SALT DISTRIBUTION IN ESTUARIES

TNO

COMMISSIE VOOR HYDROLOGISCH ONDERZOEK TNO

COMMITTEE FOR HYDROLOGICAL RESEARCH TNO

VERSLAGEN EN MEDEDELINGEN NO. 20

PROCEEDINGS AND INFORMATIONS NO. 20

SALT DISTRIBUTION IN ESTUARIES

PROCEEDING OF

TECHNICAL MEETING 30

Contents

Introduction

by ir. K. P. Blumenthal

Introduction

This 'Communication' deals with various aspects of the physical processes that take place when salt and fresh water meet. The problem is not only examined from the standpoints of theoreticians, of empiricists and of those conducting research by means of models (including both mathematical and physical models), but also the relations to practical engineering are shown. The subjects dealt with have thus been briefly characterized.

The work presented in the following series of articles would be a waste of time, were it not that a fundamental problem with which this country is confronted is involved. It is, briefly: How can we control the salt water that threatens us on all sides?
The term 'water management' covers an activity familiar to the Dutch. Apparently, however, it does not mean the same thing to everybody. No attempt will be made here to give a definition of the term, but there is a comparatively new problem connected with it which is looming large: the scarcity of fresh water which we are having to contend with and will, increasingly, have to cope with in dry periods.
Some of the causes are population growth, industrialisation, higher qualitative and quantitative standards: in short, an increasing demand. On the other hand the quality of the 'raw material' is deteriorating, in the broadest sense: an increasing number of substances are found in water, that do not naturally belong there. The usability of the water is thus more and more reduced.
One of the substances is common salt. Let us begin, for the sake of argument, by assuming that we are confronted only with the pollution of surface water by common salt from the sea; we shall forget for a moment that salt is also brought down by the Rhine. We will suppose that the Rhine is quite pure when it reaches the Netherlands and then consider this country's own state as regards salt.

Much of the country lies below average sea level, metres below it in some places. The sea is kept out by dikes and dunes, so the low part of the country could be regarded as a basin in a body of water: on the bottom and perimeter of such a basin there is a continuous pressure from outside. But the basin considered here is leaking everywhere; think of the Rotterdam Waterway and other open estuaries. Sea-locks let in salt water whenever a ship passes through them. But the bottom also leaks: the low-lying land suffers from salt seepage.
The situation with regard to salt is aggravated by several factors: by the relative sea level rise, by the increase in the volume of shipping requiring ever bigger locks, by larger and deeper harbours etc.

Fortunately, fresh water also enters the leaky basin on one side, where the Rhine, the Meuse and the smaller rivers flow into it, and from above in the form of rainfall. Besides being used for human consumption, by industries, agriculture, etc., this fresh water is used to prevent the intrusion of salt water. The following points should be noted:

1 The Rotterdam Waterway. Every tide carries salt water far inland, every ebb tide takes it out again, and the water of the Rhine and the Meuse follows it and pushes it further out.

2 Sea-locks are built in such a way as to admit as little salt as possible. There are various systems, but it is broadly true that the more effective they are, the more fresh water they use.

3 Salt seepage. Polder canals and storage areas are flushed from time to time; incidentally this removes other pollutants besides salt.

In view of 3, we must now abandon the beautiful illusion of a clean Rhine, and this brings us to another aspect of the salt and fresh water problem. The Rhine brings nearly 70 % of all our fresh water into the country, and this water therefore plays a major part in flushing polder waters. But as Rhine water is heavily polluted, not least by salt, and especially when the discharge is low, it is becoming increasingly difficult (i.e. more and more water is being needed) to reduce the high salt content in the polders by flushing. The Rhine's low discharge periods usually coincide with those in which water is urgently needed for flushing.

Some figures will be given, that carry no pretence to accuracy or completeness, but are purely intended to serve as an illustration of the foregoing. If we only consider the so-called fresh water, we find that it brings about 30 million tons of common salt into the country, in roughly the following proportions:

Rhine   18 million tons,
Locks   7 million tons,
Seepage   3 million tons, (only in the mid-west),
Meuse   1,5 million tons.

It is impossible to quantify the salt brought in by the sea in the same terms. It is better to state the amount of fresh water used in repelling it, though the operative question is: how much fresh water is actually available? This in itself is a subject requiring profound study, but let us assume for the sake of argument that in a given dry period 1000 cubic metres per second is available. This is offset by the following items:

—   600–700 cub. m. per sec. is needed to combat intrusion along the Rotterdam Waterway alone;

—   between 60 and 100 cub. m. per sec. is needed to combat the intrusion of salt through IJmuiden locks alone (but there are many more locks; for instance, in the Delta region);

8

— 50–60 cub. m. per sec. is needed merely to flush canals, etc. to counteract salt seepage.

These are just a few examples, but without indulging in quantifications, we can assume that if water is not stored when it is plentiful, it will be in short supply in dry periods.

Another approach is to examine the cost of combating salination. Here are a few illustrative points:

— the cost of raising the bed of the Rotterdam Waterway is estimated at ƒ 70 million (about $ 30.000.000);
— an air-bubble screen at IJmuiden locks will cost about ƒ 275.000 (about $ 110.000) per year. (The cost of a pumping plant for still more effective salt control, which may be installed in 1975, has been estimated at ƒ 37 million (about $ 15.000.000);
— the cost of what is called the 'Dunkirk construction' for the Kreekrak locks is estimated at ƒ 60 million (about $ 24.000.000) (requiring 20 cub. m. per sec. of fresh water);
— the cost of establishing the salt retention basin in the Alsace (which will retain 60 kg. salt per sec.) was estimated in 1974 at 34 million French francs for the Netherlands' share (this sum will presumably be out of date by the time this publication appears).
Another approach would be to work out the financial loss attributable to salination. This has been attempted, but is is a complicated business and there is not concensus as to the correct method.
The fact that we still manage to control salination fairly well is entirely due to the complex of large projects consisting of the Zuiderzee Project, the Rhine Canalisation Project and the Delta Project. The cost already runs into thousands of millions of guilders, but we must of course remember that the reduction of salination is only one of the benefits of this infrastructure. On the other hand, we should note that very much more capital needs to be invested if our fresh water supply is to be safeguarded. The construction of storage basins for drinking water is a good example, but there are many other infrastructural ways of tackling the problem of water management. We have only discussed the salt problem, but of course many other provisions are required if the quality of our water is to be ensured.

Density currents due to differences in salinity

by dr. ir. G. Abraham

1 Salt intrusion through locks: an example of the effect of differences in density on the flow pattern

The density of water increases as more salt in dissolved in it. Consequently the water in the North Sea is about $2\frac{1}{2}$ % heavier than that in the rivers of the Netherlands. The relation between the density, temperature and salinity of water, (a measure of the quantity of dissolved salts) and chlorinity (a measure of the proportion of choloride in the dissolved salts) is described in the appendix.

If water with a high salinity and high density, and water with a low salinity and low density are brought together without much mixing the water with high salinity will initially go to the bottom while the water with low salinity will rise to the surface. When the water movement involved has ceased, the resulting state of equilibrium is marked by stratification. Relatively light water is near the surface. Relatively heavy water is near the bottom. The interface or transitional zone between the two liquids is horizontal, which is typical of a state of equilibrium. Stratification becomes less pronounced as more mixing occurs between the two liquids. Mixing blurs the dividing-plane. Energy must be used to bring about mixing, because in the mixing process relatively heavy liquid is raised and relatively light liquid is lowered.

When the lock-chamber of a sea-lock is filled with fresh water, the outer gate acts as a partition between the fresh water and the salt water. When the outer gate is opened while the inner one is kept closed, the limited amount of fresh water in the chamber is brought into contact with a much greater amount of salt water, without much mixing taking place. Initially this results in the liquids moving in relation to each other. (We will come back to this later.) Gradually, a stratified state of equilibrium is reached, the lock-chamber being almost completely filled with salt water except for a relatively shallow layer near the surface. The surface of the harbour entrance is, after all, many times greater than that of the lock-chamber, so the fresh water can spread over a much greater area than that in which it was originally contained. If the outer gate of the lock is left open long enough, the fresh water originally in the chamber can be almost completely replaced by salt water. Then, when the outer gate is closed and the inner gate stays open long enough, a stratified state of equilibrium is gradually reached, the salt water originally in the lock-chamber having settled in a thin layer at the bottom of the canal full of fresh water behind the lock. Each time the lock is opened and shut, therefore, a quantity of salt water equal to the capacity of the lock-chamber intrudes into the canal behind the lock. An equal quantity of fresh water is carried out to sea and lost (see Ref. 1).

We have just explained the intrusion of salt water through locks by considering the state of equilibrium ultimately achieved after any vertical partition between salt and fresh water is removed. The intrusion of salt water can also be explained by considering

the water movement which takes place immediately after the removal of any vertical partition. The resulting flow pattern is shown in Figure 1. A salt water front penetrates into the fresh water near the bottom, while a fresh water front penetrates into the salt water near the surface. The flow pattern in the area between the two fronts is typified by two layers flowing over each other in opposite directions. The fresh water is stationary in the area in front of the salt water front. The salt water is stationary in the area in front of the fresh water fro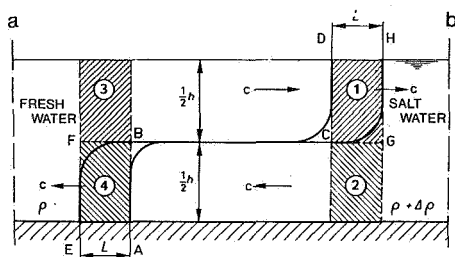nt. Potential energy is converted into kinetic energy by the exchange currents described above. Let us assume that the two fronts cover a distance L in time t (Figure 1). The potential energy converted into kinetic energy during this time is equal to the energy lost by the salt water sinking from position 1 to position 4 while fresh water rises from position 4 to position 1. Kinetic energy is gained because water that was initially stationary in positions 1 through 4 starts to move.

Figure 1. Exchange currents.

The exchange phenomenon takes on a different character when the salt water front reflects against the closed inner gate, or the fresh water front reflects against the closed outer gate. Kinetic energy is dissipated by bottom shear and internal shear. This brings the exchange currents to a halt and establishes the ultimate stratified state of equilibrium described above.

The foregoing shows that:

— density differences in fluids coming into contact with each other produce stratification;

— density differences affect current patterns (chiefly horizontal current velocities in the area between the two fronts in Figure 1, and vertical current velocities near the fronts where the liquid mass falls from 1 to 4, and the liquid mass rises from 4 to 1).

It has also been mentioned in passing that:

— energy is required to cause mixing (Conversely, mixing is inhibited by stratification).

14

2 Some more examples of exchange flows in practice

The salinity of the water in the Rotterdam Waterway varies within the tidal period. It is higher at flood than at ebb. The result is that the mean salinity of the river water is higher at flood than that of the water in a harbour situated on the river. After all, the mean salinity of the water in, say, the Botlek harbour, can only increase if the water in the harbour is replaced by river water with comparatively high salinity. The salinity of the water in the harbour reacts with a certain time lag to variations in the salinity of the river water.

Exchange currents caused by density differences are one of the mechanisms by which harbour water can be replaced by river water. If, for instance, the salinity of the harbour water is low compared with that of the river water, the exchange mechanism operates in such a way that water near the bed flows from the river into the harbour, while water near the surface flows out of the harbour into the river. This phenomenon is most noticeable around high water, when the net inflow of river water into the harbour is zero, as the level of the water in the harbour follows the variations in the level of the water in the river with a short time lag. The current pattern in the mouths of the Botlek harbours around high tide is given in Figure 2. The inflow near the bottom and the outflow near the surface are easily discernible. As the sediment content near the bed is higher than that near the surface, the inflow near the bed is a major

Figure 2.   Situation of and velocity distribution in month of Botlek Harbour at H.W.
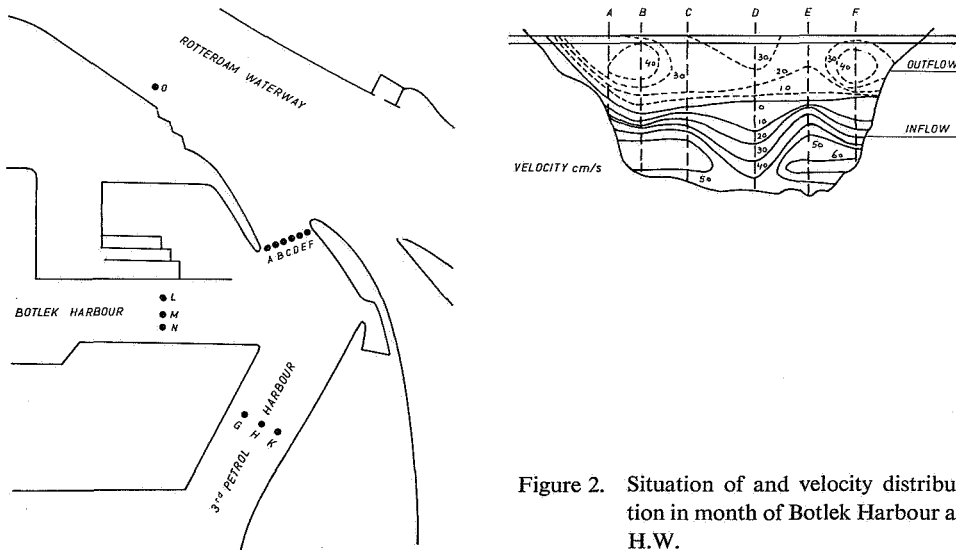
cause of the silting up of harbours on the Rotterdam Waterway (see Ref. 2). The outflow near the surface may be perpendicular to the axis of the river, and may therefore constitute a hindrance to shipping (see Ref. 3, Figure 6a, around high water).

Salt intrusion through locks, the silting up of harbours and the possible effects on the navigability of rivers are therefore three areas of civil engineering in which exchange currents caused by density differences play a part.

3 Salt intrusion in tidal rivers

If the removal of a vertical partition between salt and fresh water is associated with the introduction of a fresh water flow from A to B (see Figure 1), then the water level at A will be higher than that at B. If this were not so, there would be no net outflow of fresh water from A to B. This net outflow of fresh water makes it difficult for the salt water front to penetrate the fresh water. This situation obtains where a river discharges into a non-tidal sea, as the Rhône does into the Mediterranean. The river outflow is generally too small to remove the salt water from the river completely, so an arrested salt wedge can be found extending a certain distance up the river from the mouth, and stationary except for internal circulation (see Figure 3 and Ref. 4). The further away from the mouth, the thinner the salt wedge becomes. A certain amount of salt water intrudes over the river bed and into the river because of the circulation within salt wedge.

The stronger the tide, the more mixing occurs between the intruding salt water and the river water. The tide supplies the energy needed for mixing. Complete or partial mixing takes place, depending on the strength of the tide (see Figure 4 and 5 and Ref. 4). If mixing is partial, there will still be density differences due to the differences between the salinity of the water near the surface and that on the river bed. If mixing is complete, the differences between the salinity at the surface and that at the bottom are negligible. In that case the density only varies horizontally, i.e. from that of river water to that of sea water. The area where the density only varies horizontally lies further inland at high tide than it does at low tide. Nevertheless, even when mixing is complete, the flow over the river bed averaged over a tidal period is upstream, so as already implicitly suggested, salt water can indeed intrude over the river bed into the river.

If mixing is complete, the pressure at a point at height z above the river bed (assumed to be horizontal) will be equal to the weight of the water above that point per unit of horizontal area. The pressure increases as the depth of the water or the density of the water increases. Expressed in a formula:

$$p = \bar{\rho}g\,(h - z) \tag{1}$$

in which:

p is (hydrostatic) pressure;
g is acceleration due to gravity;
$\bar{\rho}$ is water density in cross-section of river;
h is depth;
z is distance from bottom.

CROSS-SECTION A   WATER LEVEL   CROSS-SECTION B   SEAWARDS

FRESH WATER

INTERFACE

SALT WATER

BOTTOM

SEE NOTE BELOW

→ indicates permanent seaward flow

← indicates permanent landward flow
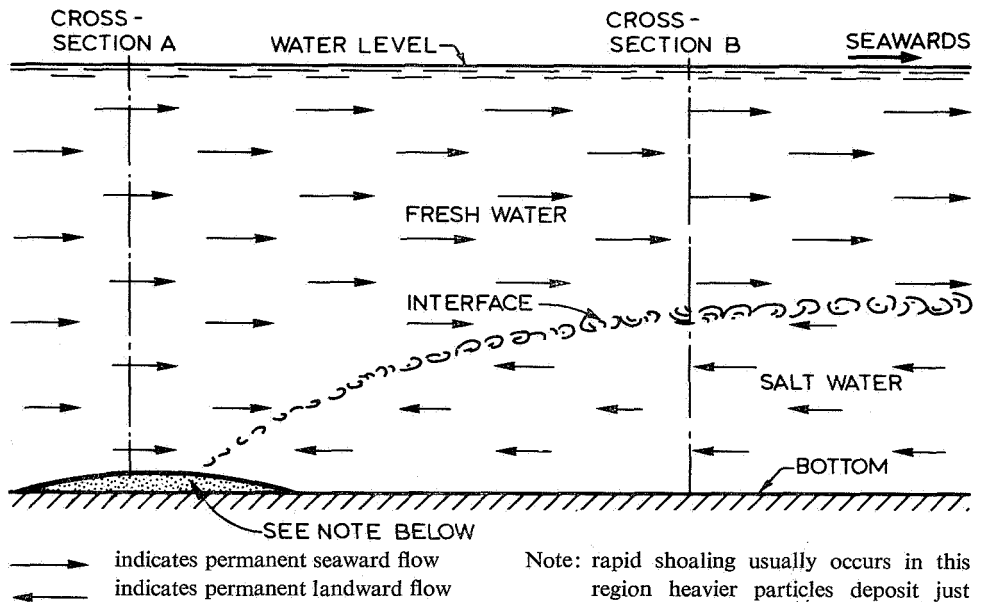
Figure 3a. Flow field.

Note: rapid shoaling usually occurs in this region heavier particles deposit just upstream from wedge tip and lighter particles just downstream from tip

SALINITY AS °/oo

VELOCITY IN ft /s

LANDWARDS   SEAWARDS

PERCENT TOTAL DEPTH FROM WATER LEVEL
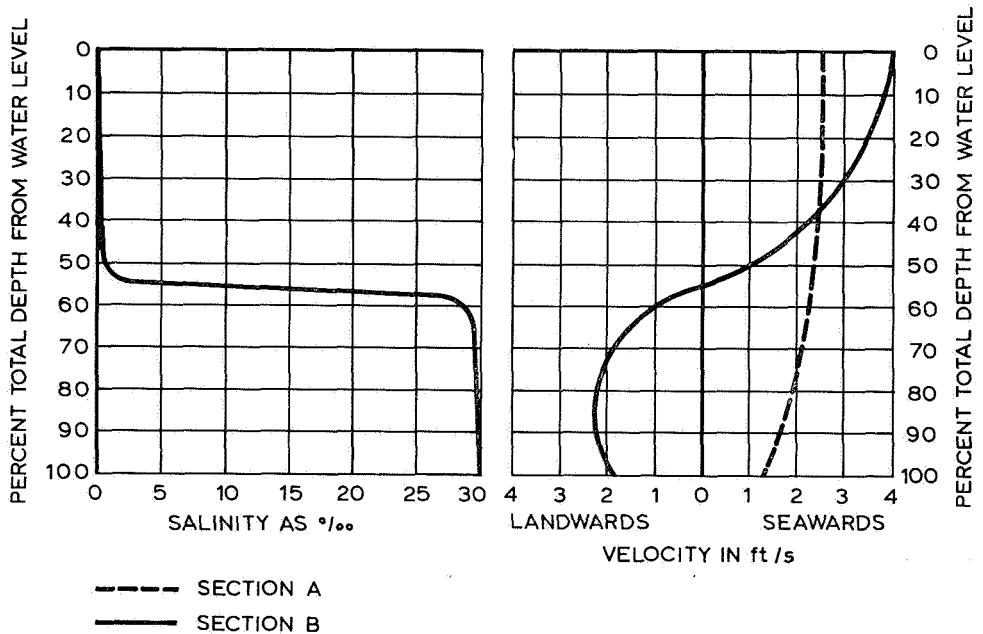
- - - - SECTION A

———— SECTION B

Figure 3b. Salinity and velocity distribution over the depth (order of magnitude).

Figure 3. Arrested salt wedge. According to Simmons (1955) (Ref. 4).

18

CROSS – SECTION A WATER LEVEL CROSS – SECTION B SEAWARDS

POSITION AND SHAPE OF INTERFACE AT: HIGH TIDE LOW TIDE
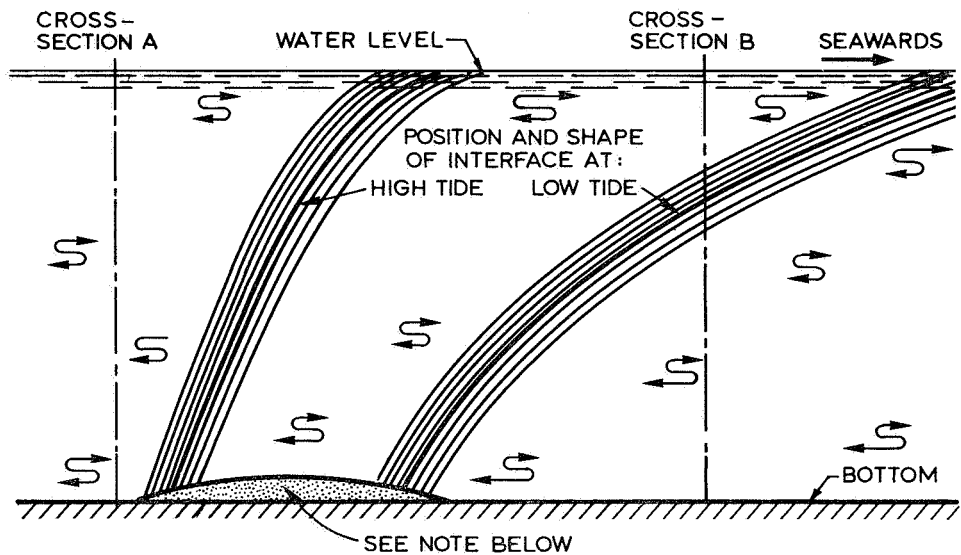
BOTTOM

SEE NOTE BELOW

indicates that direction of current reverses with tidal phase, but that predominant current is downstream

indicates that direction of current reverses with tidal phase, but that predominant current is upstream

indicates that direction of current reverses withtidal phase, but there is no predominant direction

Note: rapid deposition of both heavy and light particles of sediment usually occurs in this region

Figure 4a. Flow field

PERCENT TOTAL DEPTH FROM WATER LEVEL

HIGH TIDE

LOW TIDE

SALINITY AS °/oo

LANDWARDS SEAWARDS
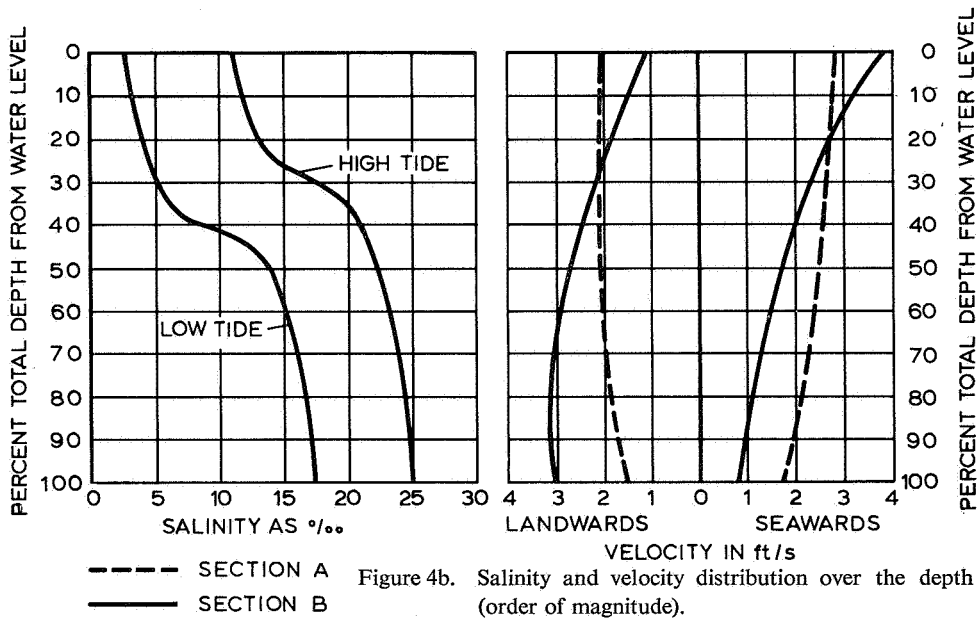
VELOCITY IN ft/s

– – – – SECTION A

———— SECTION B

Figure 4b. Salinity and velocity distribution over the depth (order of magnitude).

Figure 4. Partially mixed estuary. According to Simmons (1955) (Ref. 4).

19

SEE NOTE BELOW

$\underset{\longleftarrow}{\overset{\longrightarrow}{S}}$ indicates that direction of current reverses with tidal phase, but that predominant current is downstream

$\underset{\longleftarrow}{\overset{\longrightarrow}{S}}$ indicates that direction of current reverses with tidal phase, but that predominant current is upstream

$\underset{\longleftarrow}{\overset{\longrightarrow}{S}}$ indicates that direction of current reserves with tidal phase, but there is no predominant direction

Note: the shoaling pattern in a well mixed estuary does not appear to be related directly to the salinity pattern. Shoals form pricipally in areas of weak current velocities and where the physical configurations of the estuary produce extensive eddies and other non-uniform flow patterns
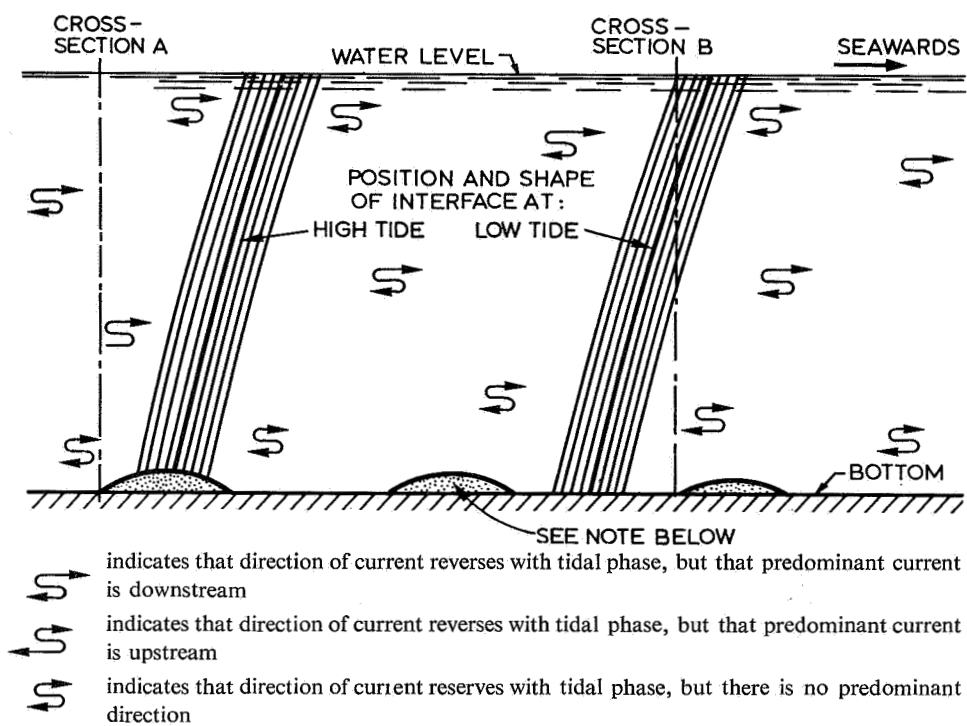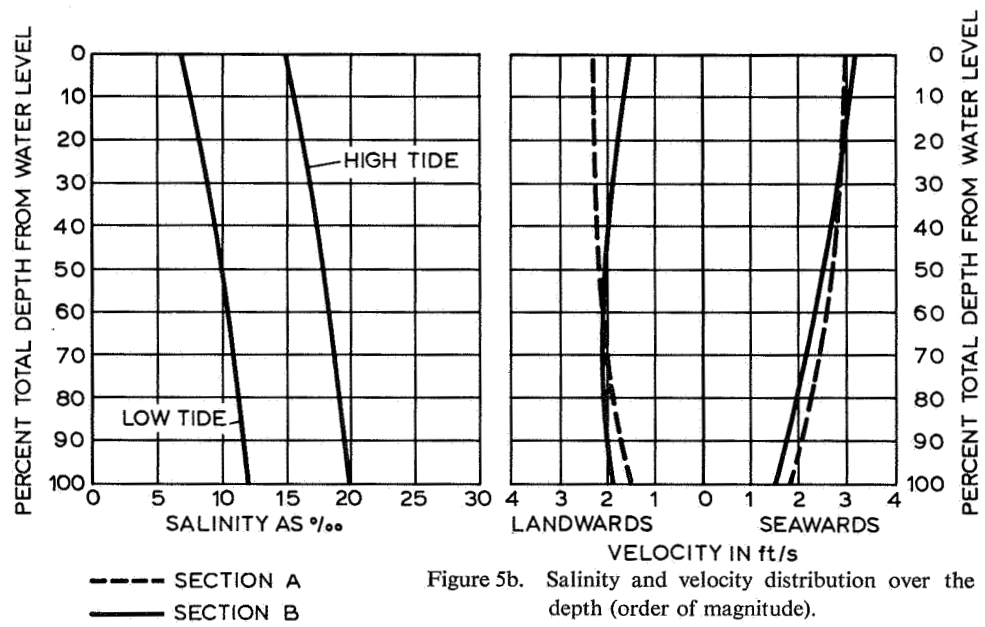
Figure 5a.   Flow field.

---- SECTION A

—— SECTION B

Figure 5b.   Salinity and velocity distribution over the depth (order of magnitude).

Figure 5.   Mixed estuary. According to Simmons (1955) (Ref. 4).

20

If the pressure at level z on the seaward side of a given mass of water is greater than that on the landward side, the difference in pressure will cause the mass of water to be subject to landward acceleration and vice versa.

Pressure differences on either side of the mass of water may have two causes, either there is a difference in depth or a difference in density. The essential difference between the two causes is that in the former the difference in pressure is the same over the whole depth, whereas in the latter the difference in pressure increases as the distance from the surface increases. The difference is illustrated in Figure 6, and it can be derived from equation 1 by differentiation of pressure p in the horizontal x direction, taking account of the fact that $\bar{\rho}$ and h vary horizontally. Therefore the following is true at any point of time t at any level z:

$$\frac{\partial p}{\partial x} = \bar{\rho} g \frac{\partial h}{\partial x} + (h - z) g \frac{\partial \bar{\rho}}{\partial x} \qquad (2)$$

The first term after the equals sign gives the difference in pressure resulting from changes in depth. This term does not vary with z. The second term gives the difference in pressure caused by the longitudinal gradient of density. The value of this term increases linearly as the distance from the surface increases, and is therefore greatest at the bottom. This explains why the tide (i.e. changes in depth) accelerates the water equally over the whole depth, while differences in density are accompanied by differences in pressure that are greater at the bottom than at the surface. Since the density decreases in a landward direction, the water at the bottom is subjected to greater force in a landward direction than is the water at the surface. This explains salt intrusion into rivers from the sea (Ref. 5).

In the area beyond the zone of salt intrusion, the time averaged flow at the bottom is seawards. In the area where salt intrusion occurs, the time averaged flow is landwards Consequently, the difference in density between sea and river water has a significant effect on sediment transport, which occurs mainly near the bottom (see Ref. 4).

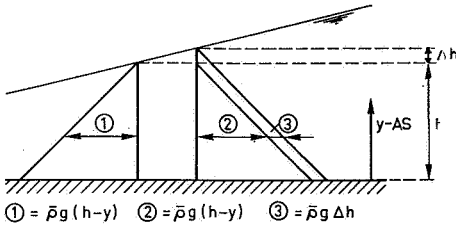① = $\bar{\rho} g (h-y)$ ② = $\bar{\rho} g (h-y)$ ③ = $\bar{\rho} g \Delta h$

Figure 6a.   Pressure gradient caused by surface gradient.

① = $\bar{\rho} g (h-y)$ ② = $\bar{\rho} g (h-y)$ ③ = $\Delta \bar{\rho} g (h-y)$
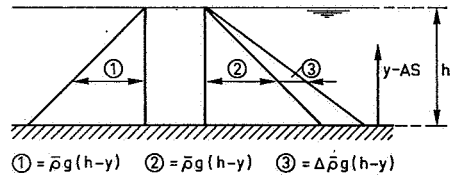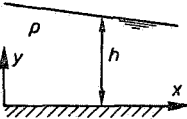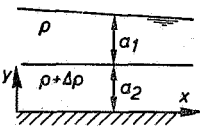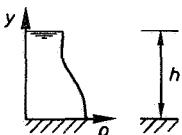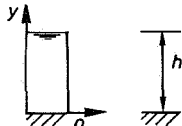
Figure 6b.   Pressure gradient caused by density gradient.

4 Advective transport versus diffusive transport; turbulent shear stress

In the foregoing introduction instances are quoted of stratified, partially mixed and mixed density currents encountered in actual practice. This classification is explained in Table 1. From now on equations will be developed to describe the various types of current. Before we do so, however, it would be useful to examine some transport and exchange mechanisms.

Table 1. Classification of density currents.

phenomenon		predominant factors
Air-water $$\frac{\partial \rho}{\partial x} = 0, \quad \frac{\partial \rho}{\partial y} = 0$$		Bottom shear Effect of h upon pressure
Stratified $$\frac{\partial \rho}{\partial x} = 0, \quad \frac{\partial \rho}{\partial y} = 0$$ except at discontinuities		Bottom shear Interfacial shear Effect of $(a_1 + a_2)$ and $\Delta\rho$ upon pressure Propagation of discontinuities
		How does mixing begin
Partly mixed $$\frac{\partial \rho}{\partial x} \neq 0, \quad \frac{\partial \rho}{\partial y} \neq 0$$		Bottom shear Effect of $\partial\rho/\partial y$ upon vertical transfer of momentum and mass Effect of h, $\partial\rho/\partial x$, $\partial\rho/\partial y$ upon pressure
Completely mixed $$\frac{\partial \rho}{\partial x} \neq 0, \quad \frac{\partial \rho}{\partial y} = 0$$		Bottom shear Effect of h and $\partial\rho/\partial x$ upon pressure

4.1 Advective transport versus diffusive transport

Figure 7 is a vertical view of running water after a quantity of dye has been injected

into it, forming a cloud of coloured liquid, this coloured liquid and the water both having the same density. The cloud moves with the current and becomes larger. The movement of the cloud illustrates advective transport. The increasing size of the cloud illustrates diffusive transport.
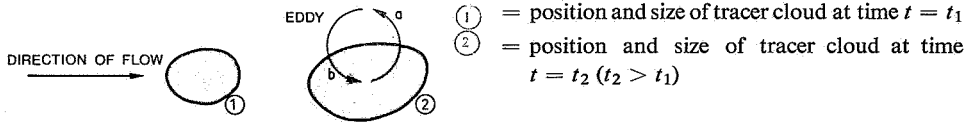
Figure 7. Cloud of tracer in steady uniform flow (displacement of tracer cloud is associated with advective transport; increase of size of tracer cloud is associated with diffusive transport (part a of eddy causes cloud to increase in size, part b of eddy brings diluting ambient fluid into cloud)).

4.1.1   Advective transport

Any substance present in running water moves with the current. The transport involved is called the advective transport of the substance. Its direction coincides with that of the current. The magnitude of the advective transport per unit of area perpendicular to the direction of flow is equal to the product of the velocity and the concentration of the substance at the spot in question. Expressed as a formula:

$$T_{adv} = u_n \, c \tag{3}$$

in which:

T_{adv} is the advective transport perpendicular to the datum plane per unit of area of the said plane;

u_n is a velocity component perpendicular to the datum plane;

c is the concentration of the substance.

The magnitude of the advective transport can only be determined if the *velocity field* is known.

4.1.2   Diffusive transport

Part a of the eddy shown in Figure 7 increases the size of the cloud of coloured fluid. Part *b* of the eddy carries non-coloured sea water into it, reducing the concentration of colour.

23

According to this example, turbulent eddies are the cause of substances in water being transported in a direction other than that of the current. Transport by eddies is called diffusive transport. Theoretically it can occur in any direction, provided the concentration of the substance varies in that direction. The extent of diffusive transport is usually equated with the gradient of the substance in the direction in question. Expressed as a formula:

$$T_{diff} : : \frac{\partial c}{\partial n} \tag{4}$$

in which:

> T_{diff} is the diffusive transport perpendicular to the datum plane per unit of area of the said plane;
>
> n is a coordinate perpendicular to the datum plane.

The turbulent *eddy field* must be known before the magnitude of diffusive transport can be determined.

4.2 Turbulent shear stress

In the example given in Figure 7, one part of the eddy carries deeply coloured liquid into the area of lightly coloured liquid, while another part of the eddy does the opposite. Similarly, part of an eddy may tend to introduce some slowly moving liquid into a mass of faster moving liquid, and vice versa. The eddies then cause a turbulent exchange of momentum relatively slow-moving liquid being accelerated and relatively swift-moving liquid being slowed down. This effect is tantamount to shear stress in the plane of contact between the two bodies of liquid. For this reason, the turbulent exchange of momentum is also called turbulent shear stress. By analogy with diffusive transport, the magnitude of the turbulent shear stress is regarded as proportional to the gradient of the velocity component parallel to the plane concerned in a direction perpendicular to the plane in question. Expressed as a formula:

$$\tau_{r,n} : : \frac{\partial u_r}{\partial n} \tag{5}$$

in which:

> τ is the shear stress in the direction of the first index in the plane perpendicular to the second index;
>
> u_r is the velocity component in the direction of the index.

24

One must also know the turbulent *eddy field* before one can ascertain the magnitude of the turbulent shear stress.

4.3   The effect on the eddy field of density differences in the body of liquid

Vertical density differences in the body of liquid slow down eddies with a horizontal axis, the larger the eddy, the more pronounced the retardation. This is explained by Figure 8. Part *a* of the eddy shown in the diagram raises heavy liquid. Part *b* of the eddy pushes light liquid down. Consequently, energy is required to initiate the eddy motion, the larger the eddy, the more energy being needed. It is then that the density difference between the bodies of liquid participating in the eddy movement increases, so that forces resistant to the eddy movement also increase. This causes the vertical diffusive transport of substances (the vertical mixing) and the vertical exchange of horizontal momentum (turbulent friction) to be suppressed by vertical density differences (Ref. 6).
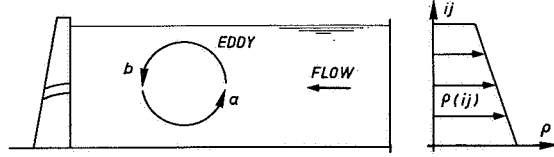
Figure 8.   Eddy in stratified surroundings.

Much research has been done on turbulence in stratified conditions. The purpose of the earliest work (Ref. 7) was to find a criterion with which to determine the conditions under which existing turbulence could be maintained. To this end two equal bodies of water were studied in conditions in which the horizontal velocity varied linearly and in which the density decreased linearly as the distance from the bottom increased. Studies were based on vertical exchange between the bodies of water over distance 1. At the end of the exchange process the heavy liquid is in the neighbourhood of the light liquid, retaining its density and vice versa, while the velocity of both bodies has become equal to the average velocity. This exchange results in an increase in potential energy, ΔE_{pot}, which is given by

$$\Delta E_{pot} = \frac{\partial \rho}{\partial z} \, g \, l^2 \tag{6}$$

and in a decrease in kinetic energy, ΔE_{kin}, which is equal to

$$\Delta E_{kin} = \tfrac{1}{4}\rho \left(\frac{\partial u}{\partial z} \right)^2 l^2 \tag{7}$$

25

in which

ΔE_{pot} is the increase in potential energy;
ΔE_{kin} is the decrease in kinetic energy;
ρ is density;
u is horizontal velocity;
l is the mixing length (see definition in the text).

The following was posited as essential for maintaining turbulence:

$$\Delta E_{pot} < \Delta E_{kin}$$

or

$$R_i = \frac{\dfrac{1}{\rho} \, g \, \dfrac{\partial \rho}{\partial z}}{\left(\dfrac{\partial u}{\partial z}\right)^2} < \tfrac{1}{4} \tag{8}$$

in which R_i is Richardson's dimensionless number as defined by the first part of equation 8.

A critical evaluation of this criterion, given in Ref. 8, shows that the numerical value $\tfrac{1}{4}$ may not be considered as valid throughout, though the analysis is correct from a dimensional point of view.
In stratified currents with a sharp interface ($\partial \rho / \partial z = \infty$, $\partial u / \partial z = \infty$) Richardson's number ceases to have significance. The stability of the interface can then be studied by ascertaining the conditions under which waves do or do not break on the interface. Equation 8 can be developed by determining the conditions under which internal waves do or do not break in a situation where there is a gradual decrease in density and velocity over the whole depth (Refs. 9 and 10).
In Richardson's number the vertical velocity gradient can be regarded as proportional to a characteristic horizontal velocity divided by a characteristic vertical length. In the same way the vertical density gradient can be regarded as proportional to a characteristic density difference divided by the characteristic vertical length. If this is substituted in the reciprocal value of Richardson's number, it produces the internal Froude number, Fr_D, which can be defined as:

$$Fr_D = \frac{U^2}{\dfrac{\Delta \rho}{\rho} \, g \, H} \tag{9}$$

26

in which

> U is a characteristic horizontal velocity;
> H is a characteristic vertical length;
> Δp is a characteristic density difference.

Derived in this way, the internal Froude number is a dimensional criterion for $\Delta E_{kin}/\Delta E_{pot}$.

Little is known about the relation between turbulent friction caused by the vertical exchange of horizontal momentum, vertical diffusive transport and about parameters indicative of the degree of stratification such as Richardson's number and the internal Froude number (Ref. 8).

4.4 Limits to the possibility of three-dimensional mathematical formulation

Newton's second law and the conservation of mass serve as exact departure points for mathematical formulation of the flow pattern. Equations that are as exact as these departure points will from now on be called exact.

Three exact equations can be developed from Newton's second law for a three-dimensional flow field. These equations express that the forces exerted on the liquid in question per unit of mass in the three main directions are equal to the accelerations which the liquid in question undergoes in the main directions. The forces are generated by turbulent shear stress, τ, and by pressure p. The accelerations are expressed in the equations in the three velocity components u, v and w. Thus Newton's second law provides three exact equations with the five unknowns u, v, w, τ and p.

The conservation of mass means that the same amount of water flows into a confined control space per time unit as flows out of it per time unit. The transport of water can be expressed in the three velocity components. Therefore the continuity of water gives a single exact equation, u, v and w being unknowns.

The conservation of salt means that the increase in the amount of salt in a fixed control volume is equal to the difference between the amount of salt that has come in across the boundaries and the amount that has gone out. Any increase in the amount of salt produces a higher salt concentration c. Salt transport across the boundaries is either advective (and equal to $u_n \cdot c$ per surface unit) or diffusive, T_{diff}. The continuity of salt therefore gives a single exact equation with the unknowns u, v, w, c and T_{diff}.

The above equations are all the exact equations that can be obtained. Thus there are only five exact equations for solving the seven unknowns u, v, w, τ, p, c and T_{diff} (see Table 2). Consequently the three-dimensional phenomenon cannot be completely expressed in exact equations. To complete the system of equations, turbulent shear stress (τ) and diffusive salt transport (T_{diff}) must be expressed in terms of the other unknowns. Then only is the number of equations equal to the number of unknowns.

We say in para. 4.3 that we only partly understand the relation between τ, T_{diff} and the other unknowns. It is therefore impossible as yet to develop a system of equations whose solution will give an exact description of the three-dimensional phenomenon.

5 Dispersion; a result of spatial averaging

The term 'dispersion' or 'dispersive transport' is used in the literature on the subject alongside the term 'diffusive transport' introduced in the foregoing. It should be noted that diffusive transport is a local quantity associated with the local eddy pattern. Dispersive transport, on the other hand, is not a local quantity. Whereas diffusive transport has a certain value at a given spot, we cannot speak of the value of dispersive transport at a given spot, because dispersive transport is linked with a reduction in the number of independent variables by spatial averaging.

The total transport of a substance (e.g. salt) across a given plane is equal to the sum of advective transport (linked with the velocity field) and diffusive transport (linked with the eddy field). Expressed as a formula:

$$T_{tot} = \int_A (u_n c + T_{diff}) dA \tag{10}$$

in which

T_{tot} is the total transport across plane A;
dA is the element of plane A;
n is the coordinate perpendicular to plane A.

It is therefore true that

$$T_{tot} = A \overline{u_n c} + A \overline{T}_{diff} \tag{11}$$

a line above the quantity in question indicating averaging over the area in question A. Since

$$\overline{u_n c} \neq \bar{u}_n \cdot \bar{c} \tag{12}$$

the total transport may be subdivided as follows:

$$T_{tot} = \underbrace{A (\bar{u}_n \cdot \bar{c})}_{1} + \underbrace{A (\overline{u_n c} - \bar{u}_n \cdot \bar{c}) + A \overline{T}_{diff}}_{2} \tag{13}$$

In the literature on the subject the total transport is usually subdivided as shown in equation 13. The second part of the total transport is called 'dispersive transport'.

29

It represents the total transport as observed by a spectator moving at speed $\bar{u}_n$, this being the average speed over the plane in question. After formal mathematical processing, the dispersive transport T_{disp} may be expressed as

$$T_{disp} = \underbrace{\int_A (u - \bar{u})\,(c - \bar{c})\,dA}_{1} + \underbrace{\int_A T_{diff}\,dA}_{2} \tag{14}$$

The first part of the dispersive transport represents the portion contributed by the irregular distribution of velocity and concentration over the plane concerned. The second part represents the portion contributed by diffusive transport.

The first part is zero when the velocity and concentration is *completely* equally distributed over the plane concerned. In this case equation 12 is not satisfied.

When applying the dispersion concept, plane A can be taken as the total cross-section of a river (dispersion by averaging over the entire cross-section), as the depth times the unit of width (dispersion by averaging over the depth), or as the width times the unit of depth (dispersion by averaging over the width).

As equation 14 shows, dispersive transport cannot be expressed in terms of the quantities $\bar{u}$, $\bar{c}$ and A. This is why, even when the number of independent variables is reduced by spatial averaging, the number of unknowns is greater than the number of exact equations available (see Table 3).

Table 2. Number of exact equations compared with number of unknowns (three-dimensional study).

Starting-point	Number of exact equations derived from starting-points	Number of unknowns
Newton's 2nd law	3 equations of motion	u, v, w, τ, p
continuity of water	1 continuity equation for water	u, v, w
continuity of salt	1 continuity equation for salt	u, v, w, c, T_{diff}
total	5 exact equations	7 unknowns

Table 3. Number of exact equations compared with number of unknowns (one-dimensional study).

Starting-point	Number of exact equations derived from starting-points	Number of unknowns
Newton's 2nd law (hydrostatic pressure distribution)	1 equation of motion in main flow direction	$\bar{u}, \bar{c}, A$
continuity of water	1 continuity equation for water	$\bar{u}, A$
continuity of salt	1 continuity equation for salt	$\bar{u}, \bar{c}, A, T_{disp}$
total	3 exact equations	4 unknowns

30

6 Equations for density currents due to salinity differences

The relation between velocity components, pressure and salinity at any point (x, y, z) in a tidal river can only be described by means of three-dimensional equations. One-dimensional equations are obtained by integrating these equations over the cross-section. They give the mean value of the velocity and salinity over the cross-section. For the stratified flow described in Table 1, the equations can be integrated over the thickness of the two layers. The equations for two layers of flow obtained in this way give the thickness of the layers and the salinity and velocity in both layers. From now on, brief descriptions of these equations will be given. For a detailed derivation, see Ref. 11.

6.1 Three-dimensional equations

When studying salt intrusion in rivers and canals situated behind locks, the vertical accelerations are small enough for the pressure to be distributed hydrostatically. As in homogeneous currents, the pressure satisfies the equation:

$$\frac{\partial p}{\partial z} = - \rho g \tag{15}$$

in which z is the vertical coordinate (positive direction upwards).

The continuity equation for salt equates salinity increase in an elementary volume dx, dy, dz per time unit dt with the net quantity of salt passing across the boundaries. Assuming advective and diffusive transport (see Chapter 4), this gives the following equation:

$$\frac{\partial c}{\partial t} + \frac{\partial uc}{\partial x} + \frac{\partial vc}{\partial y} + \frac{\partial wc}{\partial z} + \frac{\partial T_{diff,x}}{\partial x} + \frac{\partial T_{diff,y}}{\partial y} + \frac{\partial T_{diff,z}}{\partial z} = 0 \tag{16}$$

in which

u, v, w are velocity components in x, y and z directions;
x, y are coordinates in longitudinal and lateral direction;
t is time;
T_{diff} is diffusive transport in the direction indicated by the index.

The equation of motion in the two horizontal directions and the continuity equation for water are equal to those for homogeneous (incompressible) fluid.

6.2   One-dimensional eqations

The continuity equation for water is the same as for homogeneous currents:

$$\frac{\partial bh}{\partial t} + \frac{\partial A\bar{\bar{u}}}{x} = 0 \tag{17}$$

in which

b is width of river in question;
A is area of cross-section;
$\bar{\bar{u}}$ is average velocity over the cross-section.

The continuity equation for salt equates the increased amount of salt in a section of dx thickness with the net quantity of salt passing across the two boundaries of the section. Expressed as a formula:

$$\frac{\partial A\bar{\bar{c}}}{\partial t} + \frac{\partial T_{tot}}{\partial x} = 0 \tag{18}$$

where $\bar{\bar{c}}$ is mean concentration over the cross-section.
On substituting equations 13 and 14, we get:

$$\frac{\partial A\bar{\bar{c}}}{\partial t} + \frac{\partial A\bar{\bar{u}}\cdot\bar{\bar{c}}}{\partial x} + \frac{\partial T_{disp}}{\partial x} = 0 \tag{19}$$

Assuming hydrostatic pressure distribution, integration of the equations of motion in x direction over the cross-section gives:

$$\frac{\partial A\bar{\bar{u}}}{\partial t} + \frac{\partial A\bar{\bar{u}}\cdot\bar{\bar{u}}}{\partial x} + gA\left(\frac{\partial h}{\partial x} - I\right) + g\frac{Ah_c}{\bar{\bar{\rho}}}\frac{\partial\bar{\bar{\rho}}}{\partial x} + \frac{\tau_w}{\bar{\bar{\rho}}}\frac{A}{R} = 0 \tag{20}$$

in which

τ_w is friction along the boundary of the cross-section (wall and bottom friction) (τ_w positive when positively directed flow is slowed down by friction);

32

R is hydraulic radius of cross-section;

$\bar{\bar{\rho}}$ is mean density over cross-section;

h_c is distance from surface to centre of gravity of cross-section;

I is gradient of bottom (positive with downward gradient in the positive x direction).

In developing equation 20, it was assumed that velocity and salinity are distributed almost equally throughout the cross-section.

6.3   Two-layer current (without mixing)

Two-layer currents without any mixing of the two layers — and therefore constant density in both layers — occurs mostly in canals of a constant width.
The continuity equations for the two layers are:

$$\frac{\partial a_1}{\partial t} + \frac{\partial a_1 u_1}{\partial x} = 0 \tag{21}$$

and

$$\frac{\partial a_2}{\partial t} + \frac{\partial a_2 u_2}{\partial x} = 0 \tag{22}$$

in which

a_1, a_2 are the thicknesses of upper and lower layer;

u_1, u_2 are the mean velocities of upper and lower layer.

Equations 21 and 22 have the same construction as 17.

The equations of motion for the two layers can be obtained by integrating the equation of motion in x direction over the two layers. If the width in constant and the pressure distribution is hydrostatic, we get:

$$\frac{\partial u_1}{\partial t} + u_1 \frac{\partial u_1}{\partial x} + g \frac{\partial a_1}{\partial x} + g \frac{\partial a_2}{\partial x_\rfloor} - gI + \frac{\tau_i}{\rho_1 a_1} = 0 \tag{23}$$

and

$$\frac{\partial u_2}{\partial t} + u_2 \frac{\partial u_2}{\partial x} + \frac{\rho_1}{\rho_2} g \frac{\partial a_1}{\partial x} + g \frac{\partial a_2}{\partial x} - gI - \frac{\tau_i - \tau_b}{\rho_2 a_2} = 0 \tag{24}$$

in which

ρ_1, ρ_2 are densities of upper and lower layer;

τ_b is friction at bottom (positive where lower layer is slowed down when flowing in a positive direction);

τ_i is interfacial friction (positive where upper layer is slowed down when flowing in a positive direction).

In deriving equations 23 and 24 it was assumed that the velocity was distributed almost equally throughout the thickness of the layers.

6.4   Essential additional information

The equations given above do not enable the flow pattern to be fully described. To obtain a three-dimensional description of the flow pattern, additional information is needed on the relation between the magnitude of diffusive salt transport and turbulent shear stress on the one hand and parameters describing the fields of velocity and concentration on the other. Without this information, it is impossible for instance, to eliminate diffusive salt transport from equation 16. By analogy, it is essential in one-dimensional studies to express the magnitude of dispersive transport and wall shear in one-dimensional parameters which describe the fields of velocity and concentration. In two-layer currents similar considerations apply to wall shear, bottom shear and interfacial shear.

One of the difficulties encountered in the theoretical study of density currents is that the turbulence theory is not sufficiently developed to supply the essential additional information (see para. 4.3.). For this reason theoretical descriptions of density currents are usually semi-empirical. This is particularly true of the theoretical study of salt intrusion in rivers and canals situated behind locks.

34

7 Internal hydraulic jump

The formula $u_1 = 0$ applies to an upper layer at rest. If the upper layer is very thick, $a_1 \to \infty$. If these conditions are satisfied, equations 22 and 24, in steady flow conditions, change to:

$$\frac{\partial a_2 u_2}{\partial x} = 0 \tag{25}$$

and

$$u_2 \frac{\partial u_2}{\partial x} + \frac{\rho_2 - \rho_1}{\rho_2} g \left(\frac{\partial a_2}{\partial x} - I \right) - \frac{\tau_i - \tau_b}{\rho_2 a_2} = 0 \tag{26}$$

By substituting g for $\frac{\rho_2 - \rho_1}{\rho_2} g$, equation 26 changes into an equation for homogeneous currents. In homegeneous currents, sub-critical flow changes into super-critical flow when the Froude number is one, the Froude number being defined as

$$Fr = \frac{U^2}{gH} \tag{27}$$

Therefore in stratified flow satisfying the condition set for the development of equations 25 and 26, sub-critical flow changes into super-critical flow in the lower layer when the internal Froude number is one. If the upper layer is of finite thickness and not in equilibrium, the condition for this transition is (see Ref. 12):

$$\frac{u_1{}^2}{\dfrac{\rho_2 - \rho_1}{\rho} g a_1} + \frac{u_2{}^2}{\dfrac{\rho_2 - \rho_1}{\rho} g a_2} = 1 \tag{28}$$

When the currents are homogeneous, the transition from super-critical flow to sub-critical flow takes the form of a hydraulic jump. When the flow is stratified, it takes the form of an internal hydraulic jump, the fluid of both layers being mixed in the process.

8 Summary

8.1 Salt intrusion in rivers

The following phenomena are of importance in salt intrusion:

— tidal movement;
— the effect of differences in density on velocity distribution (through the pressure

——— $= x - t$ diagram of bottom water particle coming in from fresh water sea ($\Delta\rho = 0$) at beginning of flood (river discharge has caused particle to go out to sea again before end of ebb).

— — $= x - t$ diagram of bottom water particle coming in from salt water sea ($\Delta\rho \neq 0$) at beginning of flood.
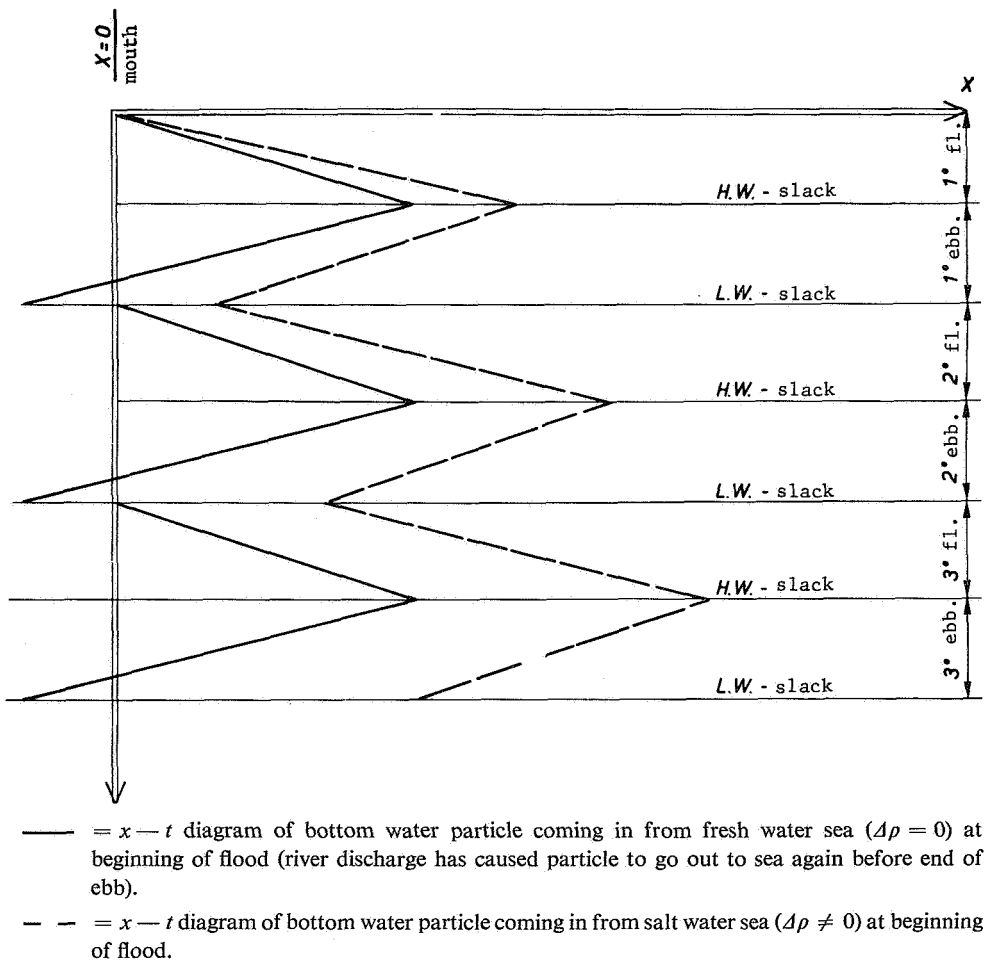
Figure 9. Effect of velocity distribution and mixing on salt intrusion into rivers.

gradient and the distribution of shear stress over the depth);
— the effect of mixing on the distance the salt intrudes.
Owing to differences in the density, the mean velocity near the bottom during the tidal cycle is directed inland to a greater degree than if there were no differences in density. Near the surface, the position is reversed. This causes salt water near the bottom to intrude further up the river than it could if there were no differences in density (see Fig. 9). One of the factors that limit the distance salt can intrude inland is vertical mixing and vertical advective salt transport, by which the salt from the bottom layers, where there is predominantly landward advective transport, is carried into the upper layers, where there is predominantly seaward transport. Salt intrusion can also be affected by exchange currents between the river and the harbours situated on it (see Chapter 2).

A hydraulic model for studying salt intrusion in rivers should therefore correctly represent:
— tidal movement;
— the effect of differences in density on velocity distribution;
— mixing;
and where necessary the effect of harbours situated on the river.

A theoritical methematical study should give:
— tidal movement;
— the effect of differences in density on velocity distribution.
It should be based on:
— a sound mathematical formulation of mixing and turbulent shear stress;
— knowledge of conditions in the estuary, insofar as this is necessary for formulating boundary conditions.

8.2   Salt intrusion in canals

If salt intrusion is combated chiefly by flushing canals with fresh water, the following phenomena effect the distance the salt intrudes:

— exchange currents in the lock (comparatively short distance travelled, comparatively high velocity, comparatively little friction);
— mixing by an internal hydraulic jump, if the canal is deepened out near the lock;
— currents due to the tendeney to stratify in the non-flushing preiod (comparatively long distance travelled, comparatively low velocities, comparatively high friction);
— currents and mixing during flushing period.

These factors should be correctly represented in a hydraulic model; alternatively, a theoretical mathematical study should be based on a sound formulation of these phenomena (problems are: mixing, shear stress, what happens at salt water fronts).

8.3 Research Methods

Salt intrusion in rivers and canals is due to a complex interaction between various factors. Consequently, research in the form of on-site measurements as well as hydraulic model research and a theoretical mathematical approach is essential. Each of these methods has its limitations. Salt intrusion in rivers and canals can only be studied by combining all these methods.

On-site measurements can only be carried out under the actual conditions obtaining (e.g. the actual depth of the Rotterdam Waterway). There can be no systematic variation of the determining variables. Provided enough samples are taken, on-site measurements can extend our knowledge of the physical situation.

Theoretically, the theoretical mathematical method can be used for extrapolation, provided the formulas which are used represent the phenomena concerned correctly. It is the present state of the turbulence theory that imposes limitations. Three-dimensional calculations are as yet impossible to effectuate and there may be difficulties in formulating boundary conditions.

Hydraulic model research may be carried out for conditions other than those actually obtaining. Three-dimensional phenomena can be studied. When the object of the research is to gain a better understanding of the physics of the subject, systematic variation of the determining variables and geometrical schematisation to simple shapes (e.g. a rectangular cross section) are possible. The limitations of hydraulic model research are due to the difficulty of correctly representing the phenomena to be studied in the model.

Appendix

The salt content of sea water, whether or not diluted with distilled water, is expressed as salinity and chlorinity. These values are defined as follows:

S (salinity): the total amount of salts in solution in grams per kilogramme of water (as $^0/_{00}$);

Cl (chlorinity): the amount of Cl^- in solution in grams per kilogramme of water (as $^0/_{00}$).

Since the density of sea water is only slightly different from 1000 kg per cub. mtr., the above definitions may be taken to mean approximately the amounts of salts in solution per liter of water.
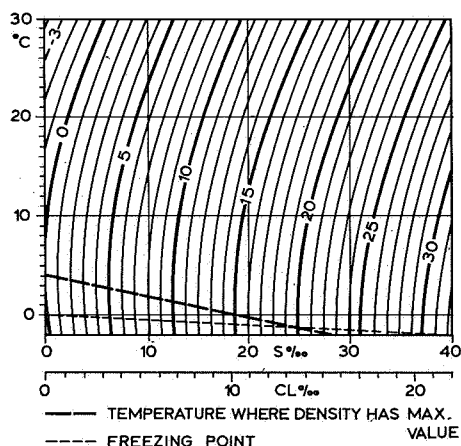
Figure 10 shows the relation between density, temperature and salt content expressed as salinity. This relation may be expressed approximately as:

$$\rho = 1000 + 805\ S - 0.0065\ (\theta - 4 + 220\ S)^2 \qquad (29)$$

In this equation ρ is in kg. per cub. mtr., and θ is the temperature in °C. If the chlorinity values are high enough, salinity can be expressed approximately by the formula:

$$S = 0.03 + 1.805\ Cl$$

For more detailed information, see Ref. 13.

Figure 10. Density as function of temperature and salinity (the figure gives the difference between the density of water of a given temperature and salinity, and that of distilled water of 4° C in kg/m³). (Ref. 14).

39

References

1 Beperking van verzilting via schutsluizen in Deltagebied, Driemaandelijks bericht Deltawerken, 1964, nr. 27, februari, blz. 354–361.
   ABRAHAM, G., VAN DER BURGH, P. AND DE VOS, P., Means to reduce salt intrusion through new and existing locks, 21st International Navigation Congress, Section 1, Subject 1, 1965, pp. 1–17.
2 SANTEMA, P., Enkele beschouwingen over de aanslibbing van de havens langs de Rotterdamse Waterweg, de Ingenieur, 8 januari 1954, pp. B1–B8.
   ALLEN, F. H. AND PRICE, W. A., Density currents and siltation in docks and tidal basins, Dock and Harbour Authority, July 1959.
3 VAN REES, A. J., VAN DER KUUR, P., AND STROBAND, H. J., Experiences with tidal salinity model Europoort, Proc. 13th Conf. on Coastal Eng., Vancouver, 1972, vol. 3, pp. 2345–2368.
4 SIMMONS, H. B., Some effects of upland discharge on estuarine hydraulics, Proc. Am. Soc. Civ. Eng., 81 (1955), paper no. 792.
5 IPPEN, A. T., Salinity intrusion in estuaries, chapter 13, Estuary and Coastline Hydraulics, Edited by A. T. Ippen, McGraw-Hill, New York, (1966).
6 MONIN, A. S., Turbulence in shear flow with stability, Journ. Geoph. Res. 64, 1959, no. 12, pp. 2224–2225.
7 RICHARDSON, L. F., The Supply of energy from and to atmospheric eddies, Proc. Roy. Soc. A 97, 1920, p. 354.
8 LONG, R. R., Some aspects of turbulence in stratified fluids, Appl. Mech. Rev. Nov. 1972, pp. 1297–1301.
9 MILES, J. W., On the stability of heterogeneous shear flows, J. Fluid Mech. 10, 1961, p. 496.
10 MILES, J. W., AND HOWARD, L. N., Note on a heterogeneous shear flow, J. Fluid Mech. 20, 1964, p. 331.
11 RIGTER, B. P., Reproductie zouttoestand getijrivieren; theoretische grondslagen getijgootonder-
   zoek, Waterloopkundig Laboratorium, Rapport M 896–3, 1971.
   VREUGDENHIL, C. B., Computation of gravity currents in estuaries, Delft Hydraulics Laboratory Publication, nr. 86, 1970.
12 SCHIJF, J. B., AND SCHÖNFELD, J. C., Theoretical considerations on the motion of salt and fresh water. Proc. Minn. Intern. Hydr. Conv., Sept. 1953, pp. 321–333.
13 KNUDSEN, M., Hydrographical tables, Copenhagen 1901.
14 DIETRICH, G., UND KALLE, K., Allgemeine Meereskunde, 1957, Borntraeger, Berlin.

Emperical methods of forecasting movement of salt in estuaries

by ir. F. Langeweg and J. J. van Weerden

1 Introduction

Salinity movement in estuaries is a subject of extensive research because of the major consequences it has on water management. It affects such things as water supplies for the population, for agriculture and for industry. Quite clearcut standards have to be applied to the quality of the water taken; moreover, a knowledge of the mechanism of salinity movement is needed in connexion with the influence it has on the current-speed pattern, affecting shipping and the carrying capacity of the water. One particular aspect worth mentioning is the carrying of sediment and the effect this has on the siltation of harbours lying along the estuary.

An attempt has been made, taking an emprirical approach, to obtain a picture of the salinity-movement mechanism. The fact that an empirical approach was taken does not, however, mean that the basis for our study will not involve a physical description of the mechanism; but there are problems in determining the constants with their physical significance in this mathematical presentation. In this area, therefore, we were forced to work empirically, with all the simplification of the problem and the consequent uncertainties this entails. Yet provided one is aware of the limitations inherent in empirical methods because of this, one finds that in practice sound results can be obtained.

2 Background to empirical methods

A one-dimensional diffusion equation generally forms the starting point for empirical methods of forecasting salinity movement in estuaries. This equation comes about from averaging in the conservation of mass equation for salt in an estuary on a time-scale for turbulence, and then again averaging over the cross-section. Finally, the following equation emerges:

$$\frac{\delta \bar{c}}{\delta t} + \bar{U}\frac{\delta \bar{c}}{\delta x} = \frac{1}{A}\ \frac{\delta}{\delta x}\ \left(AD_x\frac{\delta \bar{c}}{\delta x}\right) \tag{1}$$

where

$\bar{c}$ = concentration averaged over the cross-section;
$\bar{U}$ = velocity averaged over the cross-section;
D_x = dispersion coefficient;
A = cross-sectional area.
($\bar{c}$, $\bar{U}$, A and D_x are functions of x and t).

This one-dimensional model forms a usable starting point for forecasting salinity distribution in a tidal estuary. The change in salt content during one tidal cycle takes place over a time-scale that is considerably longer than that of the turbulence, so that when time-averages have been struck in order to eliminate turbulence fluctuations there is still sufficient detailed information remaining.

The one-dimensional diffusion model will give a physically-accurate picture of salt distribution only if the salt is homogeneously mixed over the cross-section; this is not, however, necessarily the case in all estuaries. The factors determining the extent to which mixing occurs include:
— the horizontal tidal movement in the estuary mouth;
— the outflow of fresh water to the estuary from the river;
— the geometry of the estuary.

Harleman and Abraham [1] deduced, from the work carried out by Ippen and Harleman [2], that what they term the 'estuary number' E provides a measure of the degree of stratification in an estuary

$$E = \frac{P_T \cdot F_0{}^2}{Q_f \cdot T} \tag{2}$$

where

P_T = tidal prism, i.e. the volume of seawater in m³/tide entering the estuary on the flood tide;

F_0 = Froude number = $U_0/\sqrt{gd}$, where U_0 is the maximum flood tide velocity and d is the mean depth in the estuary mouth;

Q_f = freshwater discharge in m³/s;

T = tidal period in sec.

When E is relatively small the estuary is strongly stratified and density currents occur to an overwhelming extent. As appears from (2), this will be the case with a weak tidal movement combined with a relatively high rate of outflow from the river. If, however, the estuary number is high then the salt will be mixed more uniformly by the vertical component, with the mixing effect of turbulence arising from a more marked tidal movement playing an important part where there is a relatively modest river discharge. Figure 1 gives some idea of the relationship between stratification and the estuary number.
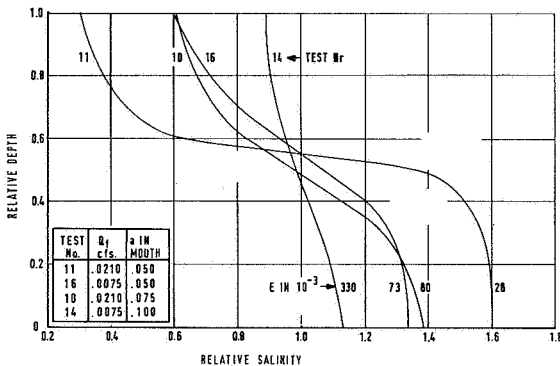
It is found that the one-dimensional diffusion model can be used for partially-mixed estuaries as well as for well-mixed ones; but for cases where density currents provide the motive force for the salt intrusion mechanism, this model will not provide an answer.

Figure 1. Vertical salinity distribution as indication of degree of stratification (from lit. 5, p. 74).

Attempts have been made in many different ways to arrive at a solution from the one-dimensional diffusion model as set out in equation (1).

There were three main problems, stemming partly from the mathematical techniques available for solving systems of differential equations and partly from the degree of understanding of the physics of the process; these problems were

1 the simultaneous solving of a system of differential equations composed of the diffusion equation, the movement equation and the continuity equation: the application of computer-based numerical methods has opened up many possibilities in this sphere;

2 the understanding of the physics of the dependence of the dispersion coefficient D on flow and geometrical parameters; these dependences were, in particular, masked by the limited mathematical techniques at hand;

3 the opportunities for forecasting the boundary conditions for the behaviour of

salt water in the mouth of the river, where the behaviour of the adjoining coastal waters need by no means always predominate.

These factors prompted a simplification of the problem aimed at reaching at least some solution, even if only one of limited applicability. In many cases the starting point was then a state of equilibrium in the estuary, with neither the tidal movement in the mouth of the estuary nor the river discharge allowed to vary with time (Ippen & Harleman, Harleman & Abraham, Van der Burgh, and others). Besides the fact that they give only a limited picture of salinity movement, the main disadvantages of these methods are that:

firstly, estuaries virtually never reach such an equilibrium, mainly because quite a long time is needed before a state occurs in nature as a result of which the boundary conditions of tide and river outflow will not alter;

secondly, the physical significance of the dispersion coefficient loses a great deal of its value, mainly because in such methods there is usually an extensive use made of averaging procedures.

For a long time, however, this equilibrium-state approach was the only one that would yield practical results for the forecasting of saline intrusion; this being so, these methods are today widely used. There was no clear picture of the limitations of these methods, however, largely because of the small amount of suitable measurement data available for empirical research into saline intrusion. Systematic testing carried out in a tidal flume at the Hydraulics Laboratory at Delft did provide useful information in this respect.

Thatcher & Harleman took a further step forward from the empirical methods of work by discarding the assumption of an equilibrium-state in the estuary; yet even in their method there was still a large measure of empiricism. Empirical methods thus fall into two main groups:

1   stationary models, based on a state of equilibrium in the estuary;
2   non stationary models, in which the estuary need not be in equilibrium.

The chapters that follow will look in greater detail at the methods in these two main groups, and will see how they cope with the three principal problems we have been discussing above.

46

3 Stationary models

The stationary models proceed from equation (1), with the assumption that the velocity $\overline{U}$ is made up of two components, one ($\overline{U}_T$) resulting from tidal movement and the other V_f the result of outflow from the river. Both these components are, basically, functions of X and t, although on different time-scales. The tidal component has a period of 12 hours 25 minutes, while the outflow component has a far longer time-scale. Assuming that the x-axis is directed towards the river, we have:

$$\overline{U} = \overline{U}_T - V_f \tag{3}$$

Equation (1) can, by substituting (3), be replaced by:

$$\frac{\delta \bar{c}}{\delta t} + \overline{U}_T \frac{\delta \bar{c}}{\delta x} - V_f \cdot \frac{\delta \bar{c}}{\delta x} = \frac{1}{\tilde{A}} \frac{\delta x}{\delta x} \left[\tilde{A} \, D_x \frac{\delta \bar{c}}{\delta x} \right] \tag{4}$$

A further simplification can be achieved by working from the salt content averaged over a tidal period. Since in a state of equilibrium V_f is constant throughout a tidal period, and furthermore

$$\int_0^T \frac{\delta \bar{c}}{\delta t} \, dt = 0; \quad \int_0^T \overline{U}_T \frac{\delta \bar{c}}{\delta x} \, dt = 0$$

we get the following equations from (4) after averaging over a tidal period of duration T:

$$- V_f \cdot \frac{d\tilde{\bar{c}}}{dx} = \frac{1}{\tilde{A}} \cdot \frac{d}{dx} \left[\tilde{A} \cdot D_X^T \cdot \frac{d\tilde{\bar{c}}}{dx} \right] \text{ or}$$

$$- Q_f \cdot \frac{d\tilde{\bar{c}}}{dx} = \frac{d}{dx} \left[\tilde{A} \cdot D_X^T \cdot \frac{d\tilde{\bar{c}}}{dx} \right] \tag{5}$$

In this equation D_X^T represents an effective value for the coefficient of dispersion over a tidal period, while $\tilde{\bar{c}}$ is the average salt content and $\tilde{A}$ is the profile averaged over a tidal period. Equations (4) and (5) provide the starting-point for the stationary one-dimensional models to be used.

3.1 Ippen & Harleman method

Ippen and Harleman [2], and later Harleman and Abraham [1], make an analytical solution possible by (on the basis of equation (4)) considering the situation at low-water slack, i.e. the moment at the end of the ebb flow at which saline intrusion into the estuary is at its least. At this moment $\frac{\delta \bar{c}}{\delta t} = 0$ and $\bar{U}_T = 0$, so that — if one works from the assumption of a constant cross-sectional area in the estuary, equation (4) becomes:

$$- V_f \cdot \frac{d\bar{c}}{dx} = \frac{d}{dx} \left(D_X^{LWS} \frac{d\bar{c}}{dx} \right) \tag{6}$$

Integration to x, bearing in mind that for a large x the values of $\frac{\delta \bar{c}}{\delta x}$ and $\bar{c}$ approach zero, gives us:

$$- V_f \cdot \bar{c} = D_X^{LWS} \frac{d\bar{c}}{dx} \tag{7}$$

Ippen and Harleman found, by analysing the results of laboratory experiments that the dispersion coefficient is an inverse function of x:

$$D_X^{LWS} = \frac{D_0^{LWS} \times B}{x + B} \tag{8}$$

Here B is the distance from the river mouth to the point where the salt content is equal to that of seawater, while D_0^{LWS} represents the dispersion coefficient at the river mouth at low-water slack.
By substitution of (8) and (7), and integration to x, we arrive at the following analytical solution to the basic differential equation in which C is the content of seawater:

$$\frac{\bar{c}}{c_z} = exp \left[- \frac{V_f}{2D_0^{LWS}B} (x + B)^2 \right] \tag{9}$$

Ippen and Harleman carried out fundamental research into saline intrusion using a flume (length 100 m, width 0.23 m and depth 0.15 m) at the Waterways Experiment Station in Vicksburg. This showed that the parameters D_0^{LWS} and B could be correlated to the 'stratification number' G/J, as defined by the following equation:

$$\frac{G}{J} = \frac{\text{rate of energy dissipation per unit mass of fluid}}{\text{rate of gain of potential energy per unit mass of fluid}}$$

The stratification number is, in practice, difficult to arrive at. Harleman and Abraham [1] found, from re-analysis of the model tests and measurements in the Rotterdam Waterway already mentioned that the stratification number correlates well to the estuary number E, defined as:
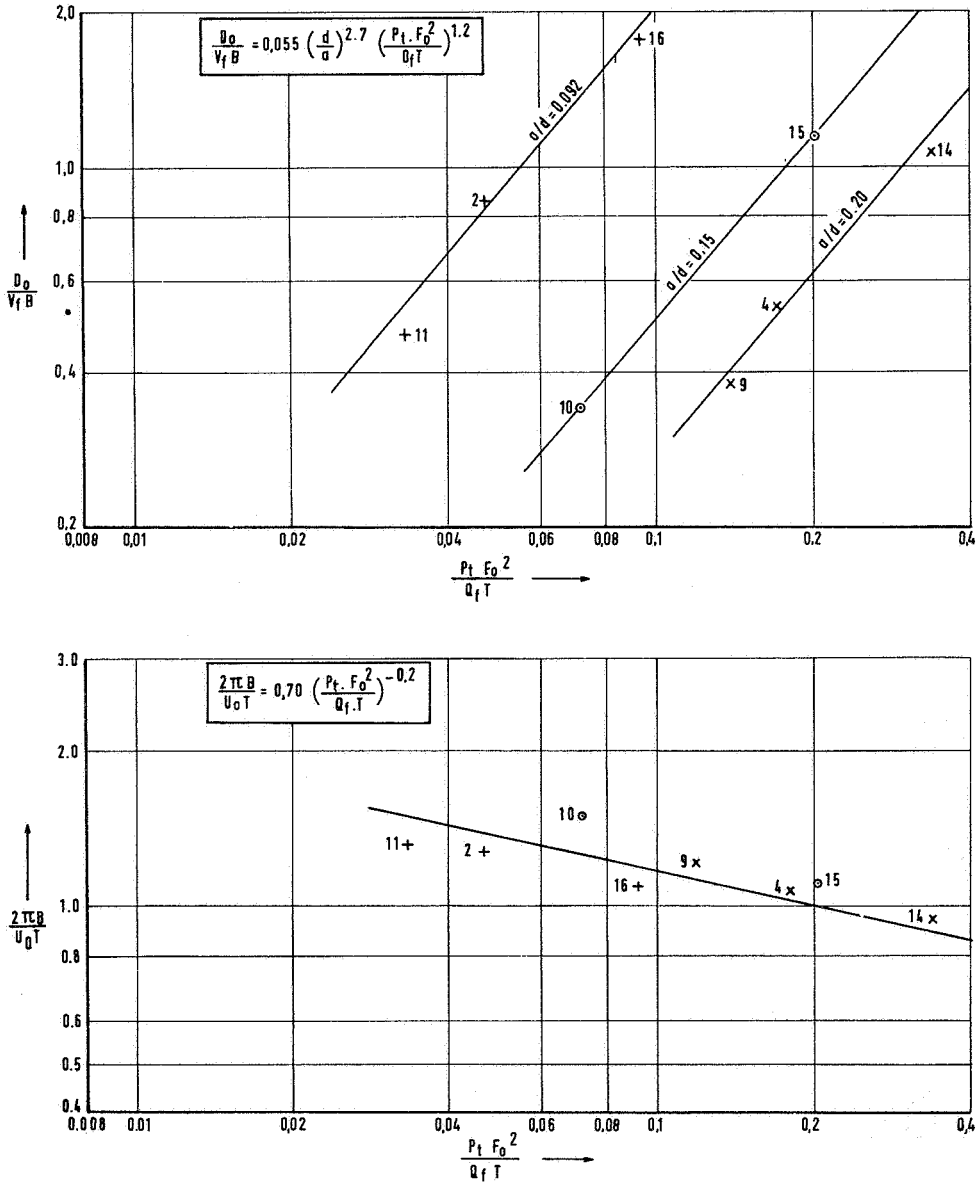

Figure 2. Determining parameters for Ippen-Harleman-Abraham model.

$$E = \frac{P_T \cdot F_0{}^2}{Q_f \cdot T} \tag{10}$$

Harleman and Abraham formulated fresh correlations between D_0^{LWS} and B using this new parameter. It was however then necessary to introduce an additional parameter a/d (tidal amplitude/depth at the river mouth). The correlations found are (see also Fig. 2):

$$\frac{D_0^{LWS}}{V_f \cdot B} = 0{,}055 \left(\frac{d}{a}\right)^{2,7} . E^{1,2} \tag{11}$$

$$\frac{2\pi B}{\bar{U}_0 T} = 0{,}70 \, E^{-,2} \tag{12}$$

Using these correlations it is possible to determine the parameters in equation (9). The salinity distribution at times other than low-water slack can be found by translating the calculated salinity distribution along the distance covered by a water particle up to the desired point in time.
Besides the limitations of the stationary model listed earlier, the Ippen and Harleman model has the further constraint of being valid only for a constant cross-sectional area A (that is to say that A is not a function of x).

3.2 Van der Burgh method

Van der Burgh [3] works from the average salinity over a tidal period, and therefore has equation (5) as his basis. He determines the salinity curve at low-water and high-water slack by translating the average salinity trend over a half-ebb or half-flood distance, as the case may be. He assumes V_f and C to be functions of x, and does not try to obtain an analytical solution but rather to solve equation (5) numerically. Since in a section of the size of Δx the magnitudes $\tilde{A}$ and D_X^T are assumed to be constant, equation (5) may be replaced by the following differential equation:

$$\frac{\Delta \tilde{\tilde{c}}}{\Delta x} = - \frac{V_f \tilde{\tilde{c}}}{D_X^T} \tag{13}$$

Van der Burgh arrived, from numerous measurements on site in the Dutch estuaries, at the following empirical equation for the dispersion coefficient:

$$D_X^T = D_0^T - K_1 \cdot \int_0^x V_f \cdot dx \tag{14}$$

50

The dispersion coefficient at the mouth of the estuary can be obtained from:

$$D_0^T = K_0 \, (\alpha.g.)^{0,5} \cdot d^{1,5} \tag{15}$$

In this equation α is the flood number introduced by Canter Cremers; this can be looked upen as a characteristic for the degree of mixing in the estuary, and defined as

$$\alpha \; = \; \frac{Q_f \cdot T}{P_T} \tag{16}$$

Also in this equation, g is the gravitational acceleration, d is the depth at the mouth of the estuary and K_0 and K_1 are constants. For salinity at the estuary mouth C_0, Van der Burgh found the empirical relationship:

$$\bar{\bar{c}}_0 = c_z \, exp(-K_2 \cdot \alpha) \tag{17}$$

He concluded, from prototype measurements in the Rotterdam Waterway, that $0.5 < K_2 < 1.0$, while in his method he applies a value of K_2 equal to 0.5. He further uses a value of $K_0 = 26$ and $K_1 = 0.9$ (see Figs. 3, 4 and 5).
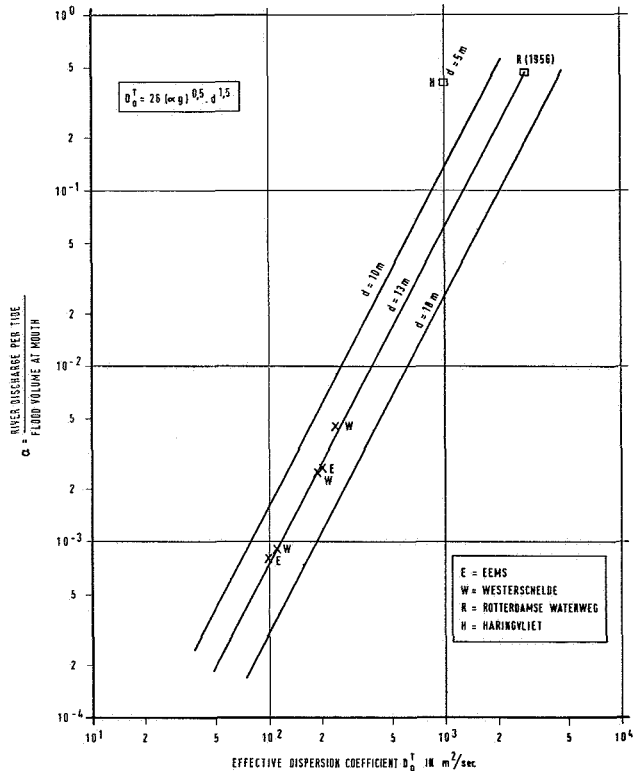

Figure 3. Effective dispersion coefficient in river mouth as function of flood number and depth in river mouth (from lit. 3, fig. 60).

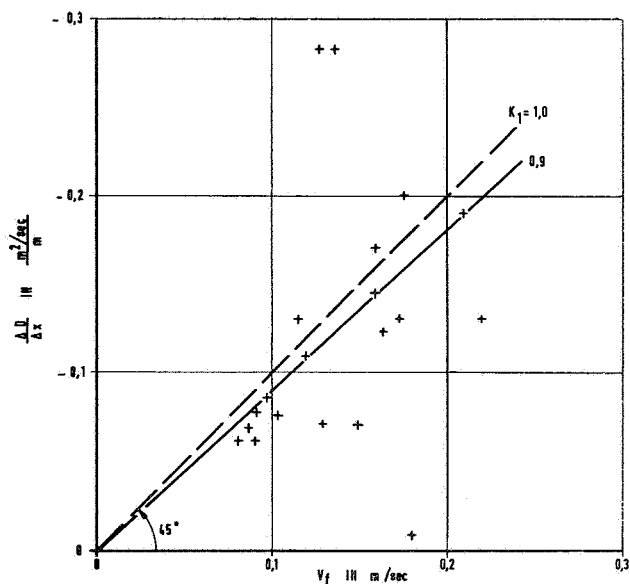Figure 4. Reduction of dispersion coefficient in x-direction as function of velocity of river discharge from (lit. 3, fig. 56).
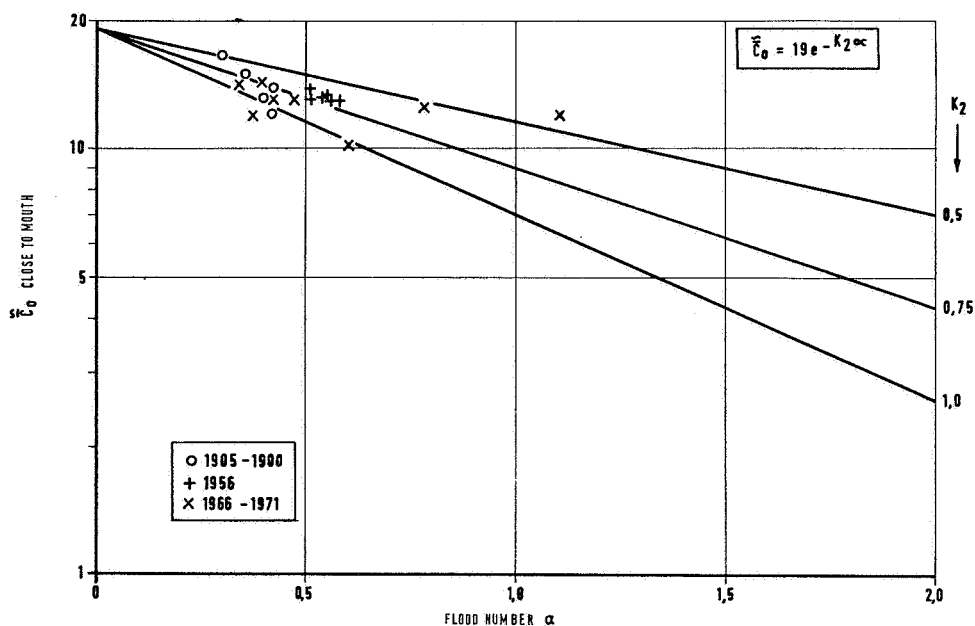

Figure 5. Average salinity in river mouth as function of flood number (from lit. 3, fig. 57).

One important advantage of Van der Burgh's method is that the cross-sectional area can be introduced as a function of x. Against this there is however the fact that the

method is based solely on prototype observations, where it is of course not possible to vary the magnitudes in a systematic manner in order to find the constants needed. Thus, the constant K_0 is based on observations for which $\alpha < 0.5$, K_1 on observations for which $V_f < 0.2$ m/sec, and K_2 on observations where $\alpha < 1.0$. Extrapolations beyond the limits just quoted must, in principle, been seen as dangerous.

3.3 Schönfeld & Van Dam method

Van Dam and Schönfeld [8] offer in their paper a method for calculating salt distribution in estuaries in stationary and non-stationary states. They work from a salt content averaged over a tidal cycle. The steady-state model thus has the same starting-point as the Van der Burgh method. Additionally, an analytical solution of equation (5) is given for stationary conditions, when a point source is present in the estuary. This makes it possible also to use the model for studying problems of pollution affecting the surface water.

In the context of salinity movement, however, the non-stationary model is more important. This model, too, works from salt-content values averaged over a tidal cycle, and should therefore be looked at as a quasi-non-stationary model. The basic equation for the model hence comes from averaging equation (1) over a tidal period:

$$\tilde{A} \frac{\delta \tilde{\tilde{c}}}{\delta t} = \frac{\delta}{\delta x} (Q_f \cdot \tilde{\tilde{c}}) + \frac{\delta}{\delta x} \left(\tilde{A} \cdot D_X^T \frac{\delta \tilde{\tilde{c}}}{\delta x} \right) \tag{18}$$

This equation is solved numerically; Eggink [7] gives some idea of the difference scheme used for this. The model assumes non-time-dependent effective dispersion coefficients. Taking this starting-point means that the model cannot yield information any more detailed than average values over an average mixing-length in the estuary. The model can also be used only when

a the diffusion system being studied is large compared to the dominant 'mixing-length', which is equivalent to about one-half the distance covered by a water particle during one tidal period, and

b the concentrations and data derived from them are based on observations averaged over distances at least equal to the 'mixing-length'.

This means that the model cannot be used if there are steep gradients caused by high resultant velocities, such as will be the case with high river discharge rates.

It is sufficient, for many applications, to consider time-averages over one or more tidal periods, and this makes it possible, in principle, to satisfy the conditions mentioned earlier. The model is used in this way for two Dutch estuaries, those of the Wester-schelde and the Eems (see Fig. 6). These estuaries have low river discharge rates and a large tidal capacity, so that a state of equilibrium will seldom be reached. Typical times for reaching a new steady state after, for example, a wet period are about 6 months for
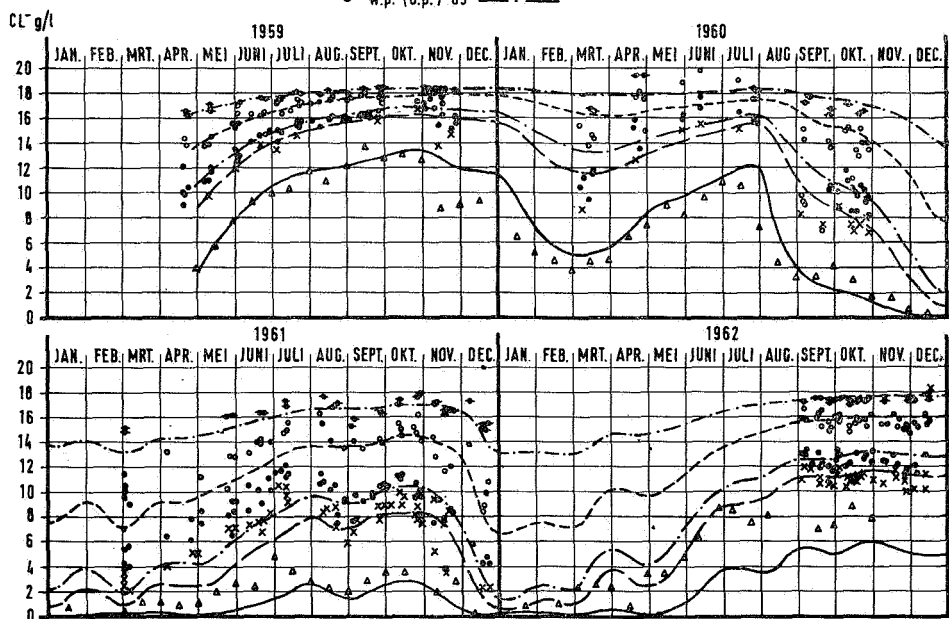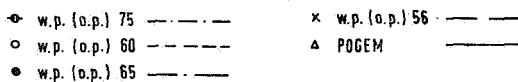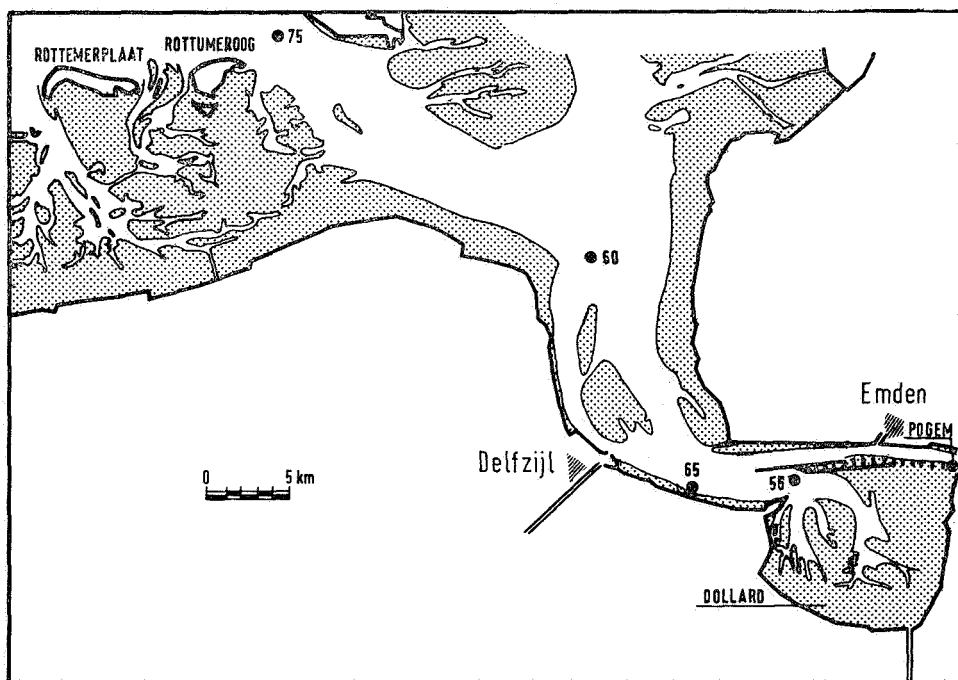
Figure 6. Chlorosity-distribution in the Eems-estuary according to measurements and the Schön-feld-van Dam method.

the Eems and 1–2 years for the Westerschelde. The effective dispersion coefficients in these estuaries are arrived at using actual 'on-site' measurements over a period of several years. Since equilibrium states virtually never occur in the estuaries, the dispersion coefficients are arrived at by applying the model in a numerical iteration process on a computer.

The deviations that remain are, in the case of the Westerschelde, erratic in nature because of variations in wind and tide and a quite large measure of uncertainty in respect of river discharge data. In the case of the Eems estuary there is a clear distinction to be made between D_X^T values that apply to dry periods and values for wet periods (see Fig. 7). The authors believe that these regular deviations are not ascribable solely to high rates of river discharge. During wet periods there are, in general, more frequently water levels above the average, wide variations in water level due to storms, and turbulence caused directly by the effects of wind. These phenomena may be the reason for the greater dispersion noted; this conclusion clashes, however, with the empirical findings of Van der Burgh, who does see there to be a clear dependence, apparent from equations (14) and (15).
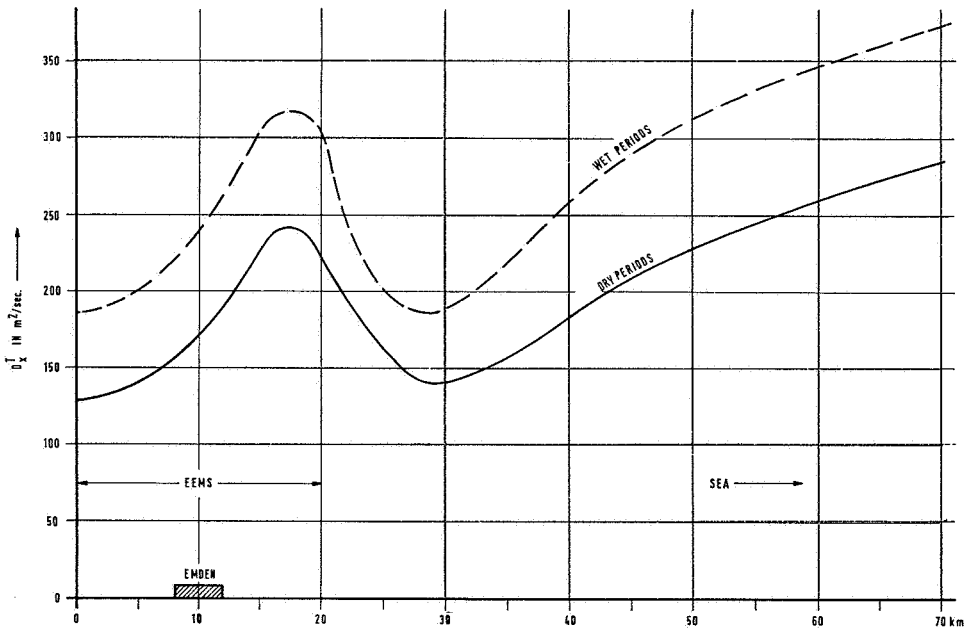

Figure 7. Effective values of dispersion coefficient according to Eggink (from lit. 8, slide 7).

4 Non-stationary models

Non-stationary models make it possible to describe salinity movement in the estuary where there is no steady state. They therefore offer simultaneously a solution for the movement equation for water, the continuity equation for water and the diffusion equation for salt. These equations take the following form:
Movement equation:

$$\frac{\delta Q}{\delta t} + \overline{U}\frac{\delta Q}{\delta x} + Q\frac{\delta \overline{U}}{\delta x} + g\frac{\delta h}{\delta x} \cdot A + g\frac{A.h.}{\bar{\rho}}\frac{\delta \bar{\rho}}{\delta x} +$$

$$+ g\frac{Q|Q|}{AC^2 R} = 0 \tag{16}$$

Continuity equation:

$$b. \quad \frac{\delta h}{\delta t} + \frac{\delta Q}{\delta x} - q = 0 \tag{17}$$

Diffusion equation:

$$\frac{\delta(A \cdot \bar{\rho})}{\delta t} + \frac{\delta(Q\bar{\rho})}{\delta x} = \frac{\delta}{\delta x}\left(D \cdot A\frac{\delta \bar{\rho}}{\delta x}\right) \tag{18}$$

Here $\bar{\rho}$ is the water density, R is the hydraulic radius, C the Chezy resistance coefficient, A the cross-sectional area, and q the lateral inflow into the river. The water density can be arrived at from the salinity, using:

$$\bar{\rho} = 0.75\,\overline{C} + 1000 \text{ (in kg/m}^3) \tag{19}$$

The problem just mentioned demands a numerical approach, as the equations involved cannot be solved analytically. For this reason the use of a computer is essential. With non-stationary models the same problem arises, when finding the boundary conditions for the salt content and the size of the dispersion coefficient, as with the stationary models.

4.1 Stigter & Siemons method

Stigter and Siemons [4] have developed a model for calculating water movement and

longitudinal saline intrusion by applying a numerical model that solves simultaneously the three differential equations considered earlier. In this model the water level and the average salinity at the estuary mouth ($x = 0$) and on the river side ($x = L$) have to be shown as boundary conditions.

Using their model Stigter and Siemons provide an insight into the effect of density currents on the size of the dispersion coefficient in partially-mixed estuaries. Analysis of measurements taken in the Rotterdam Waterway showed a clear difference to exist between 'apparent' dispersive transport, calculated by means of equation (18), and turbulent diffusive transport. This further demonstrated that the effect of density currents in partially-mixed estuaries has to be expressed through the size of the dispersion coefficient.

Stigter and Siemons subsequently applied their model to the results of the flume study by Ippen and Harleman, and to the Rotterdam Waterway. The size of the dispersion coefficient was found experimentally, strating from the assumption that D is a function only of x and not of t, with the following form:

$$D_x = D_0 \left(1 - \frac{x}{L} \right)^3 \tag{20}$$

By using the trial-and-error principle, $D_0 = 0.25 \ \text{m}^2/\text{sec}$ was found for the flume experiment, while to obtain a match with the measurements taken in the Rotterdam Waterway D_0 had to be taken as 1200 m²/sec. There is, however, no reason to suppose that these values are generally valid.

The Stigter & Siemons model must thus be regarded as one for analysis, not for forecasting. To make the model generally applicable for the purpose of providing forecasts methods would need to be developed that would allow a prediction of salinity in the estuary mouth and of the size of the dispersion coefficient. The Thatcher and Harleman method, which we shall consider next, goes a substantial way towards doing this.

4.2 Thatcher and Harleman method

Thatcher and Harleman [5], like Stigter and Siemons, apply a finite difference method to the basic equations set out in the introduction to this chapter. In a numerical scheme of this kind small steps are taken in the x direction (Δx) and time (Δt). It is usual, im order to be able to apply the finite difference scheme, to use a simplified version of the diffusion equation. For this it can be assumed that within steps Δx and Δt the cross-sectional area, the current velocity and the dispersion coefficient are constant, as a result of which (18) becomes:

$$\frac{\delta \bar{c}}{\delta t} + \bar{U} \frac{\delta \bar{c}}{\delta x} = D \frac{\delta^2 \bar{c}}{\delta x^2} \tag{21}$$

The value for $\overline{U}$ needed in this equation follows from the numerical solution of equation (16) and (17), while the value for D is obtained with the help of the results of the parametric studies to be discussed later.

Thatcher and Harleman assumed that in the saline part of partially-mixed estuaries the coefficient of dispersion is closely linked with the circulation generated by density differences. In a one-dimensional model this circulation is not directly apparent through the averaging over the cross-sectional area that is carried out. One may expect that this circulation will be greatest in areas with the greatest longitudinal saline gradient $\delta\bar{c}/\delta x$. Thatcher and Harleman thus take the dispersion coefficient to be dependent on this gradient, in the following equation:

$$D(x,t) = K \left[\frac{\delta\overset{\circ}{c}}{\delta\overset{\circ}{x}} \right] + D_G \tag{22}$$

where $\overset{\circ}{c} = \bar{c}/\bar{c}_z$ and $\overset{\circ}{x} = x/L$, L being the length of the estuary; D_G is the dispersion coefficient applicable to complete mixing.

The term $K \cdot \delta\overset{\circ}{c}/\delta\overset{\circ}{x}$ provides for additional dispersion in the area with saline intrusion. The parameter K, with the dimension of the dispersion coefficient ($l^2 t^{-1}$), is taken to be independent of x and t, yet to depend only on the degree of stratification in the estuary. Thatcher and Harleman verified this assumption by means of the model tests mentioned in chapter 3.1 above, working on the basis of an average salinity over a tidal period with a steady state (see Fig. 8).

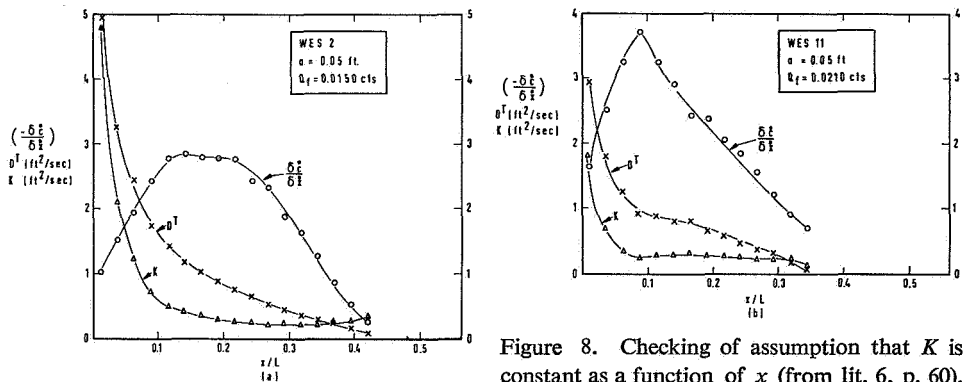Figure 8. Checking of assumption that K is constant as a function of x (from lit. 6, p. 60).

The final term in equation (22), the dispersion coefficient in the mixed part of the estuary or the freshwater area, can be described by means of current and geometrical parameters. Harleman [6] found the following relationship:

$$D_G = 77 \cdot N \cdot \overline{U} \cdot R^{5/6} \left[ft^2/\text{sec} \right] \tag{23}$$

58

where $\overline{U}$ and R are functions of x and t, while N represents Manning's coefficient of roughness.

Thatcher and Harleman assumed the dispersion parameter K to be dependent on the degree of stratification in the estuary. According to these authors, the degree of stratification can be indicated better by the internal estuary number than by the estuary number E as defined by Harleman and Abraham. The internal estuary number E_i is defined as

$$E_i = \frac{P_T \cdot F_i^2}{Q_f \cdot T} \tag{24}$$

Here, F_i is the internal Froude number, defined as

$$F_i = \overline{U}_0 / \sqrt{g \cdot d \Delta \bar{\rho} / \bar{\rho}} \tag{25}$$

where $\Delta \bar{\rho}$ is the change in density over the whole length of the estuary.

Proceeding from equation (5), we get for the dispersion coefficient

$$D^T = V_f \cdot \frac{\bar{c}}{d\bar{c}/dx} \tag{26}$$

Taking into account also equation (22), we arrive at the following equation for K, with a steady state and salinity averaged over a tidal period:

$$K = V_f L \cdot \frac{\overset{\circ}{c}}{(d\overset{\circ}{c}/d\overset{\circ}{x})} \tag{27}$$

We find from equation (27) that $K / V_f \cdot L$ gives a dimensionless reproduction of the salinity distribution under the circumstances set out above. Within the tidal movement $K / (\overline{U}_0 \cdot L)$ is a corresponding form, so that this dimensionless parameter correlates to the internal estuary number.

Thatcher and Harleman, analyzing numerous model tests and actual measurements, deduced the following relationship between the two parameters (see Fig. 9):

$$\frac{K}{U_0 \cdot L} = 0{,}002 \, E_i^{-\frac{1}{4}} \tag{28}$$

This results in the following equation for finding the coefficient of dispersion in $ft^2/\sec$:

$$D(x, t) = 0{,}002 \, \overline{U}_0 \cdot L \cdot E_i^{-\frac{1}{4}} \left| \frac{\delta \overset{\circ}{c}}{\delta \overset{\circ}{x}} \right| + 77N \cdot \overline{U} \cdot R^{5/6} \tag{29}$$
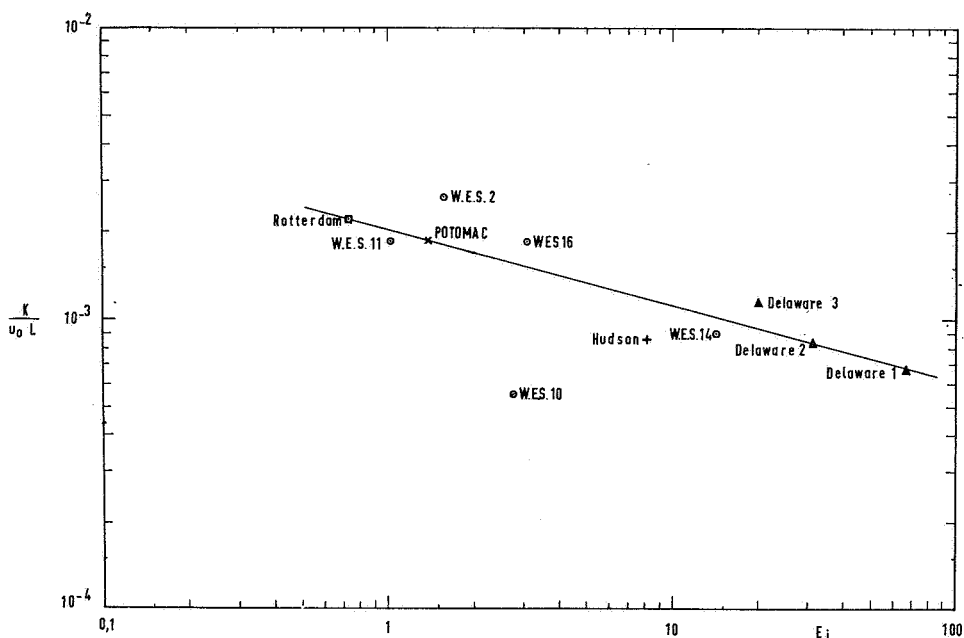
Figure 9. Correlation of dispersion parameter K with internal estuary number (from lit. 5, p. 104).

The boundary values for calculating the tidal movement are simple to specify; this is not however the case for the boundary value of salinity in the river mouth. This is due to the fact that the salinity in the river mouth is affected by the outflowing river water and the salt content of the seawater, which is not always present in the river mouth.

Thatcher and Harleman therefore divide a tidal cycle into two — a flood part and an ebb part. During the flood the salinity in the river mouth is assessed at the same level as in seawater c_z. During the ebb the boundary values are calculated by mass-balancing in the most sea-ward element at the magnitude Δx. Both advection and diffusion transport must be included in this balance.

During the ebb, salinity in the river mouth will as a result drop below c_z. When the flood starts the salt content cannot rise immediately to c_z, and for this reason a linear interpolation to c_z is made over a period of $^1/_{20} \cdot T$ before the turn of the tide. Thatcher and Harleman's way of handling boundary values is likely to present problems if the model is being used for forecasting purposes. This will be the case if the salinity in the river mouth during the flood is still affected by the water that has reached it from the river. They give an example of this kind in the River Hudson, where it was found impossible to put the boundary value for salinity sufficiently sea-wards. Here, it proved necessary to interpolate linearly from low-water slack and over a period of $^2/_5 T$, in order to estimate the actual salinity trend (see Fig. 10). An important advantage of the Thatcher and Harleman method is, however, that the

60

salinity trend in the estuary can be calculated against time. Stationary models succeed in doing this only to a limited extent.
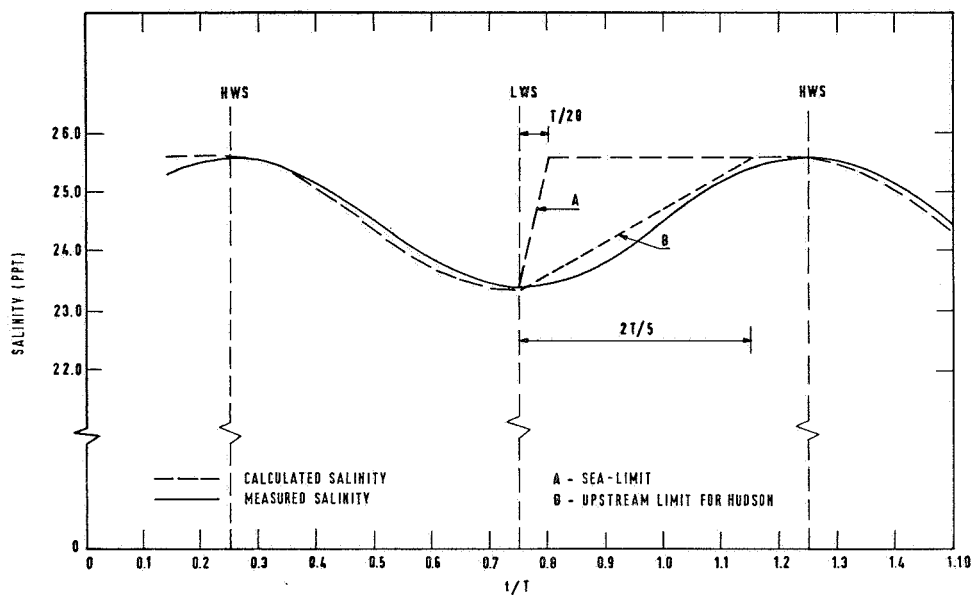

Figure 10. Reproduction of boundary values for salinity in mouth of Hudson estuary (from lit. 5, p. 181).

5 Checking stationary models by means of systematic physical model studies

The Hydraulics Laboratory has, using a tidal flume, carried out systematic research into salinity intrusion with varying boundary and flow conditions (lit. 7). The one-dimensional stationary models set out in Chapter 3 were checked against the results from the tidal flume; the work was carried out by M. Karelse, of the Delft Hydraulics Laboratory. Parts of this research work will be discussed in the chapters that follow, though without invariably adopting the same interpretation as Karelse.

When comparing the tidal flume results with the models mentioned above, it must be borne in mind that these models are, in principle, valid only for a well-mixed estuary yet are being applied also to the partially-mixed estuary. The effect of circulation currents generated by density differences is allowed for through the dispersion coefficient. These models may not, however, be applied to stratified flow. For this reason the tests carried out in the tidal flume are grouped in classes, on the basis of the estuary number E (defined earlier) and the flood number α.

Class A; stratified flow, which occurs when the volume of fresh water flowing out to sea during a tidal period is of the same order of magnitude as the flood volume, so that there is a quite sharp interface between the salt-water and freshwater layers:

$$E < 0.005$$

$$\alpha \geqslant 1.0$$

Class B; partially-mixed flow, which occurs when there is an interface between salt water and fresh water, but this is not clearcut:

$$0.005 < E < 0.2$$

$$0.1 \quad < \alpha < 1.0$$

Class C; mixed flow, which occurs when the volume of fresh water flowing out to sea during a tidal period is very small compared to the flood volume, and there is no interface:

$$E > 0.2$$

$$\alpha < 0.1$$

The majority of the tests carried out belong to Class B, so this class is subdivided into:

Class BA $0.005 < E < 0.02$

Class BB $0.02\ \ < E < 0.05$

Class BC $0.05\ \ < E < 0.2$

Table 1 gives a survey of the tests carried out during the tidal flume study, with their classification.

5.1 Checking of Ippen & Harleman stationary model

For the tests carried out in the tidal flume during the systematic study, the parameters B and D_0 were obtained from the measured salinity distribution at the moment of
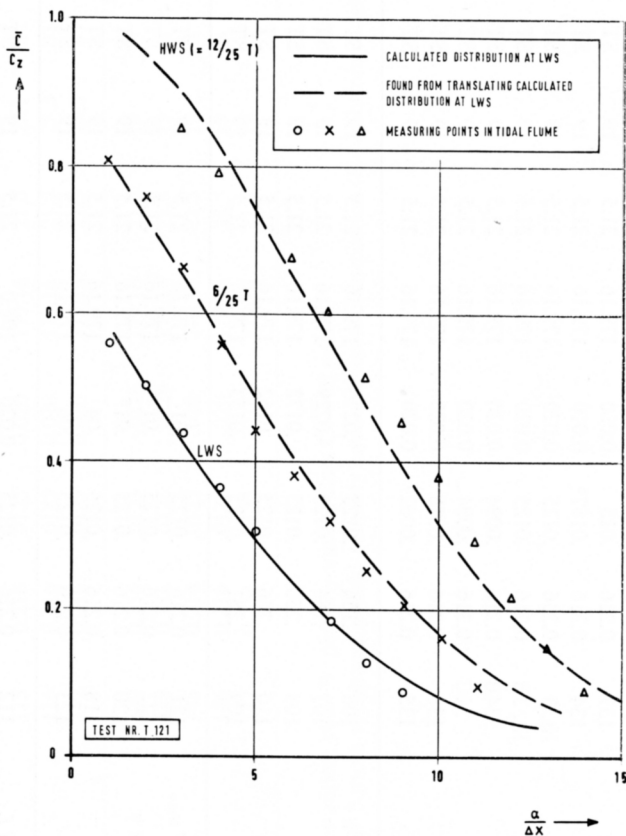

Figure 11. One-dimensional Ippen & Harleman model. Comparison of measured and calculated salinity distribution (from lit. 7, Fig 32).

Table 1. Survey of tidal flume tests (from lit. 9).

	test	h (m)	a (m)	u_{riv} (m/sec)	L (m)	$\varepsilon = \dfrac{\Delta\rho}{\rho}$ ‰	C m³/sec	type of roughness	u_0	α	E	class[1]
variation of a	136	0.216	.0375	0.020	179.16	21.5	19	ST	.249	.29	.099	BC
	137	0.216	.025	0.020	179.16	21.5	19	ST	.196	.38	.047	BB
	134	0.216	.0187⁵	0.010	179.16	21.5	19	ST	.168	.47	.028	BB
	lit. 3	0.216	.0125	0.020	179.16	21.5	19	ST	.121	.71	.009⁵	BA
	lit. 3B	0.216	.0125	0.020	179.16	21.5	19	ST	.129	.64	.012	BA
	34B	0.216	.0094	0.020	179.16	21.5	19	ST	.100	.91	.005	BA
	34C	0.216	.0094	0.020	179.16	21.5	19	ST	.103	.87	.006	BA
	138	0.216	.0078	0.020	179.16	21.5	19	ST	.097	.95	<.005	A
	135	0.216	.0062⁵	0.020	179.16	21.5	19	ST	.088	>1.10	<.005	A
variation of h	106	.156	.0125	.0276	179.16	21.5	19	ST	.098	>1.59	<.005	A
	107	.188	.0125	.0229	179.16	21.5	19	ST	.112	.95	.007	BA
	108	.250	.0125	.0172	179.16	21.5	19	ST	.125	.55	.011	BA
	110	.266	.0125	.0162	179.16	21.5	19	ST	.136	.46	.015	BA
	109	.281	.0125	.0153	179.16	21.5	19	ST	.128	.45	.013	BA
variation of u_{riv}	121	0.216	.0125	.01	179.16	21.5	19	ST	.129	.28	.028	BB
	122	0.216	.0125	.01²⁵	179.16	21.5	19	ST	.132	.35	.023	BB
	120	0.216	.0125	.01⁵	179.16	21.5	19	ST	.130	.43	.018	BA
	118	0.216	.0125	.04	179.16	21.5	19	ST	.113	≫1	<.005	A
	123	0.216	.0125	.06	179.16	21.5	19	ST	.105	≫1	<.005	A
variation of L	112	0.216	.0125	0.020	106.0	21.5	19	ST	.084	1.19	<.005	A
	104	0.216	.0125	0.020	113.3	21.5	19	ST	.091	1.05	<.005	A
	103	0.216	.0125	0.020	135.3	21.5	19	ST	.110	.80	.007	A
	101	0.216	.0125	0.020	157.2	21.5	19	ST	.122	.69	.013	A
	102	0.216	.0125	0.020	201.1	21.5	19	ST	.107	.83	.006	BA
	105	0.216	.0125	0.020	252.3	21.5	19	ST	.088	1.11	<0.05	A
	111	0.216	.0125	0.020	303.5	21.5	19	ST	.069	1.66	<0.05	A

variation of ε												
	144	0.216	.0125	0.020	179.16	35.5	19	ST	.129	.64	.012	BA
	140	0.216	.0125	0.020	179.16	29.0	19	ST	.130	.63	.012	BA
	141	0.216	.0125	0.020	179.16	13.7	19	ST	.134	.61	.013	BA
variation of C												
	114	0.216	.0125	0.020	179.16	21.5	12.7	ST	.067	1.65	<.005	A
	113	0.216	.0125	0.020	179.16	21.5	15.8	ST	.106	.84	.006	BA
	115	0.216	.0125	0.020	179.16	21.5	22.1	ST	.142	.57	.016	BA
	116	0.216	.0125	0.020	179.16	21.5	25.3	ST	.169	.46	.029	BB
	117	0.216	.0125	0.020	179.16	21.5	28.5	ST	.190	.40	.042	BB
variation of h												
	149	0.156	.0125	.0276	179.16	21.5	19	B	.129	1.01	.010	(BA)[2]
	148	0.188	.0125	.0229	179.16	21.5	19	B	.140	.69	.015	(BA)
	145	0.216	.0125	.020	179.16	21.5	19	B	.145	.55	.017	(BA)
	146	0.216	.0125	.020	179.16	21.5	19	B	.146	.55	.018	(BA)
	147	0.234	.0125	.0184	179.16	21.5	19	B	.151	.47	.021	(BB)

[1] class A: stratified; class B: partially-mixed; class C: well mixed.

[2] Tests with bottom roughness should properly have a seperate classification (B = bottom roughness, ST = bar-roughness).

low-water slack and high-water slack, using a least-squares method. It was found that the magnitudes of the parameters calculated in this way were highly dependent on the number of measuring points taken into account. Finally, those values for the parameters were selected that allow as close an approximation as possible to the measured saline distribution.

Taking the parameters found in this way, the one-dimensional saline distribution was calculated for a number of points in time, for tests T 121 (Class BB) and T 145 (Class BA). Figure 11 shows an example of such a calculation where, starting from a calculated distribution at low-water slack, the distribution at other times is found by applying the principle that an observer moving with the tide at its own speed of $\bar{U}_T$ will see no change in the saline concentration. It was found, from these and other equations worked out, that the Ippen & Harleman model will permit a reasonably accurate description of saline distribution only for more mixed cases; the model fails in the case of stratified systems.

This proves also to be so when the parameters D_0 and B (obtained as described above) are incorporated into Ippen and Harleman's correlations between the estuary number E and the parameters $2\pi B/\bar{U}_0 T$ and $D_0^{LWS}/V_f B$. In Fig. 12 the parameters for LW slack found from the tidal flume study are shown in the correlations postulated by Ippen and Harleman.
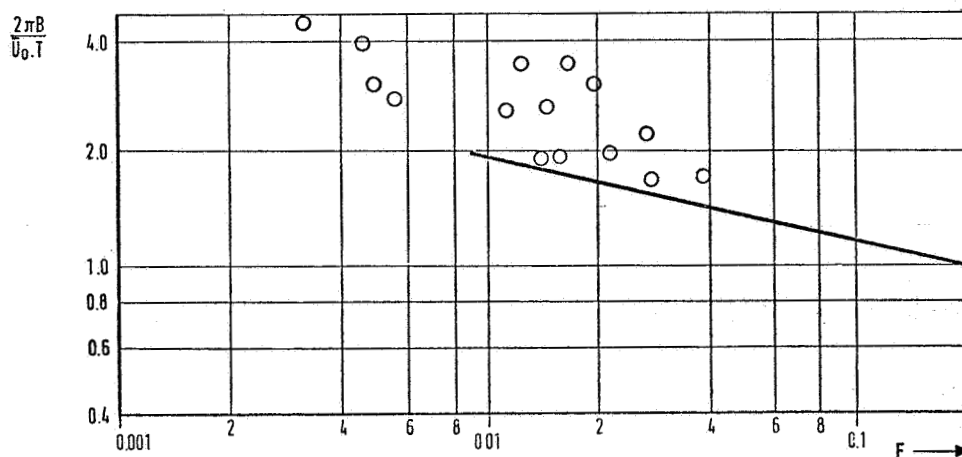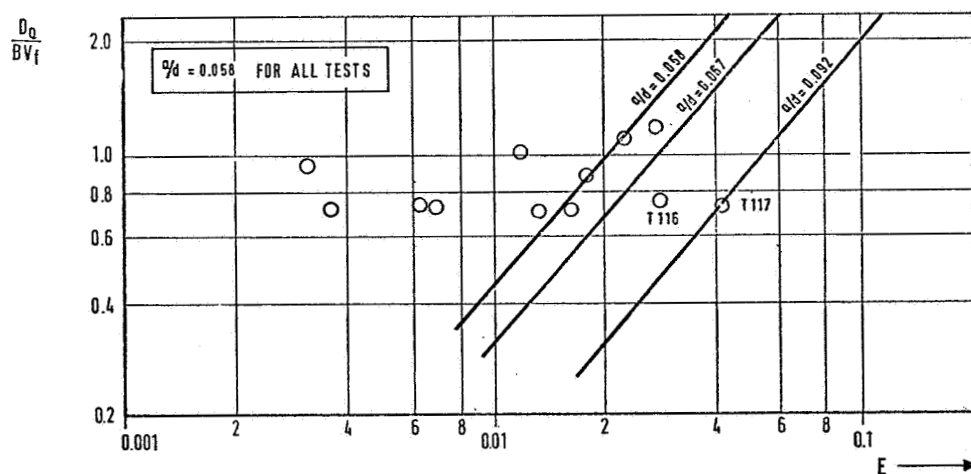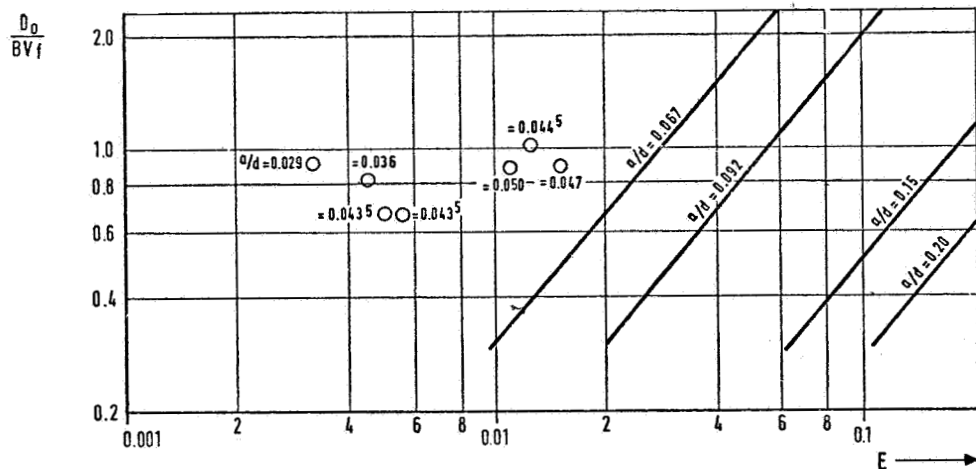
Comparison shows that the parameter relationships suggested by Ippen and Harleman do not match the results of the tidal flume study when looked at overall, $E < 0.02$, i.e. Class BA and A. There quite probably is a connexion between the parameters B and D_0 on the one hand and boundary conditions and flume parameters such as a, d, C, L, $\Delta\rho$ and Q_f on the other. It would be possible to identify these links via dimensional analysis, were it not for the fact that uncertainty in determining parameters B and D_0 makes it hardly likely that such an analysis would be successful.

Summing up, it can be said that the Ippen and Harleman one-dimensional model is, according to the tidal flume study, able to provide sufficiently accurate results only when the estuary number E is larger than 0.02 to 0.05. The Ippen Harleman model was, besides, designed on the basis of more mixed tests in the WES flume, so this conclusion should not occasion any surprise.

5.2   Checking the Van der Burgh stationary model

For the purposes of comparing the tidal flume results with the Van der Burgh method, the flume measurements were calculated back into prototype values; this was done in order to avoid scale effects. The scales involved are thus $n_x = {}^1\!/_{640}$, $n_z = {}^1\!/_{64}$, $n_u = {}^1\!/_8$

Figure 12.   One-dimensional Ippen & Harleman model. Correlation of parameters D_0 and B at low-water slack to estuary number E (processing of figs. 3.4, 3.5 and 3.6 in lit. 7). ▶

$\dfrac{D_0}{BV_f}$

2.0

1.0
0.8

0.6

0.4

0.2

$a/d=0.029$ $=0.036$ $=0.044^5$ $a/d=0.067$ $a/d=0.092$ $a/d=0.15$ $a/d=0.20$ $=0.050$ — $=0.047$ $=0.043^5$ ○○ $=0.043^5$

0.001   2   4   6   8   0.01   2   4   6   8   0.1   E ⟶

$\dfrac{D_0}{BV_f}$

2.0

1.0
0.8

0.6

0.4

0.2

$a/d = 0.058$ FOR ALL TESTS

$a/d=0.058$ $a/d=0.067$ $a/d=0.092$

T 116   T 117

0.001   2   4   6   8   0.01   2   4   6   8   0.1   E ⟶

$\dfrac{2\pi B}{U_0.T}$

4.0

2.0

1.0
0.8

0.6

0.4

0.001   2   4   6   8   0.01   2   4   6   8   0.1   E ⟶

○   RESULTS OF TIDAL FLUME STUDY   ——— CORRELATIONS ACCORDING HARLEMAN - ABRAHAM

67

and $n_c = 1$. Using the values thus arrived at, check calculations were carried out for the Van der Burgh model, in which the coefficients K_0, K_1 and K_2 have the magnitudes indicated in Chapter 3.2. The results of these calculations are seen in Table 2 in the form of an assessment of the extent to which the calculations approach the measured values. Figure 13 offers a comparison, in graph form, for a case where there is close similarity (T 121). In addition, Fig. 13 gives two examples where a match between the mathematical model and the tidal flume was found possible only by altering the parameters in the mathematical model.

Table 2. Checking Van der Burgh model against tidal flume tests.

test	fresh water discharge in m³/sec.	water-depth in m	remarks	flood-number	results of checking Van der Burgh model if the salinity in the rivermouth:	
					is calculated using eq (17)	is taken from tidal flume test
121	475	13.8	—	0.287	$\times$	$\times$
122	593	13.8	—	0.364	$\times$	$\times$
120	712	13.8	—	0.443	$\times$	$\times$
3	949	13.8	—	0.706	O/—	O/—
3 B	949	13.8	—	0.642	O/—	O/—
118	1898	13.8	—	2.53	—	—
123	2847	13.8	—	8.57	—	—
106	949	10.0	—	1.599	—	—
107	949	12.0	—	0.943	—	—
108	949	16.0	—	0.538	$\times$	$\times$
110	949	17.0	—	0.464	$\times$	$\times$
109	949	18.0	—	0.462	$\times$	$\times$
141	949	13.8	$\dfrac{\Delta\rho}{\rho} = 13.7^0/_{00}$		O	O
105	949	13.8	$L/L_R = 1.242$	1.110	O	$\times$
111	949	13.8	$L/L_R = 1.494$	1.697	O	$\times$
117	949	13.8	$C = 90\,\mathrm{m}^{\frac{1}{2}}/s$	0.395	—	—
136	949	13.8	$2a = 4.8\,\mathrm{m}$	0.342	—	—
145	949	13.8	bottomroughness	0.608	—	—
147	949	15.0	bottomroughness	0.473	—	—

$\times$ = good approximation,
O = unsufficient approximation,
—— = bad approximation.

Closer analysis of the comparison shown in Table 2 reveals that the Van der Burgh model produces strikingly good results when the flood number α is smaller than 0.5 ($E > 0.01$), although the tidal amplitude in the river mouth must then correspond
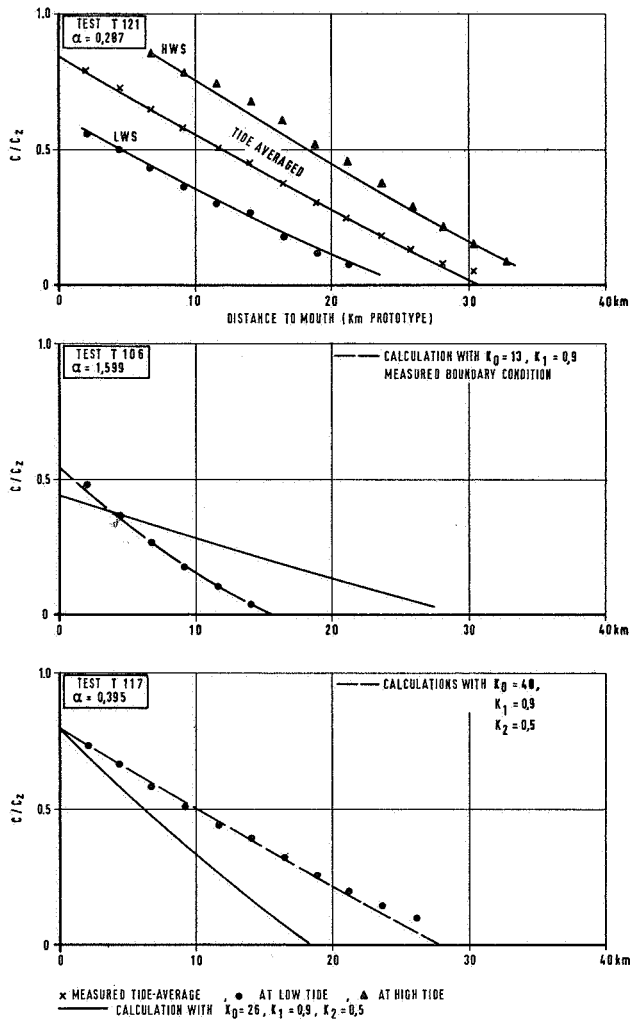
Figure 13. One-dimensional Van der Burgh model, measured
and calculated salinity distributions (from lit. 7,
Figs. 5.1 and 5.2).

to an average value actually found in the Rotterdam Waterway. This means that at higher river discharge rates the match between the mathematical model and the tidal flume is lost. This can be put right by altering the parameters in the mathematical model ($K_0 \ll 26$ and, possibly, $K_1 > 0.9$).

When the water depth is reduced the Van der Burgh is again inadequate, although in the cases studied α also reached values greater than 0.5. It is therefore uncertain whether the poor match can be ascribed solely to the depth of water. The mathematical

model achieves good results again, however, if one takes $K_0 \ll 26$ and, possibly $K_1 > 0.9$, and in a few cases $K_2 < 0.5$.

Changes also have to be made in the parameters when there are variations in the tidal amplitude, the length of the estuary (i.e. the flume) and the bottom roughness.

The general conclusion that can be drawn from the foregoing is that — to judge from the results of the tidal flume study — the Van der Burgh model has a limited range of applicability. For forecasts outside this range to be possible using this model, it is necessary to determine relationships between the parameters K_0, K_1 and K_2 on the one hand and magnitudes such as α, a ,L/L_R and C on the other.

6 Checking stationary and non-stationary models against actual observations

6.1 Processing of measurements, and measuring method

The one-dimensional stationary models set out in Chapter 3 will be checked against actual measurements taken in the Rotterdam Waterway. This river lends itself particularly well to this, since over the years a great many measurements have been made of the salinity values, current velocities and water levels, using both vessels and fixed continuous-recording equipment. Among these, we may mention:

a   a programme in 1951–1959, as part of which water samples were taken at a large number of points, at high-water and low-water slack, from the bottom and from the surface along the centre-line of the channel.

b   a network of continuous-recording salinity meters that has been operating efficiently since the end of the 1960s, and which yields mainly data on salinity close to the surface; these instruments are generally sited on the bank, so that there is often no information for the deeper parts of the river cross-section.

Since in both these kinds of measurement there is an inadequate density of information as to place and/or time, simultaneous measurements of water and salinity movement were regularly made from vessels.

When checking stationary models, the estuary needs to be in a state of equilibrium at the moment of measurement. Since, however, tidal movement in the river mouth and the river discharge rate are constantly altering, such a steady state virtually never exists. This means that there has to be an approximation to a steady state, by manipulation of the observation data.

Working from equation (3.3), which forms the basis for the stationary models, it can be deduced that at a location x from the river mouth, in a state of equilibrium,

$$In \; \tilde{\tilde{c}} = In \; \tilde{\tilde{c}}_0 - \frac{x \, Q_f}{\tilde{A} \, D_X^T} \tag{30}$$

It is a natural step, therefore, to seek a correlation for $ln \, \tilde{\tilde{c}}$ and Q_f for high-water and low-water slack. The spread in these correlations will give an indication of the extent to which tidal movement, changes in river discharge, local wind effects and so on influence the movement of the salt water. From the correlations it is now possible, if there are enough observation points available, to work out the salinity trend at HW and LW slack in an imaginary equilibrium situation. Processing of this kind has
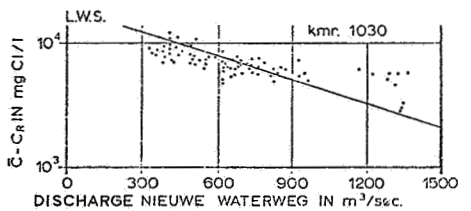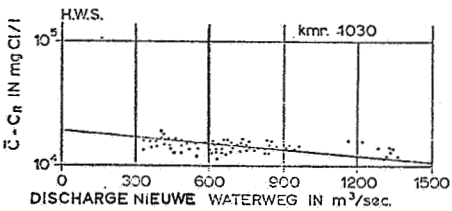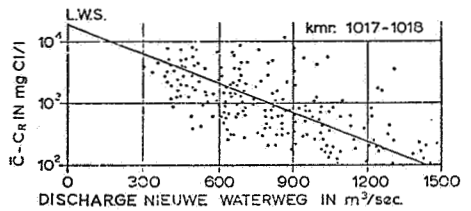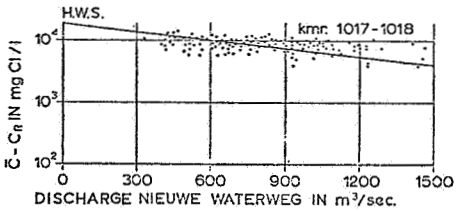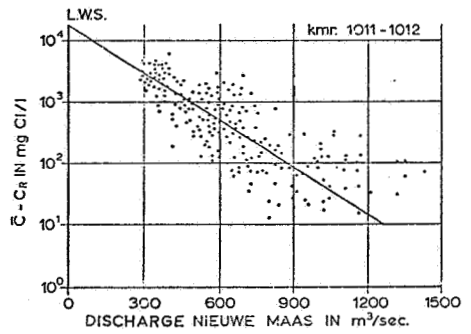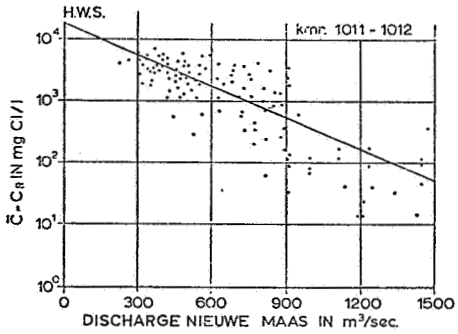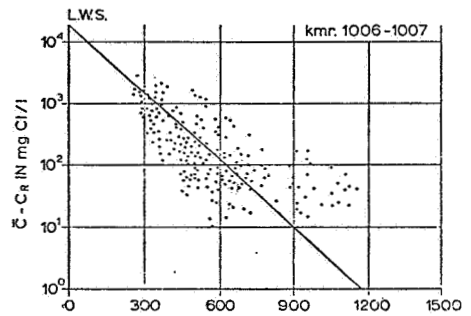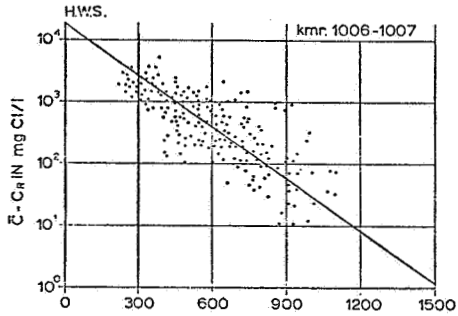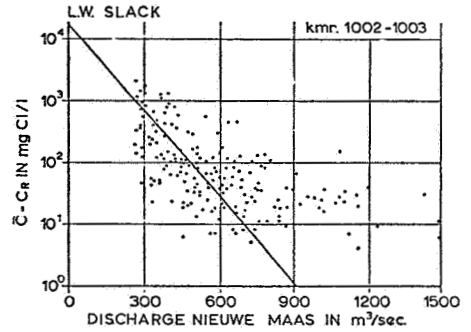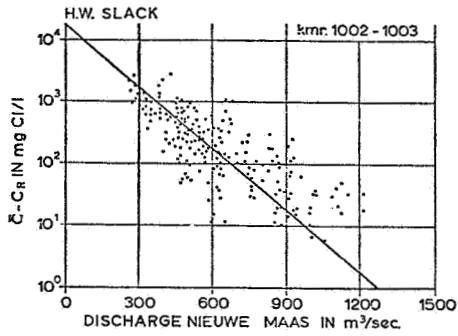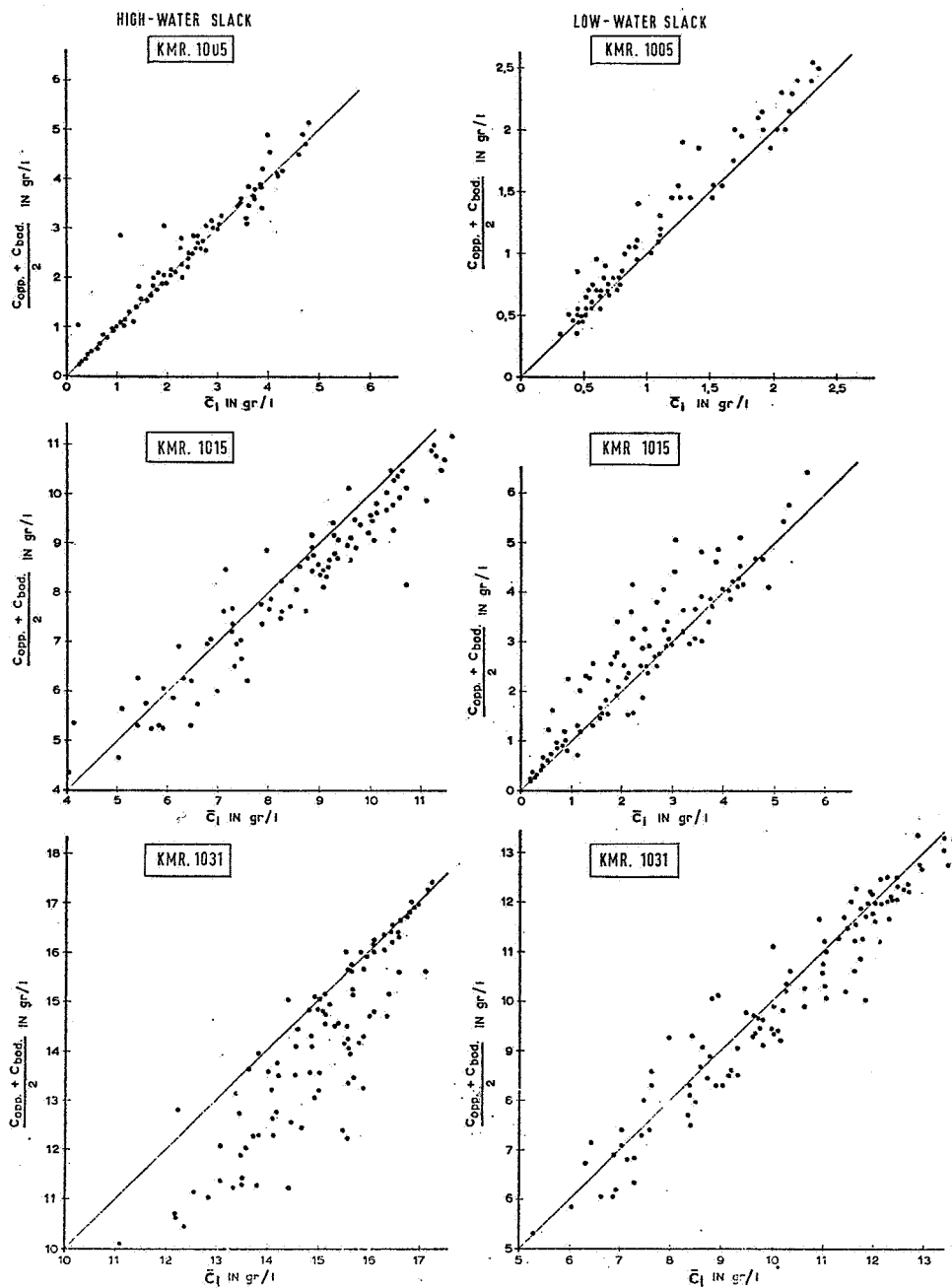
Figure 15.   Correlations between average chlorosity in a vertical and average of salinity at surface and bottom of Rotterdam Waterway.

Figure 14.   Correlation between the chlorosity at HW and LW-slack and the fresh water discharge ◄   of the Rotterdam Waterway.

been carried out on the measurements taken during the 1951–59 campaign in the Rotter-dam Waterway at a large number of measuring points (see Fig. 14). It is found that problems arise in interpreting the correlations at points where the sea exerts an influence in an occasional fashion. Less weight has to be given to these points, because the picture of correlation is incomplete in that observations where the sea does not reach the measuring-points do not appear in the correlation due to the fact that the starting-point is taken as $ln\ \tilde{\bar{c}}$.

In the foregoing we have passed over without comment the fact that in these measure-ments what was being measured is not $\bar{c}$ but salinity at the bottom and at the surface. A number of river measurements were carried out during the years 1963–1965 and examined by the Rotterdam Public Works Department; one objective was to arrive at a correlation between the magnitudes mentioned above (see lit. 10). This study showed that it can be assumed, with reasonable accuracy, that the average of the surface and bottom salinity is equal to $\bar{c}$. Using all the measurement data, km. 1031, 1015 and 1005 were found to have correlation coefficients of, respectively, 0.86, 0.96 and 0.99. As is seen from Fig. 15, however, there is not a linear correlation at all states of tide.

The results obtained from continuous-recording instruments lend themselves less well to such treatment, since they tell little about the deeper layers of water. These results need to be looked at in even closer connexion with simultaneous river measurements, and therefore are of more limited value for the checking described below. Simultane-ous river measurements, supplemented with data from continuous-recording instru-ments, will be used to check on the situation since the closing-off of the Haringvliet. We have given above methods by which the data observed from the Rotterdam Waterway can be put to use in checking stationary models. This however does not mean in the least that it would be advisable to carry out measurements in the way described. To be able to apply one-dimensional models in general, a non-observable value of $\bar{c}$ needs to be arrived at with a certain accuracy from point measurements along the river profile. Theoretically, the following integration is necessary for this:

$$\bar{c} = \frac{1}{A} \iint_A c(ij, z)\, dij \cdot dz \tag{31}$$

In practice this integral is approached by the summation of a number of verticals measured in the river profile:

$$\bar{c} = \frac{1}{A} \sum_{i=1}^{m} bi \cdot di \cdot \bar{c}i \tag{32}$$

where

$\bar{c}$ = calculated average salinity,
bi = width of the ith section in the river profile,

74

d_i = depth in the ith section,
$\bar{c}_i$ = average salinity in the ith vertical,
m = the number of sections or verticals.

The error that occurs when determining $\bar{c}$ is compounded from two components, viz.

a errors arising from measurement of the magnitudes b_i, d_i and the separate measurements of salinity needed to find $\bar{c}_i$, and
b approximation to the integral (31) by the summation (32).

The ISO (International Standards Organization) took an approach of this kind when determining discharge rates from velocity measurements (see lit. 11), and a similar approach is needed to find $\bar{c}$ from actual measurements. This will provide an idea of the degrees of accuracy that can be achieved in determining $\bar{c}$. To this end, specifically-selected measurements will need to be made from vessels so that the necessary statistical analysis can be undertaken.

As has already been found, there has to be a substantial density of information over time if stationary models are to be applied; and this is scarcely, if at all attainable with the type of measurements as carried out in the Rotterdam Waterway. If continuous-recording salinity meters would be used, it could be investigated:

a whether a vertical can be selected for which, with the least possible error, $\bar{c}_i = f(\bar{c})$;
b what number of points in this vertical need to be measured.

A consequence of applying this method will probably be that the achievable accuracy will be less than with the intensive measurement of the crosswise profile referred to earlier.

Looked at from the viewpoint of measurement technique, however, there could also be problems. If sampling from a vessel is decided upon, the location of the vertical on the crosswise profile is a free choice; when using continuous-recording equipment, however, there is usually no longer any freedom of choice (e.g. because of restrictions that may be imposed by shipping). Moreover, the network of measuring stations must be closeknit enough in the longitudinal direction to allow an accurate picture of the salinity distribution. Here reference must again be made to the problems encountered when determining the parameters in the Ippen and Harleman model from the results of the tidal flume study.

Where the Rotterdam Waterway is concerned, study must be concentrated on the aspects outlined above, so that a measuring network results that can serve several purposes. The financial consequences of this must certainly not be lost from view.

6.2 Checking the Ippen and Harleman stationary model

Harleman and Abraham [1] made an analysis of actual measurements in the Rotterdam Waterway carried out in 1908, 1956 and 1963. For the first two of these years

the Waterway came close to a constant crosswise profile; but this was not so in 1963, because of the construction of the access channel to the Europoort docks complex. The question is, therefore, whether the Ippen and Harleman model can be applied to the situation obtaining in 1963.

Since the estuary number is affected by the width-to-depth ratio at a constant crosswise profile, we need to define very closely how the estuary is to be represented diagrammatically. Harleman and Abraham represented the Waterway as a shallow, wide profile and a deep, relatively narrow profile, as set out in the following table:

	1908		1956		1963	
	profile I	profile II	profile I	profile II	profile I	profile II
d (m)	5.8	7.7	9.3	13.0	11.0	13.8
A (m²)	3600	3600	5300	5300	5900	5900

The authors give an extensive description of the available data and the way in which these are handled so as to be able to find the parameters in the Ippen and Harleman model. As shown in Fig. 16, there is a close match with the results of the flume study on which Ippen and Harleman based their model. An exception must be made for the measurements carried out in 1963, which it is found do not fit into the correlation between $2\pi B/\overline{U}_0 T$ and E. Harleman and Abraham further note that special attention must be paid to an estuary that splits up into several arms. The mathematical model is not in fact designed to allow calculation of the salinity intrusion into an estuary of this kind, at least when the intrusion passes the point at which it divides.

The Ippen and Harleman model is also proved against measurements carried out in the Rotterdam Waterway in the 1950s and 1970s (see also Chapter 6.1). Direct application of the model generally gives an unsatisfactory match between calculation and measurement (see Fig. 17). For this reason the parameters of the Ippen and Harleman model are computed afresh on the basis of the actual measurements made. These are shown in Fig. 16 in the correlations suggested by Harleman and Abraham. There is found to be a reasonable match in respect of the correlation between $2\pi B/\overline{U}_0 T$ and E. The match in the correlation between $D_0/V_f B$ and E is however insufficient, with the measurements from the 1950s providing the worst results.

Summing up, it can be said that the checks made using actual measurements do not contradict the conclusions of the tidal flume study. There is thus reason to assume that the Ippen and Harleman model is valid only when E is larger than 0.02–0.05. It must however be borne in mind here that the magnitudes B and D_0 can be found accurately only with difficulty, as the tidal flume and other studies have shown.

6.3 Checking the Van der Burgh stationary model

Checking of the Van der Burgh stationary model was based on measurements made
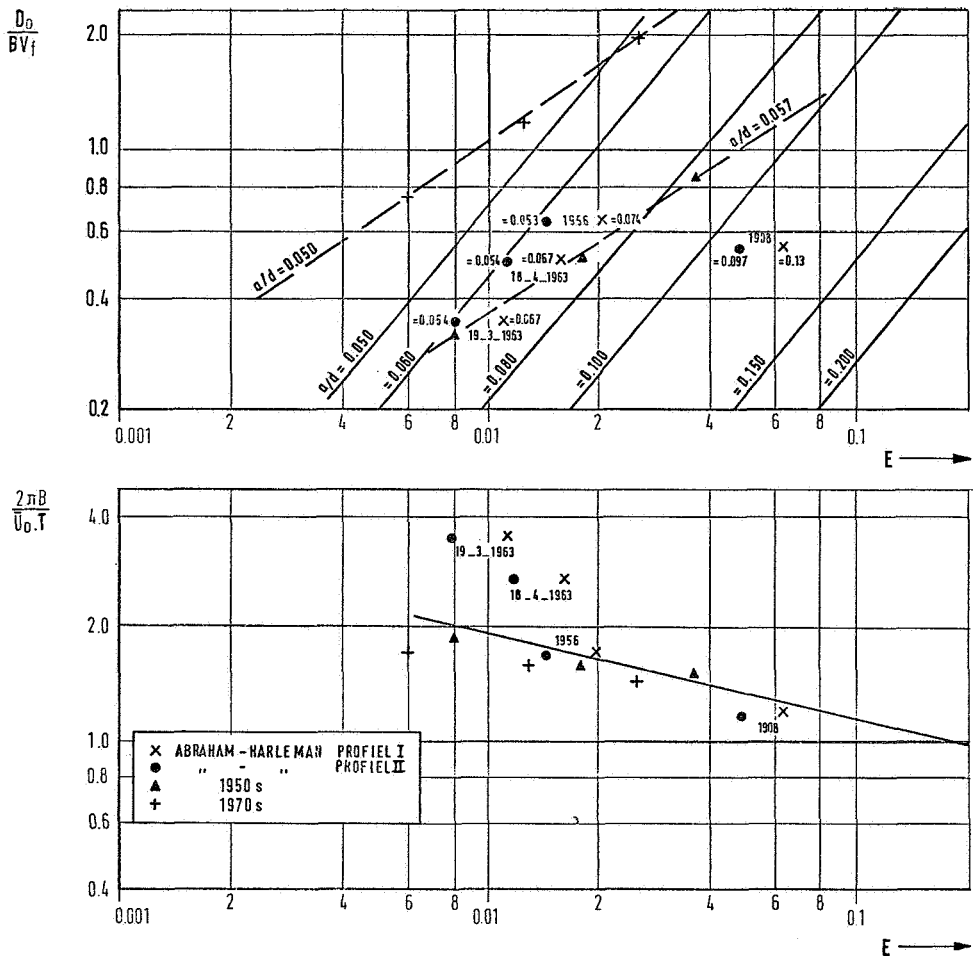
Figure 16. Checking Ippen & Harleman model against measurements taken in Rotterdam Waterway.

during the years 1950–1960 and 1971–1973, processed by the method described in Chapter 6.1. Attention was paid in the first place to the description given by Van der Burgh for the level of salinity in the river mouth (see equation 17). Van der Burgh noted a relatively wide spread in this relationship. Re-analysis of the measurements involved now shows that this spread can to a large extent be explained by salinity in the mouth of the Waterway being affected by the outflow from the Haringvliet. The measurements taken in 1971–1973 provide a clear indication of this, since during this period the discharge from the Haringvliet was very low (about 10 — 60 m³/sec). This is connected with the fact that the Haringvliet sluices were brought into operation on 2 November 1970, there then being little or no sluicing during periods of relatively low river discharge. Fig. 18 gives a picture of the realtionship between α and $\tilde{c}_0$, with
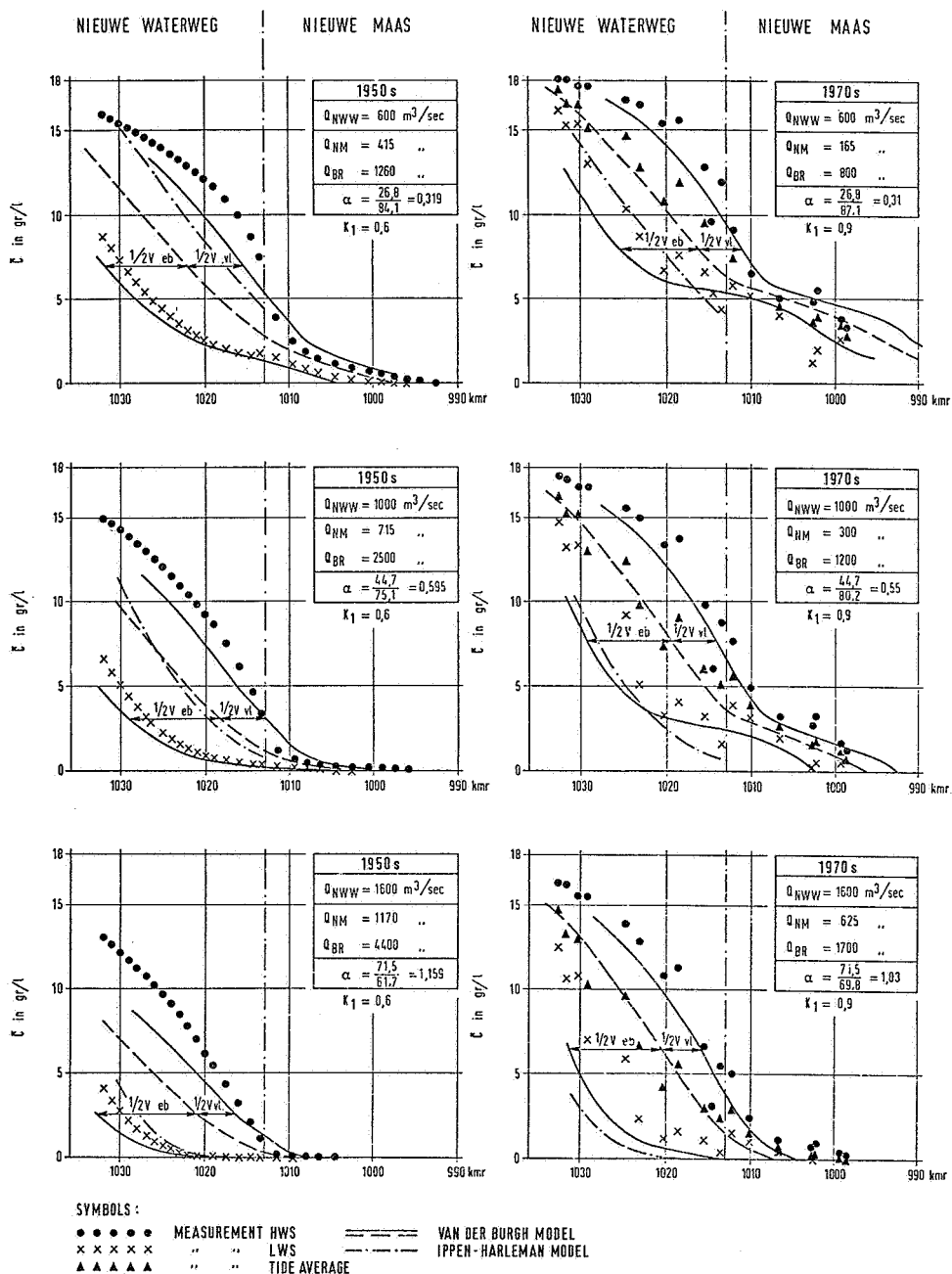
Figure 17. Checking Ippen & Harleman and Van der Burgh models against measurements taken in Rotterdam Waterway.

the discharge from the Haringvliet (Q_{HVL}) introduced as an extra parameter. All this leads to the following empirical equation:

$$\tilde{\bar{c}}_0 = c_z \cdot f(Q_{HVL}) \cdot \exp\left(-K_2 \cdot \alpha\right)$$

where

$$f(Q_{HVL}) = -0{,}00015 \cdot Q_{HVL} + 0{,}885$$

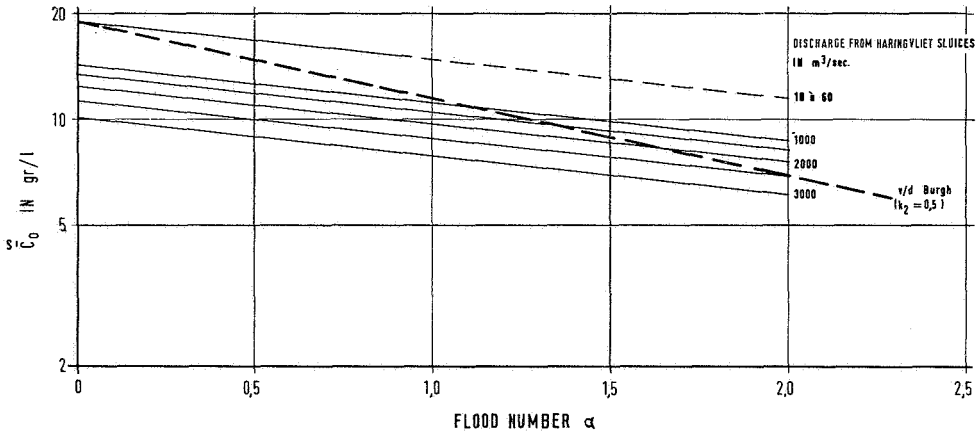$$(Q_{HVL} \geqslant 1000 \text{ m}^3/\text{sec}, K_2 = 0{,}25)$$

Figure 18. Boundary conditions for salinity in mouth of Waterway.

The above equation could be applied to an estuary without subsidiary arms by taking $Q_{HVL} = 0$. How far the resulting equation for $\bar{c}$ is generally valid has not been investigated.

Using the newly developed equation for $\tilde{\bar{c}}_0$, check calculations were made for the measurements referred to above. A distinction was made, in equilibrium states in the Rotterdam Waterway, with a number of discharge rates from this arm of the river (Fig. 17). It was found that for the measurements carried out in the 1970s there is in general a close similarity to the mathematical model. At higher discharge rates from the river, however, the calculated estimate of salt intrusion was too low. This means that coefficient K_1, for example, must be reduced.

For the measurements from the 1950s the similarity to the mathematical model is not sufficiently close, the model giving too low an estimate of intrusion. A sharp reduction in the coefficient K_1 to 0.6 is found to be necessary in order to bring the measurements and calculations into line with each other. This adaptation is needed despite the fact that the parameters in the model for the 1950s and 1970s do not differ greatly in magnitude. One reason might be that initial mixing can occur in the Rotterdam Water-

79

way because of docks, groins and so on. These additional factors affecting mixing were not identical in the 1950s and the 1970s.

6.4   Checking of the Thatcher and Harleman non-stationary model

Thatcher and Harleman based their non-stationary model on data from the flume study that was also used by Ippen and Harleman in constructing their model, and on measurements in the Rotterdam Waterway described in lit. 4. Data was also considered from three estuaries on the eastern seaboard of the United States, namely the Delaware, Potomac and Hudson. These estuaries were chosen since salinity distributions in them were available for a state of equilibrium. These various figures resulted in the relationship seen in Fig. 8 for the dispersion parameter K.

The model is designed for application to non-stationary conditions, where the saline distribution is continuously subject to changes with time. One of the difficulties encountered by Thatcher and Harleman in demonstrating the validity of their model is the lack of reliable 'on site' measurements. The authors chose the Delaware, Potomac and Hudson for checking the model against the prototype; there was a number of known series of measurements of the salinity at HW slack in these estuaries, although in the case of the Hudson the time of day of taking the measurements was not known. Thatcher and Harleman found a satisfactory correspondence between model and prototype, allowance being made for the limited opportunities offered by the actual measurements available.

As a typical example of this we may take the comparison with the Delaware, using measurements of surface salinity taken in 1932. Other studies showed that since the estuary is well-mixed the surface salinity provides a satisfactory yardstick for salinity averaged over the crosswise profile. Fig. 19 provides a comparison between calculated and measured salinity levels, for a period of 110 tidal cycles, demonstrating the close correspondence already mentioned. In this check the model was used purely as a forecasting model where, making use of the astronomical tidal movement in the river mouth, it was only found necessary (by means of actual measurements):

a   to find the salinity of the seawater (in the case in question 32 parts per thousand), and

b   to find the initial salinity distribution in the estuary as a starting condition for the calculation.

It was not necessary to adjust the parameters; at the end of each tidal period the internal estuary number E_i was calculated, and from this — with the help of equation (28) — the dispersion parameter K was found for the following tidal period.

It seems desirable, given the favourable results already obtained, to check the Thatcher and Harleman model more thoroughly against actual measurements. In doing so,

80

greater attention should be paid to the variations in salinity during a tidal cycle. Preparations for work along these lines are currently being made by the Public Works Department and the Delft Hydraulics Laboratory.
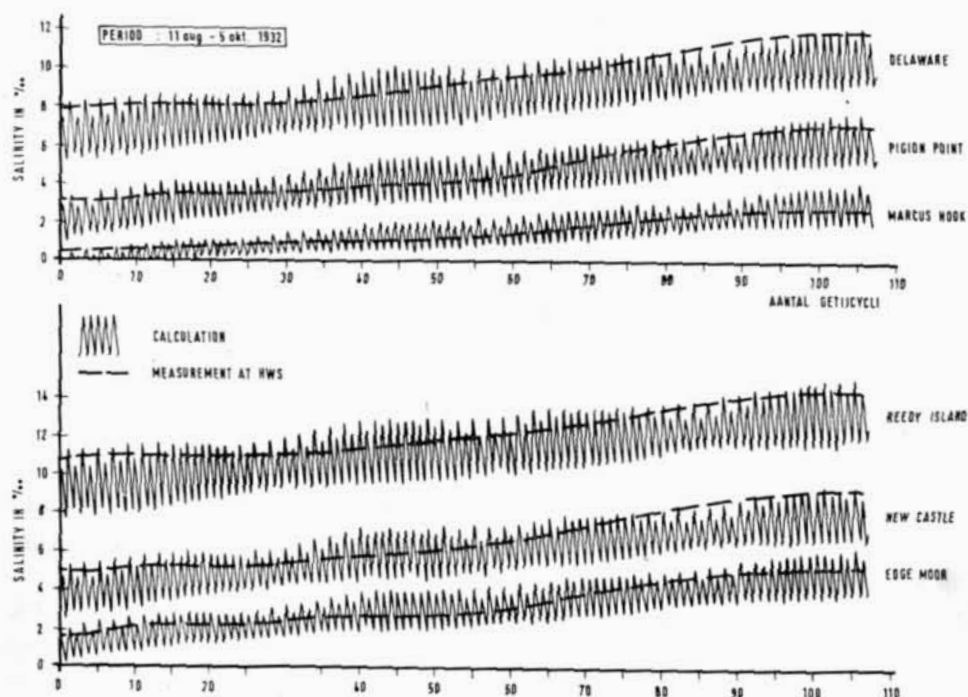

Figure 19. Checking Thatcher & Harleman model against prototype measurements.

7 Summary

1   The Ippen and Harleman model describes salinity distribution at low-water slack with a steady state in the estuary. The parameters in the model are obtained from laboratory studies. Salinity at other points in time can be found by translating the distribution at LW slack over the distance travelled by a particle of water.

2   Checking of the model against the tidal flume study carried out by the Delft Hydraulics Laboratory and against measurements taken in the Rotterdam Waterway suggest that the model is valid only for more mixed estuaries (with the estuary number E larger than 0.02–0.05).

3   The Ippen and Harleman model has the important limitation that it is valid for an estuary without subsidiary arms, that can be approximated by a constant cross-sectional area over the entire length.

4   The Van der Burgh model describes salinity distribution, averaged over the tide, with a steady state in the estuary. The parameters in the model are obtained from measurements in a number of Dutch estuaries. Salinity distribution at HW and LW slack can be arrived at by translating the distribution averaged over the tidal period along one-half of a flood or ebb distance, as the case may be.

5   Checking the model against the tidal flume study shows that the model yields strikingly good results with a vertical tidal movement in the river mouth, matching circumstances in the Netherlands, provided that the flood number α is less than about 0.5.

6   According to the tidal flume study the model is unsatisfactory if the tidal amplitude in the river mouth, the roughness of the bottom or wall, the length of the estuary or the salinity of the seawater are changed. In such cases the parameters of the model need to be adjusted. Systematic study of the way these parameters depend on flow and geometrical parameters appears desirable.

7   Checking the Van der Burgh model against measurements taken in the Rotterdam Waterway reveals a satisfactory match for the presentday situation, although not for the situation that existed in the 1950s. Alteration of the parameters was seen to be necessary, although in the opposite direction to that indicated by the flume study.

8   The reason for this contradiction can perhaps be found in the fact that Van der Burgh based his model on measured data where initial mixing due to docks, groins and so on is relatively large compared to that in the 1950s.

9   The Stigter and Siemons model describes salinity distribution in a non-stationary state. It is not, however, a forecasting model, since the boundary value for salinity in the mouth of the estuary has to be supplied. Moreover, the Chezy coefficient and the dispersion coefficient are found by trial and error.

10 The Thatcher and Harleman model is a forecasting model for salinity distribution in non-steady states. The model needs to be supplied with boundary values for river discharge, vertical tidal movement in the sea, salinity in the sea and initial values for salinity distribution in the estuary.

11 Further checking of the model against actual measurements is desirable, the necessary attention being directed towards salinity distribution during a tidal cycle.

12 The Van Dam and Schönfeld/Eggink model can act as a forecasting model in non-steady states, with respect to salinity levels averaged over one or more tidal periods. The effective dispersion coefficient in this model is assumed to be only a function of x. This assumption is probably true only in very well-mixed estuaries, and then the dispersion coefficient must be found experimentally on the basis of actual measurements.

13 Within the context of one-dimensional models, that of Thatcher and Harleman offers the best hopes for the future. Carefully-planned measurements on site need to be made for the proving and operational application of this model.

14 The salinity measurements to be carried out must start by making allowance for errors, in a way similar to the method developed by the ISO for determining discharge rates from velocity measurements. Where continuous-recording apparatus is concerned, a study should be made of whether it is possible, using a number of measuring points (to be determined) in a chosen vertical, to arrive at a sufficiently accurate approximation to the average salinity in the crosswise profile.

It should further be investigated how many measuring stations there need to be in the lengthwise direction in order to obtain a sufficiently accurate description of salinity distribution in the estuary.

Symbols used

c = salinity
$\bar{c}$ = salinity averaged over the flow profile
$\tilde{\bar{c}}$ = salinity averaged over flow profile and tidal cycle
$\overset{\circ}{c}$ = relative salinity $\bar{C}$ as against seawater salinity c_z
c_z = salinity of seawater
$\bar{\rho}$ = density averaged over the flow profile
$\Delta\rho$ = difference in density between freshwater and seawater
x = Cartesian coordinate in horizontal direction along axis of river
y = Cartesian coordinate in horizontal direction perpendicular to axis of river
z = Cartesian coordinate in vertical direction
d = depth
a = amplitude of vertical tidal movement
h = water level
R = hydraulic radius
B = distance from river mouth at which seawater salinity is present
L = length of estuary
L_R = resonance length of estuary
A = cross-sectional area
N = Manning's coefficient of roughness
U = velocity in x direction
V = velocity in y direction
W = velocity in z direction
$\bar{U}$ = velocity in x direction, averaged over flow profile
$\bar{U}_0$ = maximum flow velocity at flood in river mouth
V_f = flow velocity as result of river discharge
$\bar{U}_T$ = flow velocity as result of tidal movement
Q_f = river discharge
Q = discharge
P_T = flood volume in river mouth
D = dispersion coefficient
D^T = dispersion coefficient with averaging over a tidal period
D^{LWK} = dispersion coefficient at low-water slack
D_G = dispersion coefficient in area with complete mixing
K = dispersion parameter
F = Froude number
E = estuary number

84

F_i = internal Froude number
E_i = internal estuary number
α = flood number

Literature

[1] D. R. F. HARLEMAN AND G. ABRAHAM, One-dimensional analysis of salinity intrusion in the Rotterdam Waterway, Delft Hydraulics Laboratory Publication 44, October 1966.

[2] AT. IPPEN AND D. R. F. HARLEMAN, One-dimensional analysis of salinity intrusion in estuaries, Technical Bulletin No. 5, Committee on Tidal Hydraulics, Corps of Engineers, US-Army Vicksburg, Miss., June 1961.

[3] P. VAN DER BURGH, Ontwikkeling van een methode voor het voorspellen van zoutverdelingen in estuaria, kanalen en zeeën, Rijkswaterstaat, Deltadienst, Afdeling Waterhuishouding, rapport 01–72, januari 1972.

[4] C. STIGTER AND J. SIEMONS, Calculation of longitudinal salt-distribution in estuaries as function of time, Delft Hydraulics Laboratory Publication No. 52, October 1967.

[5] M. L. THATCHER AND D. R. F. HARLEMAN, A mathematical model for the prediction of unsteady salinity intrusion in estuaries, Department of Civil Engineering, M. I. T. report No. 144, February 1972.

[6] D. R. F. HARLEMAN, Estuary and Coastline Hydrodynamics, Chapter 12 and 14, A. T. Ippen, Editor, Mc Graw-Hill, New York – 1966.

[7] H. J. EGGINK, Het estuarium als ontvangend water van grote hoeveelheden afvalstoffen, Mededeling nr. 2, 1965, Rijksinstituut voor de Zuivering van Afvalwater.

[8] G. C. VAN DAM EN J. C. SCHÖNFELD, Experimental and theoretical work in the field of turbulent diffusion performed with regard to the Netherlands' estuariess and coastal regions of the North Sea, General Assembly IUGG, Berne, Switzerland Sept./Okt. 1967, Rijkswaterstaat – Mathematische Fysische Afdeling, nota MFA 6807).

[9] M. KARELSE, Reproduktie zouttoestanden getijrivieren. Toetsing ééndimensionale en tweedimensionale rekenmodellen aan getijgootresultaten, Waterloopkundig Laboratorium Delft M 896–XX.

[10] — Sediment-, chloormetingen Rotterdamse Waterweg, Gemeentewerken Rotterdam, Afdeling Havenwerken, rapport 0–63–18.

[11] I.S.O. — INTERNATIONAL ORGANIZATION FOR STANDARDIZATION, Investigations of the total error in measurement of flow by velocity-area methods, part 1, 2 and 3, august 1971.

Mathematical investigation of stratified flow

by dr. ir. C. B. Vreugdenhil

1 Introduction

The mathematical model method of investigating stratified flow is being used more and more widely, both for obtaining an insight into the underlying principles and for the solving of practical problems. The purposes of the models differ considerably, so a range of models of varying complexity are used. In detailed investigations, our limited knowledge of turbulence, especially in stratified conditions, and the limited use that can be made of computers must be taken into account.

Generally speaking, the mathematical and physical formulation of a problem must be schematised to make it numerically workable. Schematization primarily involves reducing the original four independent variables (i.e. three space coordinates and time) to a smaller number, usually by averaging with respect to one or more of the coordinates or time. This introduces empirical coefficients, the determination of which requires great experimental effort. Consequently there is a tendency to schematize (i.e. average) as little as possible and spend considerable numerical effort, the extent of which depends, of course, on the nature of the problem (Fig. 1). As the cost of computer time is decreasing, the optimum combination of schematization and computer effort is shifting as indicated. Moreover, the actual position of the optimum depends on the relative importance accorded to each of the two factors, which varies from problem to problem.
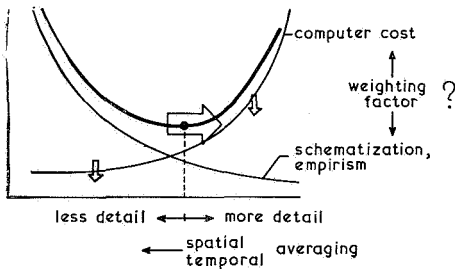

Figure 1. There is for each problem an optimum between schematization and computer cost, depending on the weighting factor between these properties. As computer costs tends to decrease, the optimum tends to shift towards more detailed models (see arrows).

89

2 Consequences of averaging

The following basic hydrodynamic equations are stated for reference purposes. They include some assumptions regarded as acceptable for the project concerned, namely:

— that the flow is turbulent; fluctuations are eliminated by averaging;
— that density differences are only retained in the gravity terms of the momentum equations (Boussinesq approximation);
— that geostrophic effects are disregarded, which makes the outcome applicable only to relatively narrow basins or estuaries;
— that boundary-layer or shallow-water approximation is adopted.

$$\frac{\partial u}{\partial t} + \frac{\partial}{\partial x}(u^2) + \frac{\partial}{\partial y}(uv) + \frac{\partial}{\partial z}(uw) + \frac{1}{\rho}\frac{\partial p}{\partial x} - \frac{1}{\rho}\frac{\partial \tau_{xz}}{\partial z} = 0 \tag{1}$$

$$\frac{\partial p}{\partial z} = -\rho g \tag{2}$$

$$\frac{\partial u}{\partial x} + \frac{\partial v}{\partial y} + \frac{\partial w}{\partial z} = 0 \tag{3}$$

$$\frac{\partial \sigma}{\partial t} + \frac{\partial}{\partial x}(\sigma u) + \frac{\partial}{\partial y}(\sigma v) + \frac{\partial}{\partial z}(\sigma w) + \frac{\partial T}{\partial z} = 0 \tag{4}$$

u, v, and w are the velocity components in x, y, and z directions, ρ is the density and σ the density surplus due to salinity or temperature. The other terms are defined in appendix 1. An equation similar to (1) holds good for the v-component.
Averaging may take the following forms:

— vertical: integration from bottom to surface;
— lateral: integration from bank to bank;
— cross-sectional: a combination of the preceding two;
— n-layer: vertical averaging over part of the depth, sometimes combined with lateral averaging;
— tidal: integration with respect to time to eliminate tidal fluctuations.

90

The outcome of these procedures can be analyzed in detail; only the main effects are described here.

Lateral averaging does not introduce any serious errors into the equations, provided the lateral distribution of flow and density is reasonably uniform, i.e., if the flow is taken to be more or less unidirectional (e.g. in estuaries, rivers). However, difficulties may be encountered when applying relations between the turbulent and mean quantities given in section 6.

Vertical averaging introduces into (4) such terms as

$$\frac{\partial}{\partial x} \overline{(\sigma - \bar{\sigma})(u - \bar{u})} \tag{5}$$

where a bar denotes averaging (vertically in this case). If there is appreciable stratification, these terms are not negligible compared with the other terms. They are called dispersion terms due to shear. Essentially (5) cannot be expressed in terms of vertical mean quantities, so a major empirical factor is introduced. This is also the case for the bottom friction which remains from the stress term in (1).

The difficulties arising from vertical averaging can be overcome by averaging over two or more layers, because shear is then largely accounted for [24]. On the other hand, differential pressures then become much more important and vertical averaging over a layer introduces errors into the pressure terms like

$$g \frac{\partial}{\partial x} \overline{\{(\sigma - \bar{\sigma})(z - z_b) a_2\}} \qquad \text{(for the bottom layer)} \tag{6}$$

which for a two-layer model can be some 10 % of the relevant pressure term

$$g \frac{\partial}{\partial x} \{\tfrac{1}{2}(\rho_2 - \rho_1) a_2{}^2\} \tag{7}$$

This can be considered acceptable for many purposes. Unfortunately, the layered model introduces several empirical factors at the interface or interfaces, such as a shear stress (direction and magnitude), and salt flux and water flux, about which little is known.

Tidal averaging introduces errors of the type given in (5) into all coordinate directions in both the momentum and the salt balance equations (1) and (4). The relation between turbulent and mean quantities is again a source of difficulty. Consequently detailed models using time-averaged equations are very problematic. By making gradient transport assumptions for the resulting transport terms, however, we can obtain typical solutions [7] with which estuaries may be classified by determining the diffusion coefficients involved empirically.

In conclusion, it should be noted that lateral averaging only does not produce empiri-

cal coefficients if it is used in connection with more or less unidirectional flow such as that obtaining in estuaries and rivers.

Consequently, two-dimensional models (in a vertical plane) are preferable or three-dimensional ones for larger basins, in which any tidal variations are retained. The details of such models are dealt with further in sections 5 and 7.

3 One-dimensional models

Only one space dimension is left when averaging over a complete cross-section of a river or estuary. This is a procedure especially adopted for well-mixed systems in which there are no appreciable differences of salinity in a cross-section, but one which can also be used for more stratified conditions. Moreover, even if the salinity is uniform over a cross-section, longitudinal differences of salinity give rise to a differential pressure which can cause the velocity distribution to differ from that in homogeneous flow; this is evident from Abraham's contribution.

The most effective application of a one-dimensional model to an estuary appears to be that by STIGTER AND SIEMONS [20] to the Rotterdam Waterway. This estuary belongs to the partly mixed class; yet the results obtained are very satisfactory, as is shown in Fig. 2. They are, however, greatly dependent on the empirical dispersion coefficient D, as given in

$$\iint (\sigma - \bar{\sigma})(u - \bar{u})\, dA = AD\, \frac{\partial \bar{\sigma}}{\partial x} \tag{8}$$

The magnitude and variation of D are selected empirically. This precludes any extrapolation to unknown situations unless a relation between the dispersion coefficient and certain characteristic parameters is found.

The superposition of two contributions to D [8] will serve the purpose: a 'Taylor type' dispersion coefficient similar to homogeneous flow, and a term proportional to the longitudinal salinity gradient to account for the effect of stratification.

Several other applications have been published which do not take the density gradient into account in the momentum equation [21]. It is evident from [20] that this gradient may have an appreciable effect (Fig. 3) so that its omission restricts the applicability of the method, to situations in which salinity acts as a passive contaminant. Some two-dimensional applications have also been published [10, 14]. In the latter, the dispersion coefficient is taken as a constant.
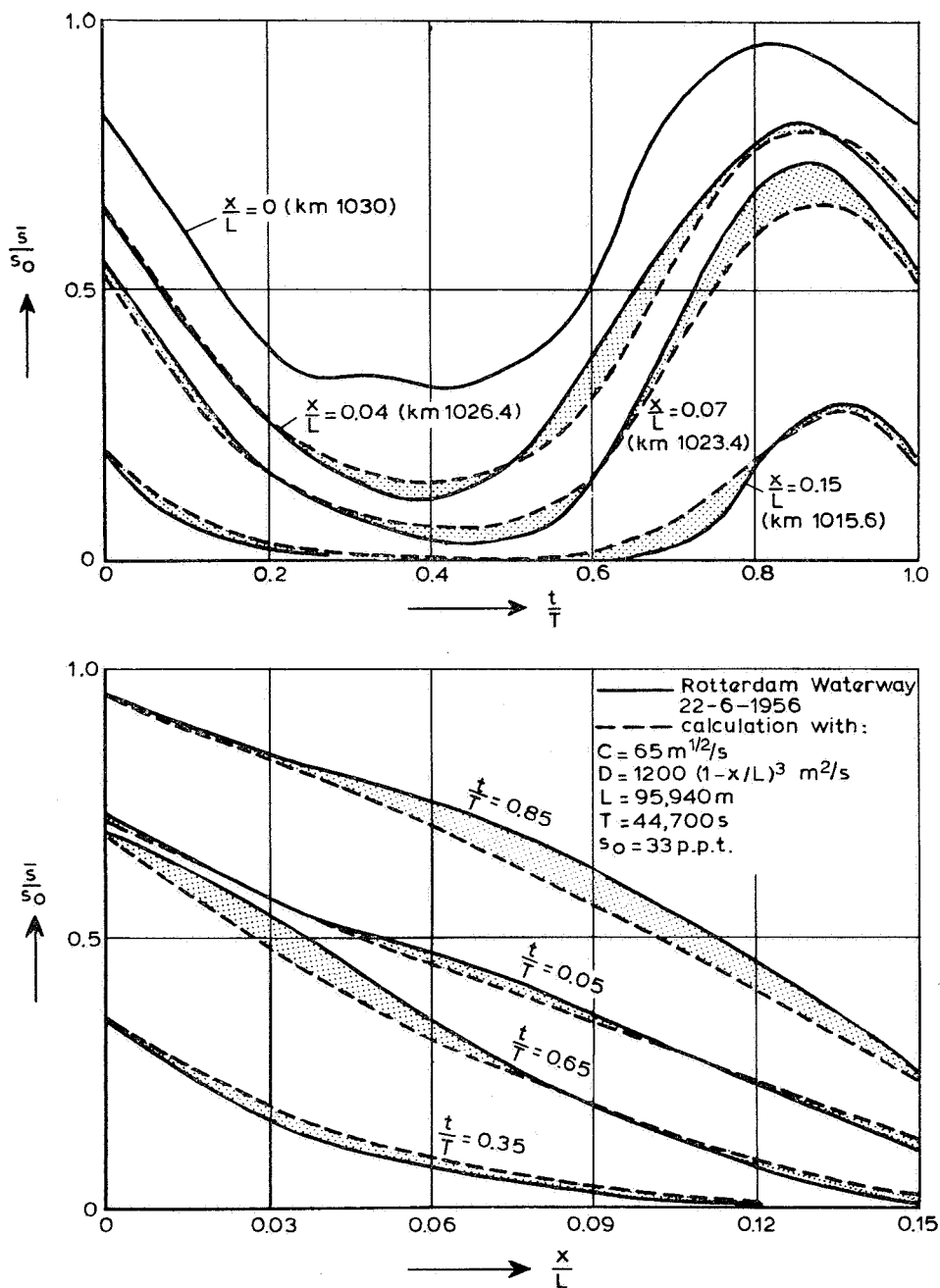
Figure 2. One-dimensional model of the Rotterdam Waterway after Stigter and Siemons (1967). Measured salinities (drawn lines) are compared with calculated ones (broken lines).
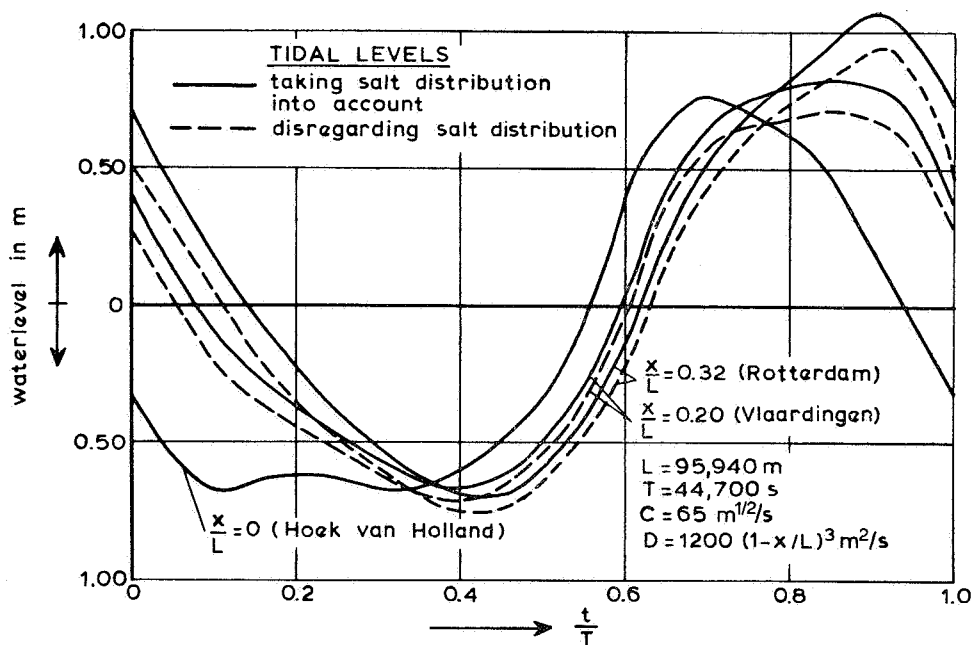
Figure 3. Effect of density gradient on water levels in Rotterdam Waterway after Stigter and Siemons (1967).

4 Two-layer model

An initial approximation of the density currents is obtained by schematizing the salinity and velocity structure in a cross-section in two layers [24]. The errors made by averaging over each of the layers cannot be entirely disregarded but they lie within reasonable limits. Difficulties are encountered when defining the exchange of mass and momentum at the interface, and when establishing boundary conditions, e.g. where the river meets the sea.

Figure 4. Two-layer model of Rotterdam Waterway after Vreugdenhil (1970). The position of the interface is compared with measurements (dots). The two lines result from slightly different expressions being used for the interfacial shear stress. Mass exchange between the two layers was not taken into account.

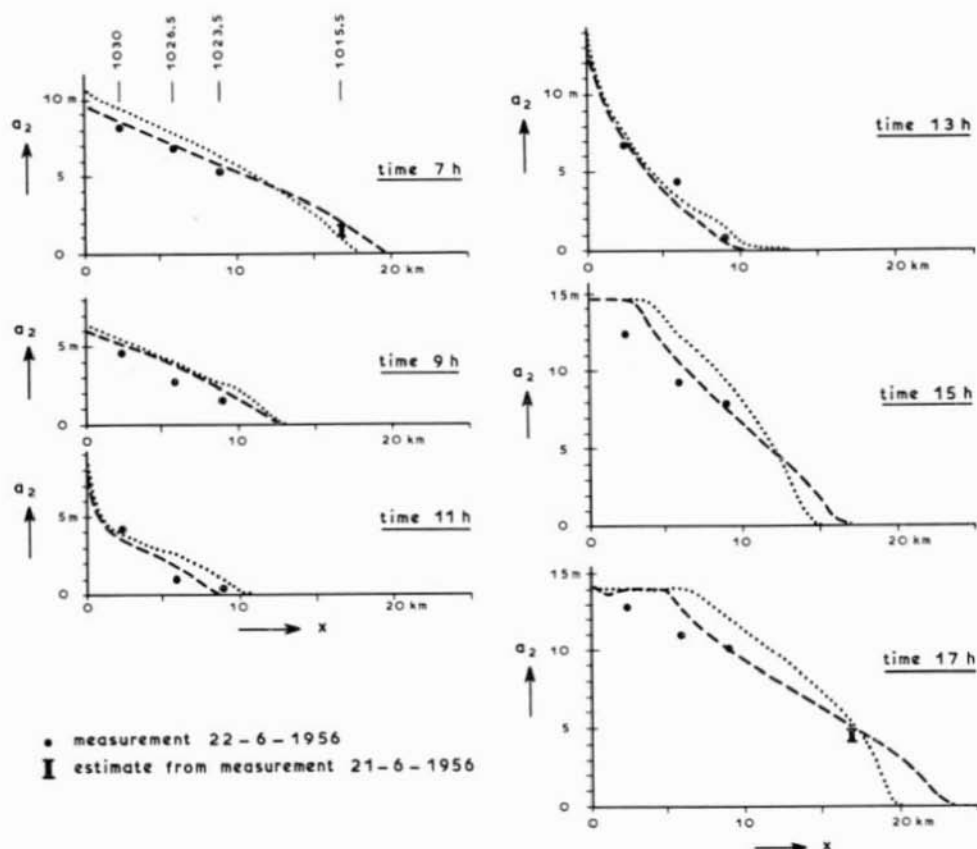If the tidal movement is so small that there is no appreciable mixing of the layers, only the shear stress at the interface need be determined. It has been argued that the stress will depend on the relative velocity of the two layers in much the same way as the bottom stress and the wind stress at the surface. If we remember that there will always be a certain residual shear stress when there is no longer any stratification, we can assume that [24]

$$\tau_i = \rho_2 \, k_b \, \frac{a_1}{h} \, u_2 | u_2 | + \rho_2 \, k_i \, (u_1 - u_2)| u_1 - u_2 | \qquad \qquad (9)$$

Experimental data on the frictional coefficient k_i are widely scattered. The effect of the Reynolds number is very much in evidence; the internal Froude number (or overall Richardson number) probably has some effect, too. Computations employing (9) (either with or without the relatively unimportant first term) have been prepared for the River Rhône, which has a small tidal range [1], and for the Rotterdam Waterway, where tidal movements are more marked [24]. Some of the results of the latter computation are shown in Fig. 4 (broken curves). Curves obtained by using (9) without the first term are also given. A reasonable representation of the situation is evidently feasible.

measurement 22-6-1956
computation

VELOCITIES IN UPPER LAYER

measurement 22-6-1956
computation

VELOCITIES IN LOWER LAYER

measurement 22-6-1956
computation

DENSITIES IN UPPER LAYER

measurement 22-6-1956
computation
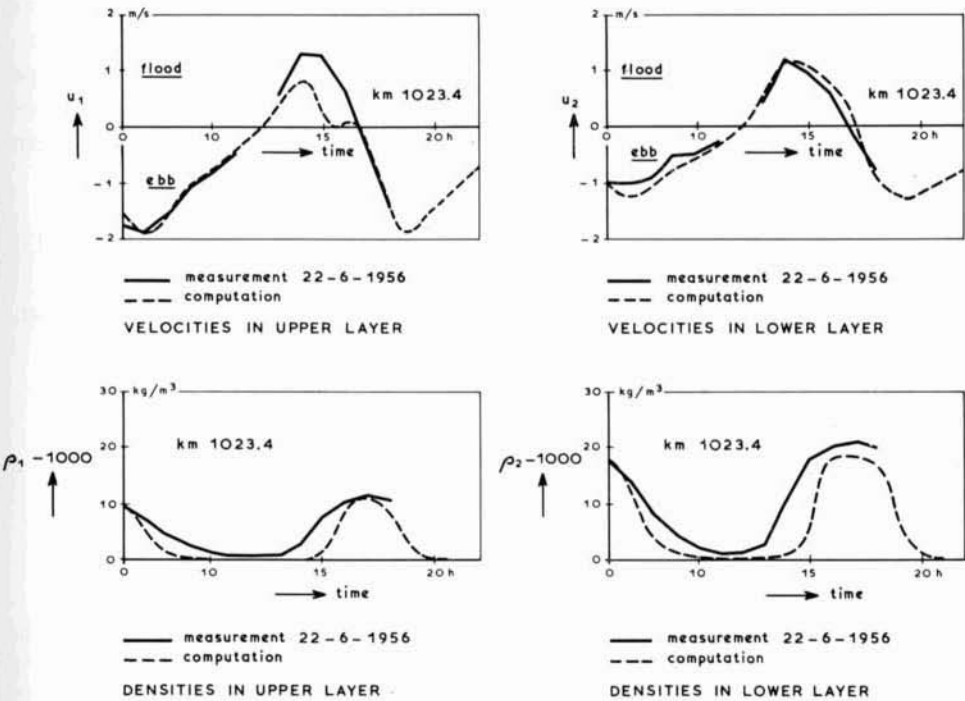
DENSITIES IN LOWER LAYER

Figure 5. Two-layer model of Rotterdam Waterway, taking mixing between the two layers into account, after Vreugdenhil (1970).

97

The model becomes much more complicated if mixing between the layers is taken into account. Exchanges of water and salt have to be treated separately and little is known of these processes in a turbulent flow without a sharp interface. Some tentative results for the Rotterdam Waterway [24] are given in Fig. 5 but extrapolation to other situations is difficult.

Numerically, the two-layer model is peculiar in that surface and internal waves have quite different propagation velocities, being approximately

$$c_s \sim (gh)^{\frac{1}{2}} \tag{10}$$

$$c_i \sim (\frac{\Delta\rho}{\rho} ga_1 a_2/h)^{\frac{1}{2}} \tag{11}$$

so c_i is about 5 % of c_s. In most numerical methods the intervals Δx and Δt at which the solution of the differential equations is determined must satisfy a relation like

$$|c_{max} \Delta t/\Delta x| < 1 \tag{12}$$

for the sake of numerical stability or accuracy. The maximum velocity of propagation is clearly c_s so the ratio $c_i\Delta t/\Delta x$ will be very much smaller than unity (Fig. 6). This may have serious effects on the accuracy of the computation for internal waves. Fortunately, the two types of waves can be separated by eliminating the surface slope from the two momentum equations for the two layers. The resulting equation describes the internal motion [24]. Only the internal-wave speed c_i is then retained in the system and such space and time intervals may be selected that

$$c_i \Delta t/\Delta x \sim 1 \tag{13}$$

(Fig. 6). In this approximation the water surface is assumed to be horizontal, and that,
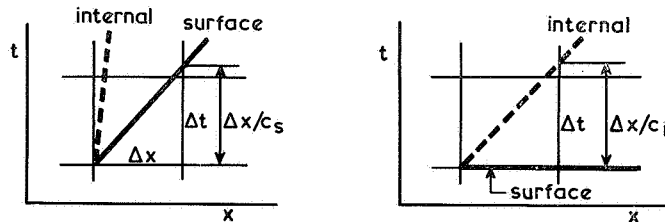
Figure 6. Stability criteria. In the left-hand diagram the surface-wave velocity c_s determines the time step. The internal waves are then represented inaccurately. In the right-hand diagram baroclinic approximation is resorted to, which eliminates the surface waves. The time step can then be chosen in the light of the internal wave velocity c_i which gives a much better approximation. Note that the time steps in the two pictures are not identical.

98

consequently, surface waves run at an infinite speed. In the extreme case of one of the layers being very thick the remaining equations are those for a single water layer with reduced gravity and increased friction, a feature also used by several other authors.

References to two-dimensional two-layer models are also found in the literature on the subject. Empirical information is still more complicated in this case because the direction as well as the magnitude of the interfacial shear stress must be specified. Methods like that described in section 5 can shed some light on the problem. Analytical studies for a schematized lake are reported by CSANADY [2, 3, 4]. Numerical techniques for this class of problems have not yet become matters of routine, but efforts to solve single-layer problems (e.g. those concerning tides or storm surges) yield valuable information. In the present case the conservation of mass and momentum should be watched if there are jumps in the interface. Some figures pertaining to cases without mixing and [25] cooling water circulation with entrainment have been published [9, 11, 22], but none of them contains any verification by measurement. Consequently it cannot yet be said that two-dimensional two-layer models are available for practical calculations.

5   Quasi two or three-dimensional models

As stated before, the type of model which does not involve the use of empirical coefficients caused by averaging is either the two-dimensional (lateral average) or the three-dimensional one, though the computer requirements for three-dimensional cases are exacting, especially if they are time-dependent. Although this will not continue to be a restricting factor, what is called quasi two or three-dimensional models are coming to the fore. Even in the long run they may be useful together with more comprehensive numerical approaches, as certain applications do not require such complicated methods (Fig. 1).

Quasi three-dimensional models, (the two-dimensional model is similar) can be obtained by means of the weighted residuals method [6]. The idea is to schematize the variation in velocity and salinity in one of the coordinate directions by means of a possible small number of parameters which depend on the other space variables and
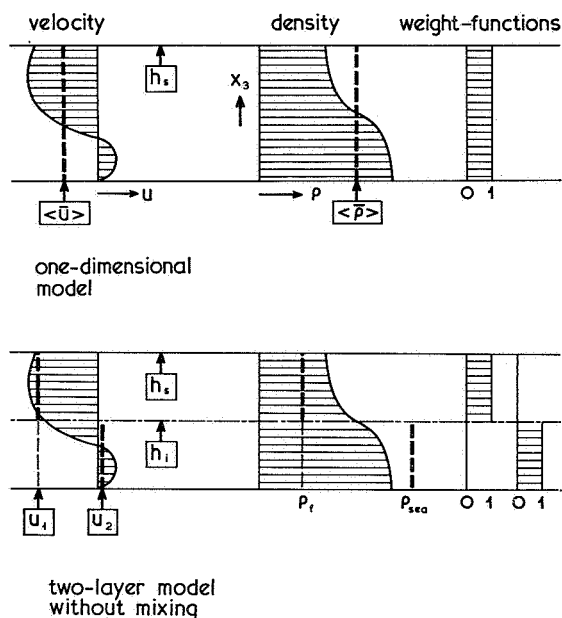
Figure 7.   Two illustrations of the weighted residuals method. In the one-dimensional model only the parameters h_s, $\langle \bar{u} \rangle$ and $\langle \bar{p} \rangle$ are used; in the two-layer model 6 parameters characterize the profiles.

100
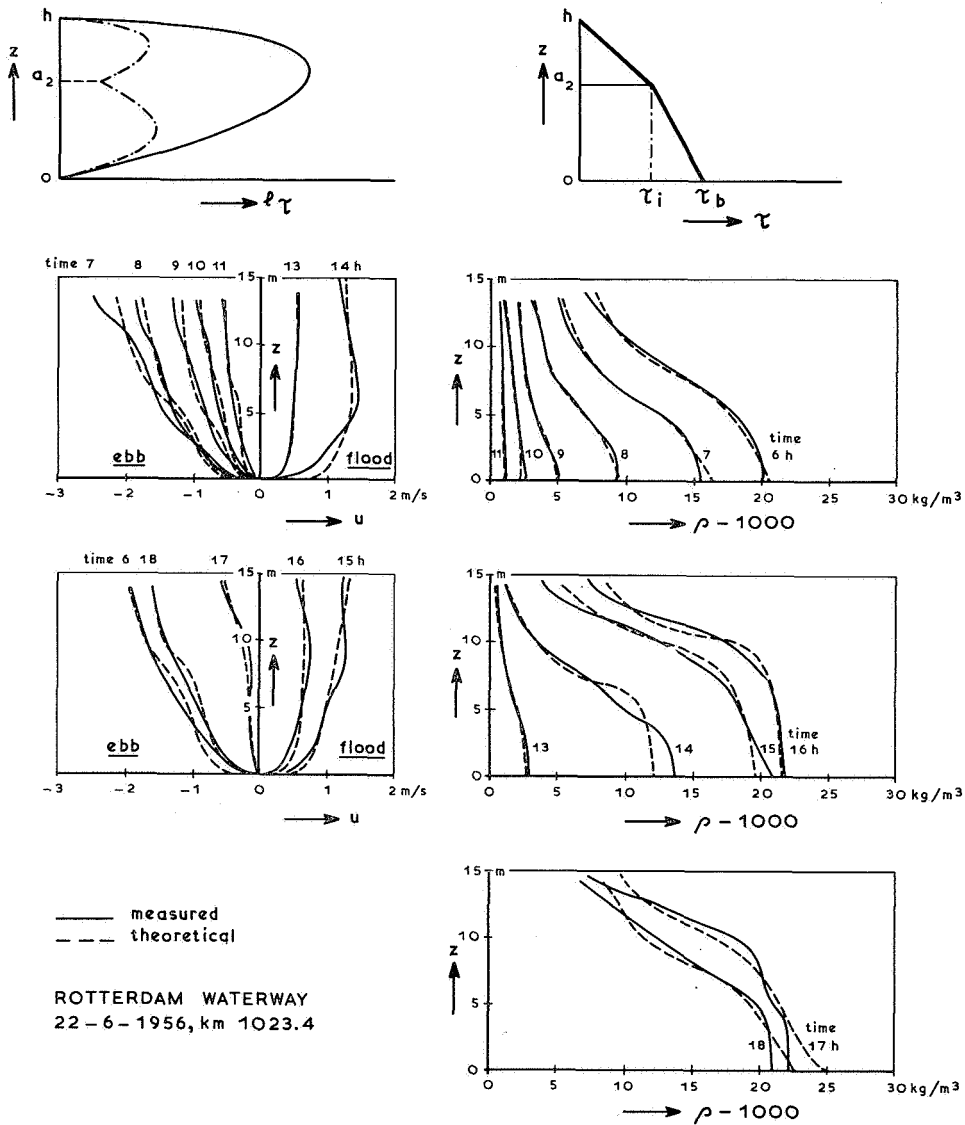
Figure 8. Examples of velocity and density profiles using a limited number of parameters. The profiles are based on a mixing-length theory using the mixing-length and shear-stress distributions shown in the upper graphs. Combining the 7 parameters involved with measured data give the curves shown in the bottom graph.

time, thereby reducing the number of independent variables in the problem. These methods are intermediate between the averaged models already dealt with and fully two or three-dimensional models. For example, the density surplus σ could be repre-
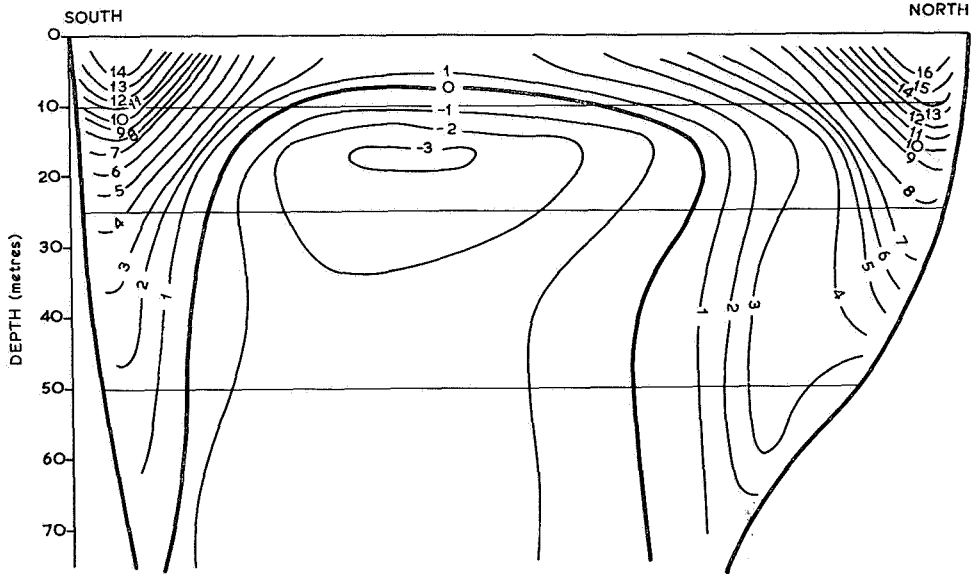
Figure 9. Results obtained from a four-layer model of Lake Ontario after Simons (1972). The lines of equal velocity (E-W direction) in a cross section of the lake are shown. The horizontal lines mark the layers.

sented as

$$\sigma(x, y, z, t) = \sum_{k=1}^{n} S_k(x, y, t) W_k(z) \tag{14}$$

in which $W_k(z)$ indicates a set of functions (polynomials, Fourier components or others) with which the density profile can be approximated. Equation (14) and similar ones for the velocity will not satisfy the differential equations (1) to (4) but an approximate solution can be found by integrating the equations after multiplication with a weight function $G_m(z)$ [whether or not identical to $W_m(z)$]. The first term of (4) would, for instance, give

$$\int_{z_b}^{z_w} G_m(z) \frac{\partial \sigma}{\partial t} dz = \sum_{k=1}^{n} \frac{\partial S_k}{\partial t} \int_{z_b}^{z_w} G_m(z) W_k(z) \, dz = \sum_{k=1}^{n} \alpha_{km} \frac{\partial S_k}{\partial t} \tag{15}$$

in which α_{km} is a set of predetermined coefficients.

The preceding methods (sections 3 and 4) are special instances of this technique as shown in Fig. 7. The representation can be systematically improved by introducing more parameters (such as S_k) with suitable weight functions. Some idea of what is possible may be gathered from Fig. 8 [24], in which velocity and density profiles

102

from measurements in the Rotterdam Waterway are represented by 7 parameters in all, though in a somewhat different form than in (14). In the two-layer approach 5 parameters are involved, viz. u_1, u_2, ρ_1, ρ_2 and a_2/h.

An additional advantage of this type of method is that derived quantities, such as the interfacial shear stress in a two-layer system, can be realistically approximated from the equations given in section 6.

Several three-dimensional instances of this approach have been published, some of which pertain to stratified flow. LEE AND LIGGETT [11, 12] assume a two-layer structure with uniform densities and use a solution of a simplified form of the differential equations for $W_k(z)$; the weight functions $G_m(z)$ are unity. Computations for a schematic lake are given without comparing them with prototype data. SIMONS [18] proposes a technique using an arbitrary number of layers, regarding the two-layer model as a special case. If the layers are thin in proportion to the gradients of density and velocity, the technique actually becomes a finite-difference method for the full three-dimensional equations. However, in view of the small number of layers used (four) the method is, in fact, quasi three-dimensional The method is very flexible, both geometrically and as regards eddy viscosity. Some provisional results are given for Lake Ontario (Fig. 9). No details into eddy viscosity and diffusion coefficient are given. These figures, too, have yet to be compared with prototype data.

6 Physical aspects of turbulence in stratified flow

The physical behaviour of turbulence in a stratified fluid is one of the main problems. The unknown functions of turbulence in (1) to (4) are the shear stress (magnitude and direction) and the turbulent mass flux. The conventional method is to assume the gradient transport, stating that the shear stress and mass flux are proportional to the velocity and density gradients respectively. Some recent theoretical considerations have given support to this assumption [13, 15]. These theories are based on transport equations describing the generation, transport and dissipation of quantities such as $\overline{u'w'}$:

$$\underbrace{\frac{d}{dt}(\overline{u'w'})}_{1} + \underbrace{\frac{\partial}{\partial z}(diffusion)}_{2} + \underbrace{\overline{w'^2}\frac{\partial u}{\partial z}}_{3} + \underbrace{g\,\overline{\sigma'u'}}_{4} + \underbrace{c_1\frac{\sqrt{e}}{l}\,\overline{u'w'}}_{5} = 0 \tag{16}$$

d/dt in term 1 is the substantial derivative $\partial/\partial t + u\partial/\partial x + v\partial/\partial y + w\partial/\partial z$. Term 2 comprises some molecular and turbulent diffusive effects. Term 3 represents the 'generation' of $\overline{u'w'}$. Term 4 is the buoyancy representing the effect of stratification. Term 5 is a 'distribution' term covering the interaction between various components of the turbulent stress tensor by means of pressure fluctuations. Further details will be found in the original publications. (16) is based on the assumption that turbulence is fully developed. Low Reynolds or high Richardson number effects such as internal waves are not included.

Terms 1 and 2 can be disregarded under certain conditions (see below). A similar equation for mass flux is:

$$\overline{\sigma'w'}\frac{\partial u}{\partial z} + \overline{u'w'}\frac{\partial \sigma}{\partial z} + c_2\frac{\sqrt{e}}{l}\,\overline{\sigma'u'} = 0 \tag{17}$$

The Richardson flux number (Rf) is defined by

$$Rf = -g\,\overline{\sigma'w'}\left(\overline{u'w'}\frac{\partial u}{\partial z}\right)^{-1} \tag{18}$$

Quantities $\overline{\sigma'u'}$ and $\overline{\sigma'w'}$ can be eliminated from (16), (17) and (18). Using additional equations for $\overline{w'^2}$ and $\overline{\sigma'^2}$, we get

$$-\frac{\tau_{xz}}{\rho} = \overline{u'w'} = -\varepsilon\frac{\partial u}{\partial z} \tag{19}$$

and, similarly,

$$T = \overline{\sigma' w'} = -\varepsilon_\sigma \frac{\partial \sigma}{\partial z} \tag{20}$$

in which the eddy viscosity ε and the diffusion coefficient ε_σ are defined as

$$\varepsilon = l \sqrt{e} \, f_1 \, (Ri)$$

$$\varepsilon_\sigma = l \sqrt{e} \, f_2 \, (Ri) \tag{21}$$

the Richardson gradient number (Ri) being defined by

$$Ri = -\frac{g}{\rho} \frac{\partial \sigma}{\partial z} \left(\frac{\partial u}{\partial z} \right)^{-2} = \frac{\varepsilon}{\varepsilon_\sigma} Rf \tag{22}$$

The functions f_1 and f_2 are not determined by this theory; they also contain the dependence of the length scale l on the Richardson number. Nevertheless the main result is that the gradient transport assumption is supported and with it, by a slight reformulation, the mixing length hypothesis. Secondly, the effect of stratification is seen only in the Richardson number. To a certain extent, this is confirmed by measurements [16], although they are widely scattered. Finally, in the three-dimensional case the shear stress is found to have the same direction as the vertical gradient of the velocity vector [15].

The foregoing analysis also gives some indication of the conditions under which results (19) and (20) are valid. One of the main points is disregarding the first two terms in (16) and its companions. Considering a flow having a length scale L and a time scale T (for tidal flow in an estuary L and T will be the tidal wavelength and period respectively), the ratio between the time derivative in term 1 and term 5 can be estimated as $l(e^{\frac{1}{2}} T)^{-1}$ which for an estuary is of the order of 10^{-3}. The convective terms are even smaller. The diffusion terms (2) may be approximated for the purpose as

$$\varepsilon \frac{\partial}{\partial z} \, (\overline{u'w'})$$

so that the estimated ratio between term 2 and term 5 works out as $(l/h)^2$, which is of the order of 10^{-1} or 10^{-2}. The conclusion is that the gradient transport assumption can be used, provided that the length and time scales involved are sufficiently large, in other words, the flow is quasi-steady and quasi-uniform. The approximation is not suitable for very unsteady or non-uniform flows and more elaborate methods [13] will have to be used.

105

7 Numerical methods for two- or three-dimensional turbulent flow

One of the main jobs in the numerical computation of general two or three-dimensional flow, either laminar or turbulent, is determining the pressure field in such a way that the equation of continuity (3) is satisfied. This usually calls for the solution of a Poisson equation for the pressure at each time step, which involves considerable computational effort. In the present case, however, the pressure distribution is hydrostatic due to the shallow-water approximation, so the pressure is a simple function of the density. There remains a coupled set of non-linear convection-diffusion equations within what is usually complicated geometry. Considerable experience has already been gained of the use of finite-difference methods for such systems. Finite-element methods are not dealt with in this paper, because yet little is known of their efficiency.

Two crucial points in a finite-difference method are stability and accuracy. An explicit finite-difference method using time and space increments Δt, Δx, Δy, Δz for a linear convection-diffusion equation is subject to the stability requirements [17]

$$ u \, \frac{\Delta t}{\Delta x} < 1 \qquad 2\varepsilon \frac{\Delta t}{\Delta z^2} < 1 \tag{23} $$

assuming the vertical mesh width Δz to be much smaller than the horizontal ones. For example, assume that

$$ u \sim 1 \text{ m/s} \qquad \Delta x \sim 100 \text{ m} \qquad \varepsilon \sim 0.05 \text{ m}^2/\text{s} \qquad \Delta z \sim 1 \text{ m}. $$

Then (23) will give $\Delta t < 100$ s and $\Delta t < 10$ s respectively, the latter being a rather serious limitation. The use of implicit methods removes the limitations of (23) but involves the adoption of a more complicated computational method. Moreover, values of the two parameters that are too far from unity in (23) result in inaccuracies. A balance has therefore to be struck between accuracy and economy.

The convective terms in the equations can give rise to non-linear instability. Exhaustive analysis of this effect is difficult, but useful heuristic criteria have been devised by Hirt (see [17]), which state that the effective diffusion coefficient (physical + numerical) should be positive. For an accurate solution, moreover, the numerical contribution to the diffusion coefficient should be small compared with the physical one. Using central differences for the convective terms, the non-linear stability criterion is seen to be

$$ \varepsilon > \tfrac{1}{2} \Delta x^2 \frac{\partial u}{\partial x} + \tfrac{1}{2} u^2 \Delta t \tag{24} $$

which may cause difficulty if $\varepsilon \sim 0.05$ m^2/s, $\Delta x = 100$ m, $\partial u/\partial x \sim 10^{-5}$ s^{-1}. The numerical diffusion coefficient, represented by the right-hand member of (24) will at any event, not be small compared with ε, so an accurate solution will not be possible. However, the two terms on the right-hand side of (24) can be removed by using special difference approximations of a higher order [17].

A major difficulty is the treatment of boundary conditions, at both fixed and free surfaces. Most of the instances published involve quite simple geometries into which hypothetical image points outside the region can be introduced to satisfy vanishing normal flow conditions. This procedure cannot be used if the bottom topography is irregular. Moreover, the mathematical formulation does not take care of the viscous layer at the wall. Consequently, the computed velocity profiles should be fitted to the wall layer in the lowest grid interval. The technique adopted in SUMMAC (see [17]) is preferable for the free surface provided the shore lines do not vary. In this method the surface elevation is computed at fixed grid points, using an implicit representation of the free surface condition.

Two examples of these techniques are given. The first [5] pertains to laminar flow, calculated by the marker-and-cell technique and an additional equation to determine the density in each cell.

There are significant vertical accelerations, so the shallow-water approximation is not used. Instead, the pressure is calculated from a Poisson equation at each time step. The numerical treatment of the momentum equation is explicit with additonal numerical diffusion in order to obtain a positive, effective diffusion coefficient. The interface is not dealt with separately but traced by means of the markers. In the same publication a 'two fluid' approach is described in which the interface is explicitly taken into account. The numerical results compare favourably

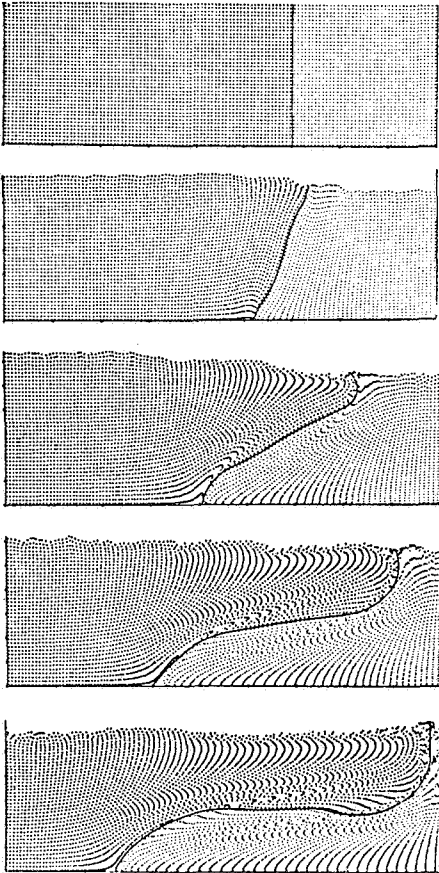Figure 10. Two-dimensional laminar flow of two fluids with different densities after Daly and Pracht (1968, reproduced by permission of the authors), obtained by the marker-and-cell method.

107
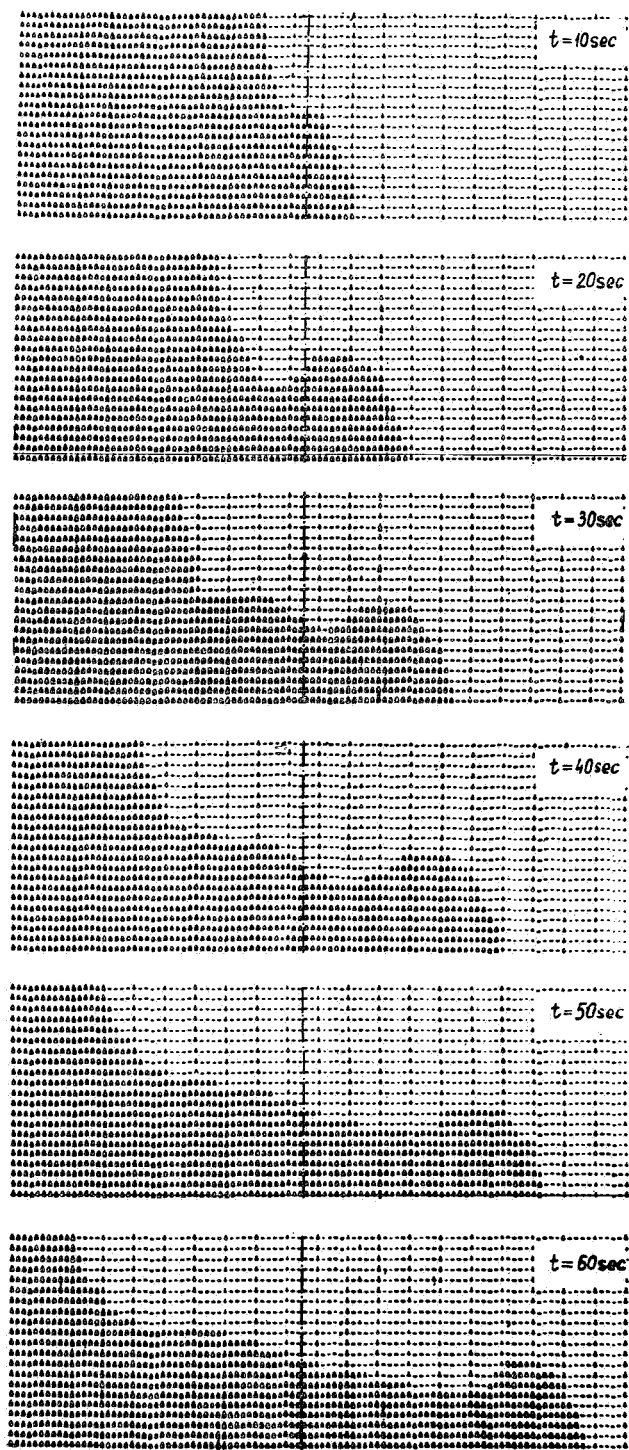
Figure 11. Two-dimensional turbulent flow of a stratified fluid after Vasiliev et al. (1973). Stratification in this example is due to temperature differences.
A specific isotherm is shown at several instants.

with the outcome of experiments. Some of them are given in Fig. 10, which shows the detail obtained from such calculations.

The second example pertains to a similar case with turbulent flow [23]. The hydrostatic assumption is used together with (19) and (20), in which the turbulence energy e is determined from a transport equation, which incidentally takes the form of a convection-diffusion equation. The length scale l is established by extending Von Kármán's similarity principle. An implicit finite-difference method is used but no details are given. Some results are shown in Fig. 11. They are not compared with figures obtained from experiments.

Three-dimensional calculations for turbulent stratified flow do not appear to have been attempted yet. The extension of two-dimensional techniques would seem to be a straightforward matter, but one should gain some experience of two-dimensional and quasi three-dimensional models first in order to get some idea of the type of problem to be encountered.

8 Conclusions

Some conclusions on the mathematical models used for stratified flow can be drawn from the foregoing.
— From the physical point of view, two or three-dimensional time-dependent models are preferred, since they enable one to avoid the obscuring effects of averaging.
The description of the turbulence process has been greatly simplified. More fundamental descriptions are being developed.
— From the numerical point of view, mathematical models for three-dimensional flow still have their limitations. Otherwise, numerical techniques are comparatively well developed, with the exception of the treatment of complicated boundaries. There is still too little verification against measurement.
— Next to comprehensive numerical models there is room for simpler ones for problems requiring rough information only.

References

[1] BOULOT, F. ET A. DAUBERT — Modèle mathematique de la remontée de la salinité sous une forme stratifiée en régime non-permanent, IAHR Congr., Kyoto 1969, C 38.

[2] CSANADY, G. T. — Large-scale motion in the Great Lakes, J. Geoph. Res. 72, 16 (1967) 4151–4162.

[3] CSANADY, G. T., — Wind-driven summer circulation in the Great Lakes, J. Geoph. Res. 73, 8 (1968) 2579–2589.

[4] CSANADY, G. T., — Motions in a model Great Lake due to a sudenly imposed wind, J. Geoph. Res. 73, 20 (1968) 6435–6447.

[5] DALY, B. J. AND W. E. PRACHT — Numerical study of density current surges Phys. Fluids 11, 1 (1968) 15–30.

[6] FINLAYSON, B. A. — The method of weighted residuals and variational principles, Acad. Press, New York 1972.

[7] HANSEN, D. V. AND M. RATTRAY — New dimensions in estuary classification, Limnology and Oceanography 11, 3 (1966) 319–326.

[8] HARLEMAN, D. R. F., M. L. THATCHER AND J. E. DAILEY — Predictive models of salinity and water quality parameters in estuaries, Proc. Conf. 'Tools in coastal zone management' Washington 1972, 185–195.

[9] KASAHARA, A., E. ISAACSON AND J. J. STOKER — Numerical studies of frontal motion in the atmosphere I, Tellus 17, 3 (1965) 261–276.

[10] KATO J., S. HAGINO AND I. AKIZUKI — On diffusion of salinity in sea area with tributary rivers, IAHR Congr. Kyoto 1969, C 22.

[11] LEE, K. K. AND J. A. LIGGETT — Computation for circulation in stratified lakes, J. ASCE 96, HY 10 (1970) 2089–2116.

[12] LIGGETT, J. A. AND K. K. LEE — Properties of circulation in stratified lakes, J. ASCE 97, HY 1 (1971) 15–29.

[13] LUMLEY, J. L. AND B. KHAJEH-NOURI — Computational modeling of turbulent transport, 2nd IUGG-IUTAM Symp. Atm. Diff. and Envir. Pollution, Charlottesville, Va. 1973.

[14] MASCH, F. D. AND N. J. SHANKAR — Mathematical simulation of two-dimensional horizontal convective dispersion in well-mixed estuaries, IAHR Congr. Kyoto 1969, C 32.

[15] MONIN, A. S. — Structure of an atmospheric boundary layer, Izv. Atm. and Oceanic Phys. 1, 3 (1965) 153–157.

[16] NELSON, J. E. — Vertical turbulent mixing in stratified flow, a comparison of previous experiments, Dept. Civ. Eng., Univ. Calif., Berkeley 1972.

[17] ROACHE, P. J. — Computational fluid dynamics, Aerodyn. Res. Dept. Sandia Lab., Albuquerque, N.M. 1972.

[18] SIMONS, T. J. — Development of numerical models of Lake Ontario, II, 15th Congr. Great Lakes Res., Madison Wisc. 1972.

[19] STEWART, R. W. — The problem of diffusion in a stratified fluid, Adv. Geoph. 6 (1959) 303–311.

[20] STIGTER, C. AND J. SIEMONS — Calculation of longitudinal salt distribution in estuaries as function of time, Delft Hydr. Lab. Publ. 52, 1967.

[21] TRACOR — Estuarine modelling, an assessment, Env. Prot. Agency, Water Quality Office, Washington 1971.

[22] Türkel, E. L. — Frontal motion in the atmosphere, Courant Inst. Math. Sci., New York Univ., Rep. IMM 385 (1970).

[23] Vasiliev, O. F., V. I. Kvon and R. T. Chernyshova — Mathematical modelling of the thermal pollution of a water body, IAHR Congr. Istanbul 1973, B 17.

[24] Vreugdenhil, C. B. — Computation of gravity currents in estuaries, Thesis Delft 1970, also Delft Hydr. Lab. Publ. no. 86, 1970.

[25] Wada, A. — Numerical analysis of distribution of flow and thermal diffusion caused by outfall of cooling water, IAHR Congr. Kyoto 1969, C 36.

Appendix 1. Notation

$a_{1,2}$ = thickness of layer 1, 2
A = cross-sectional area
c_i = propagation velocity, internal waves
c_s = propagation velocity, surface waves
D = dispersion coefficient
e = kinetic energy of turbulence
g = acceleration due to gravity
$G(z)$ = weighting function
h = depth of water
k_b = frictional coefficient, bottom stress
k_i = frictional coefficient, interfacial stress
l = length scale, turbulence
L = length scale, overall flow pattern
p = pressure
Rf = Richardson flux number
Ri = Richardson gradient number
t = time
T = time scale, overall flow pattern
T = vertical turbulent salt flux
u = velocity in x-direction
$u_{1,2}$ = mean velocity in layers 1, 2
u' = turbulent fluctuation of u
v = velocity in y-direction
w = velocity in z-direction
w' = turbulent fluctuation of w
$W(z)$ = weighting function
x = longitudinal coordinate
y = lateral coordinate
z = vertical coordinate
z_b = bottom level
Δt = time step
Δx = mesh width in x-direction
Δy = mesh width in y-direction
Δz = mesh width in z-direction
Δp = density difference
ε = eddy viscosity

113

ε_σ = turbulent diffusion coefficient, salt

ρ = density

$\rho_{1,2}$ = mean density in layers 1, 2

σ = density exceeding that of fresh water

σ' = turbulent fluctuation of σ

τ_b = bottom stress

τ_i = interfacial stress

τ_{xz} = turbulent shear stress

The use of hydraulic models for the study of salt-fresh water currents in aid of measures to prevent salt water penetration

by ir. P. A. Kolkman

1 Introduction

Physical models are used when the laws that govern the actual conditions are known and — by applying known scale conversion factors — can be related to phenomena occurring in the model. These models are particularly suitable when the peripheral conditions can be reproduced in the model relatively simply; for water flow these conditions include, for example, the configuration of the river, coast and canal profiles, tidal movements, river discharge, and so on. Various magnitudes within the area covered by the model can then be found by measurement. It has been shown that water flow models (hydraulic models) are often the best suited to reproduce flow phenomena, though even here there are certain limitations. Since water is the medium used for flow in the model, allowance has always to be made for the fact that, for instance, the viscosity of the water in the model may be having a disproportional influence; in some cases the surface tension is too high, and this again poses a limitation.

We find that the scale conversion factors used in reproducing free surface water flow remain valid when the flow of two media of differing density has to be reproduced. This applies to both stratified flow and to mixture phenomena of the two media; however the difference in the rate of movement between the layers is often smaller by one order of magnitude than the flow-rate over the ground, and because of this the effect of the viscosity is more readily noticeable.

In certain cases, as when reproducing a large area which features slowly-varying stratification or mixing, it is possible to use a model that is compressed horizontally in relation to the vertical scale chosen; this can compensate to some extent for the excessive viscosity effect in the model.

In what follows we shall see, from practical examples, that the model technique has a host of applications. Our examples cover both studies connected with the forecasting of flow patterns and salt-water intrusion in harbours and estuaries, and investigations into technical means of as far as possible preventing salt water from penetrating through engineering works.

Without going into any details it can be stated here that the same scaling laws apply to density differences between fluids due to salt and fresh water, due to contamination or due to temperature differences; likewise air currents, such as draughts or smoke extraction in air with a thermal stratification, can be studied not only by means of air models but — sometimes even more effectively — also with water models.

Another sphere we shall not enter into here is the flow pattern of salt and fresh water in porous media. These flow patterns can sometimes be studied very well in models, but because the timescale is longer molecular diffusion can play, relatively speaking, a far more important part. This cannot be reproduced in a model, although it is frequently sufficient to apply a correction factor to the results of measurement.

2 Scaling laws

A number of examples will serve to demonstrate the laws used for calculations of scale. In working out the scaling laws it is assumed that the flow pattern is shown completely conform in the model, and we look to see what the conditions for velocity scale and time scale are that will provide a clear picture of the true values for all the pressures and shear stresses in the fluid.

2.1 Stratified flow, marked by small vertical accelerations and thus approaching a hydrostatic pressure distribution; ideal case without friction. The acceleration of a water particle in the upper layer may be written as:

$$\frac{du_1}{dt} = \frac{\partial u_1}{\partial t} + u_1 \frac{\partial u_1}{\partial x} \tag{1}$$

If a similar condition is to be shown in the model as well, then we take it that all the factors u_1, u_2, t(time) that occur in the model are, in the model, a value n_{u_1}, n_{u_2}, n_t-times as large (it is found that if $n_x = n_z =$ longitudinal scale of, for example, $1 : 10$ or $1 : 100$, then n_u and n_t are also $\ll 1$). Coupled with the acceleration is a pressure gradient in the x-direction that causes this acceleration.
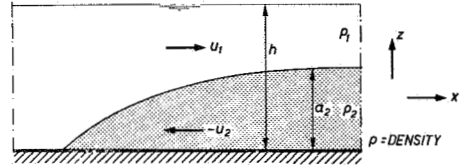
Figure 1. Two-layer flow.

$$-\left(\frac{\partial p}{\partial x}\right)_1 = -\rho_1 g \frac{\partial h}{\partial x} = \rho_1 \frac{\partial u_1}{\partial t} + \rho_1 u_1 \frac{\partial u_1}{\partial x} \tag{2}$$

If this equation (2) is also to be satisfied in the model, then we must have (h being reduced on the same scale as all factors in the z-direction):

$$n_{\rho_1} n_g \frac{n_z}{n_x} = \rho_1 \frac{n_{u_1}}{n_t} = n_{\rho_1} \frac{n_{u1}^2}{n_x} \tag{3}$$

n_{ρ_1} is of no concern here, but we have found:

$$n_t = n_x/n_{u_1} \tag{4}$$

$$n_{u_1} = \sqrt{n_g} \cdot n_z \tag{5}$$

We can also write (5) in a different way, as:

$$n\left(\frac{u_1}{\sqrt{gh}}\right) = n_{F_r} = 1, \text{ or}$$

the (external) Froude number must be equal in the model to that in the prototype $(F_r = u/\sqrt{gh})$.

We now continue with the examination of the lower layer:

$$-\left(\frac{dp}{dx}\right)_2 = -\rho_1 g \frac{dh}{dx} - (\rho_2 - \rho_1) g \frac{da_2}{dx} = \rho_2 \frac{\partial u_2}{\partial t} +$$

$$+ \rho_2 u_2 \frac{\partial u_2}{\partial x} \tag{6}$$

It is now seen that all pressure gradients and the acceleration terms coupled with them have, in the model as well, the same relation to each other when:

$$n_{\rho_1} = n_{\rho_2} \tag{7}$$

$$n_{u_2} = \sqrt{n_g} \cdot h_2 \tag{8}$$

(8) and (5) thus give the same velocity scale for the flow in the upper and the lower layers.

The time scale using (4) also remains valid.

In fact we have still made no use of a length scale in the model: n_x and n_z still could be selected independently of each other. The velocity scale is coupled solely to the height scale, and the time scale derives from the ratio between the length scale and the velocity scale. This does not however mean that, as we are assuming that there is a hydrostatic pressure distribution in the fluid, we can just make a distorted model.

It means that a distorted model may be used only on condition that the vertical accelerations are small (which in practice means that the vertical velocities, too, have to be small). There can be no abrupt steps in the river or sea bottom, while in a distorted model all eddies with a

Figure 2. Two-layer flow with friction.

horizontal axis (inclusing, for example, the spiral current that occurs in bends) are not reproduced accurately.

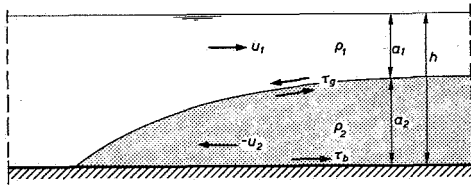## 2.2 Stratified flow with effect of shear stresses along the bottom and at the interface. Equation (2) now becomes:

$$-\left(\frac{\partial p}{\partial x}\right)_1 - \frac{\tau_g}{a_1} = \rho_1 \frac{\partial u_1}{\partial t} + \rho_1 u_1 \frac{\partial u_1}{\partial x} \tag{9}$$

If the force relationships in model and prototype are to correspond, then again we must have $n_p = n_{\tau_g} \cdot \dfrac{n_z}{n_x}$, and thus:

$$n_{\tau_g} = n_p \cdot \frac{n_z}{n_x} = n_{\rho_1} n_{u_1}^2 \frac{n_z}{n_x} \tag{10}$$

If we look also at the equation for the lower layer, we find that this scale must also be valid for the shear stress on the bottom.

In a flow where the viscosity can be ignored, the roughness of the bottom and the corrugations waves and turbulence at the interface will determine τ; the shear stresses are then proportional to the square of the velocity (or differential velocity).

$$\tau = \lambda \cdot \rho \cdot u^2 \text{ and thus } n_\tau = n_\lambda \cdot n_u^2 \cdot n_\rho \tag{11}$$

If the model is not contracted, i.e. $n_x = n_z$, and if the viscosity is to be ignored, then the λ in the model is seen to be as large as in the prototype, and it follows from (11) that equation (10) is satisfied.
If the effect of viscosity in the model is too great, then n_λ is greater than unity.
In a distorted model we find, as a condition for λ (cf (10) and (11)):

$$n_\lambda = \frac{n_z}{n_x} \tag{12}$$

It is normal practice, with distorted models, to provide extra bottom roughness. Resistance bars are also used, which affect the flow in both the upper and lower layer. The extra roughness required is, furthermore, a means of applying empirical correction to the model where it is found that — through the distorsion or because there has been a change in the topography of the bottom in the prototype in the meantime — a flow condition measured 'in nature' is not being completely reproduced in the model.

120

It is also possible to correct to some extent a λ that is wrong in the model because of the viscosity effect: the advantage of a contracted model is that the λ can also be reduced (this being usually no longer possible in a non-contracted model).

2.3 Flow with substantial vertical velocities

If a flow pattern is no longer approximately stratified, then it can be deduced from the comparison of three-dimensional movement that, provided that viscosity does not have any substantial effect, this pattern can be reproduced in a model. The scale of velocities follows, again, from the condition at the free surface, that is:

$$n_u = \sqrt{n_g n_z} = \sqrt{n_g n_x}, \text{ and furthermore we must again have}$$

$$n_{\rho_1} = n_{\rho_2} = 1$$

The illustration below shows that where the flow has substantial vertical velocities, the distortion does lead to false results.

Since the two models are identical, the flow pattern will be unaffected by the contraction.

UNDISTORTED
MODEL

HORIZONTALLY
CONTRACTED
MODEL
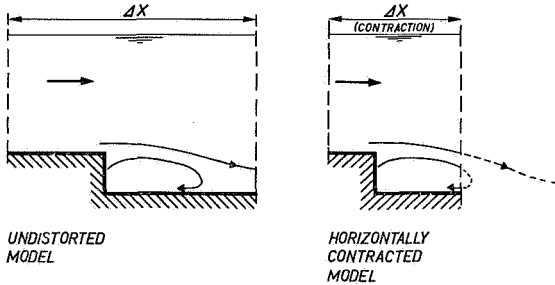
Figure 3. Flow at step in bottom; model with and without contraction.

2.4 Flow where disturbance at the free water surface plays no part

In a fairly large number of cases disturbances in the free water surface prove to have only a minor influence on the flow pattern, and in such a case there is no need to satisfy the condition used for (3) that these disturbances have to be reproduced on the height scale of the model. This applies also to flows in a closed pipe.
For the case, already discussed, of the two-layer flow we can illustrate this by comparing (2) and (6), which can now be written as
Upper layer:

$$-\left(\frac{dp}{dx}\right)_1 = \rho_1 \frac{\partial u_1}{\partial t} + \rho_1 u_1 \frac{\partial u_1}{\partial x}$$

121

Lower layer:

$$-\left(\frac{\partial p}{\partial x}\right)_2 = -\left(\frac{\partial p}{\partial x}\right)_1 - (\rho_2 - \rho_1)\, g\, \frac{\partial a_2}{\partial x} = \rho_2 \frac{\partial u_2}{\partial t} +$$

$$+ \rho_2 u_2\, \frac{\partial u_2}{\partial x}$$

If it is now further assumed that $\rho_2 - \rho_1 = \Delta\rho$ is small in respect to ρ_1 and ρ_2, then only the following condition applies for the velocity scale

$$n_{u_1}^2 = n_{u_2}^2 = \frac{n_{\Delta\rho}}{n_\rho} \cdot n_g \cdot n_z \tag{13}$$

while there is no longer any need to satisfy $n_u = \sqrt{n_g \cdot n_z}$ and $n_{\rho_1} = n_{\rho_2}$.
We can also write this differently, as:

$$n\left(\frac{u}{\sqrt{\dfrac{\Delta\rho}{\rho}\, gh}}\right) = n_{F_i} = 1 \qquad , \text{or} \tag{14}$$

the internal Froude number $F_i = u / \sqrt{\dfrac{\Delta\rho}{\rho}\, gh}$ must have the same value in the model
as it does in the prototype.

This internal Froude number is extremely important, since many phenomena that are connected with, for example, selective water extraction from the upper or lower layer or with mixing phenomena can be expressed in nondimensional parameters where the internal Froude number is seen to be the only hydrodynamic parameter (the others being geometrical).

Example: velocity and concentration at the centre of a freshwater jet spilling into salt water (salt concentration at orifice c_0, velocity at orifice v_0, diameter of orifice D, distance from orifice x):

$$\frac{c}{c_0} = f_1\left(\frac{x}{D},\ \frac{v_0}{\sqrt{\dfrac{\Delta\rho}{\rho}\cdot g \cdot D}}\right) = f_1\left(\frac{x}{D},\ F_{intern}\right)$$

$$\frac{v}{v_0} = f_2\left(\frac{x}{D},\ \frac{v_0}{\sqrt{\dfrac{\Delta\rho}{\rho}\cdot g \cdot D}}\right) = f_2\left(\frac{x}{D},\ F_{intern}\right)$$
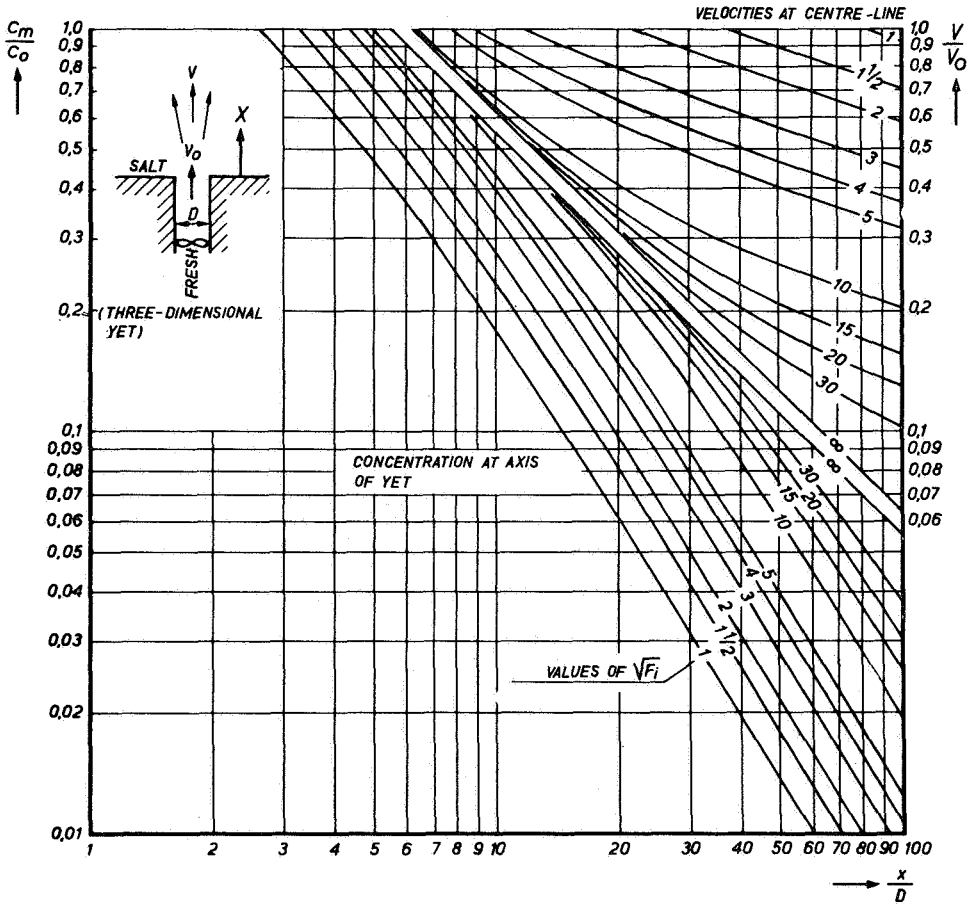
Figure 4. Velocity and concentration at axis of an upard jet of fresh water in a salt-water medium.

2.5 Influence of viscosity in a distorted model

How small the model may be made depends on the influence of the viscosity forces to which a water particle is subjected — these cannot, for instance, become dominant in the model if such is not the case in reality. Shear stresses occur in the fluid, caused by the velocity gradients in the fluid, e.g. with declining velocities parallel to the bottom

$$\tau = \mu \frac{\partial u}{\partial z} \tag{15}$$

These shear stresses must, in their nature, be clearly related to the pressures, so that $n_\tau = n_p$. Now, we had already found in (2) that:

$$\frac{n_p}{n_x} = n_{\rho_1} \frac{n_{u1}^2}{n_x} \text{ or } n_p = n_{\rho_1} \cdot n_u^2$$

123

If we introduce $n_p = n_\tau$, then it folllows from (10) that:

$$n_\mu \cdot \frac{n_u}{n_z} = n_\rho \cdot n_u{}^2 \text{ or } \frac{n_\mu}{n_\rho} = n_u\, n_x \tag{16}$$

This condition is also written as follows for the case where $n_x = n_z = n_L$

$$n_{Re} = n\left(\frac{u \cdot L}{\mu/\rho}\right) = 1 \tag{17}$$

The Reynolds number $\left(R_e = \dfrac{u \cdot L}{\mu/\rho}\right)$ must be the same in the model as in the proto-type.

This does not have to be so if the viscosity forces in the prototype, as well as in the model, have only a relatively slight effect on the accelerations of a particle of water, that is to say if the Reynolds number is large enough. Where the limit value lies has to be discovered experimentally for various circumstances.

The velocity scale deriving from (17) is wholly contradictory to what we found in (5) for models with free surface flow, and what was again found via (8) for stratified free surface flow; scaling laws are therefore valid for a flow with a free surface or for stratified flow only in those cases where the effect of viscosity is negligible in both the prototype and the model.

3 Models applied to the problems of rivers and estuaries

3.1 Tidal flume

This flume [1], with a height of 0.50 m, a width of 0.67 m and a length variable up to 100 m, is fed at the upstream end with a permanent discharge of fresh water, and
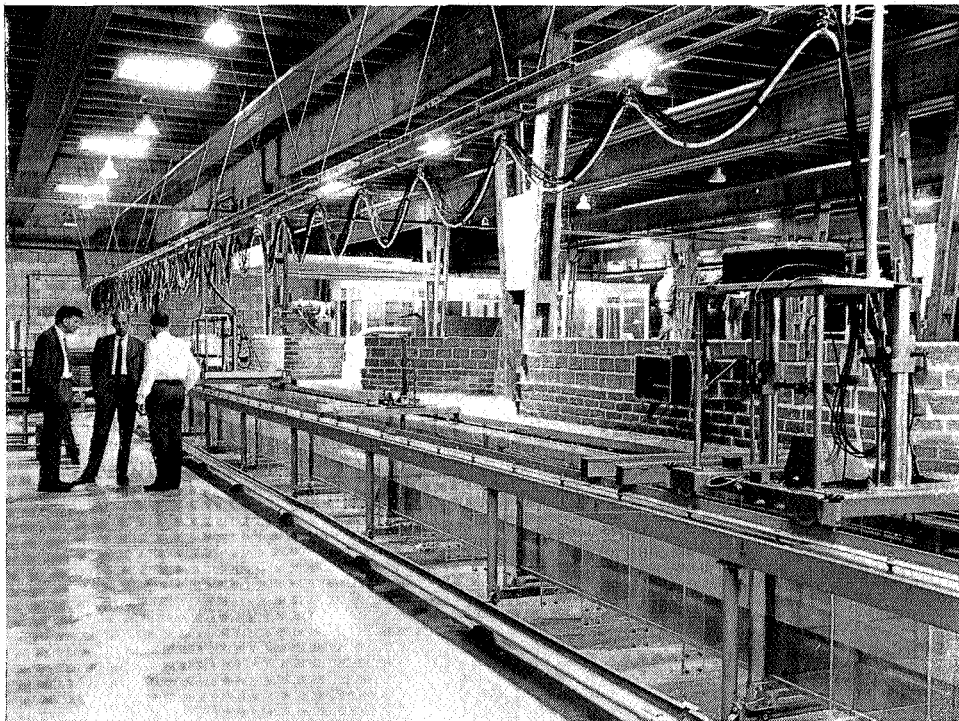
Figure 5. General view of tidal flume.

opens into a salt-water basin in which a pure periodic vertical tide is induced. The flume serves a number of functions, and can be regarded as:

a   a model in which, by systematic variations in the tidal period, tidal amplitude, flume length, water depth, upper water discharge and density difference between salt and fresh water, there is implicitly also a variation in the extent of the distorsion. The

125

effect the distorsion has on the degree of salt intrusion, local mixing, etc. can be studied in this way.

b a model that can be used to determine coefficients to be used in a mathematical model.

c a model to further develop model technique in respect of distorted models, with the application of bottom roughness, bars reaching up into the upper layer, and air bubbles. These devices will affect simultaneously both the flow resistance and the mixing of the fluids.

d a very simplified model of the Nieuwe Waterweg.
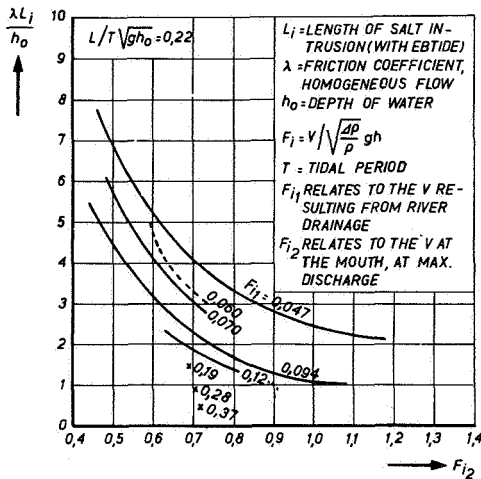
Figure 6. Salt intrusion length, measured with systematic variation of parameters.

It will be seen from fig. 6 that a model that is distorted in the horizontal direction still gives virtually the same results as one that is undistorted. The distorsion takes the form of a shortening of the flume and a speeding-up of the tidal period, the wavelength of the tidal wave being reduced in proportion to the length of the flume.

3.2 Lower river reaches and Europoort model

The tidal model [2], included reproduction of density currents, was built to serve the needs of shipping in the Europoort. On the one hand the final design had to be such that even large tankers and carriers of considerable draught could enter the port without excessive difficulty from currents and bank suction, while on the other the building programme had to be arranged so that the harbour would not be temporarily less accessible while building was going on. The flow pattern to be expected is, alone, a highly complex affair: the Nieuwe Waterweg is long (almost infinite), while the Caland Canal is of limited length so that the tidal wave reflects in a different time and

126

cross-currents varying with time occur; moreover, the freshwater upper outflow in the Nieuwe Waterweg plays an important role, the condition at the mouth is partway between stratified and mixed, and the fresher upper water upstream will to a certain extent also penetrate into the Caland Canal.

Figure 7.   Area reproduced in model.

Fig 7 shows the area reproduced in a tidal model with salt seawater and fresh river-water, with a vertical scale of 1 : 64 (i.e. with a velocity scale of $\sqrt{n_g \cdot n_z} = 8$) and a horizontal scale of 1 : 640 (i.e. time scale $n_t = n_x/n_v = 80$). Though we have not so far mentioned this, the greatly reduced time-scale is also one of the advantages of distorted models, in that it makes information available relatively rapidly. This is important, because some measurements have to be collected in a very laborious manner; the local discharge during the tide is obtained by measuring the velocity at many points on a transverse profile, and the same holds for measuring the amount of salinity penetrating into the waterway. The compressed time-scale makes it possible to provide a number of consecutive tides on a single day, so that each time only part of the local velocities or salt contents need be measured.
The velocities are measured by taking photographs, with a given exposure time, of

the tracks followed by floats; the length of the floats is varied within the range of draught of the ships using the waters.

Figure 8. Harbours area, with mobile salinity pick-up (for measuring the salt vertical).
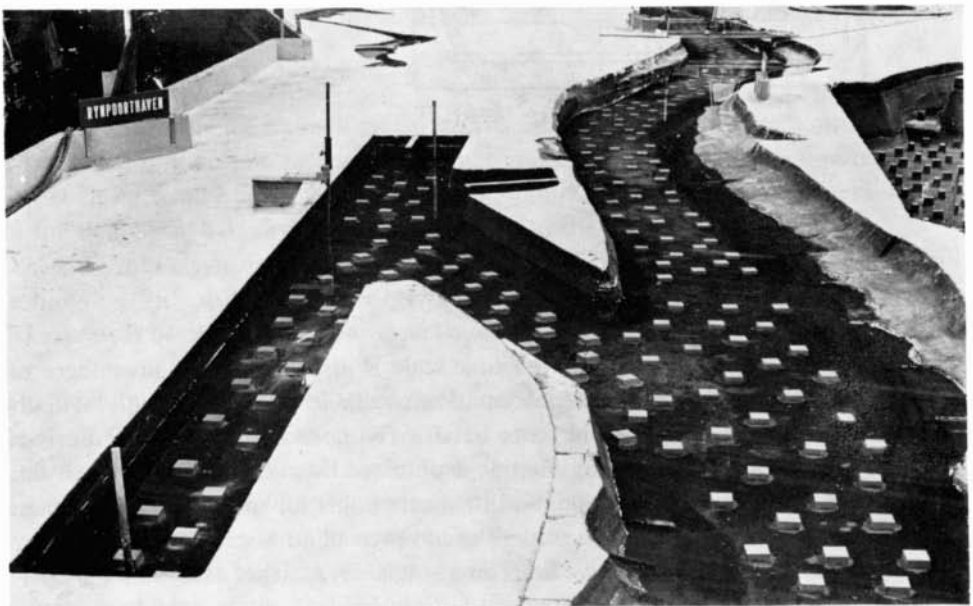

Figure 9. Blocks on bottom, creating artifical roughness.

As has already been mentioned, the immediate reason for constructing the model was for dealing with problems at the harbour mouth of the Europoort, an important consideration being to have a working model available while construction was going on. The design of the model was, however, to be so arranged that a satisfactory reproduction of salt and current conditions further inland would also be attainable, to allow the effect of the works on salt penetration (and any other water conservation problems) to be studied. From information now available it is found that this reproduction is better than would appear to be the case from studies of principle in the tidal flume. An important consideration here is probably that as a result of all the dock areas, the groins, the irregular profile of the river, etc. the flow is far more turbulent than in the tidal flume, so that the viscosity of the water itself plays a subordinate role in the model. Now that the works around the Europoort are coming to an end, it is becoming possible to investigate the salinity in the rivers, and the changes occurring in this through harbour berths, the building of bars and so on. One study that has been made, for instance, was of the extent to which an open link between the Hartel Canal and the Oude Maas affects the tide and the associated salt intrusion: this was in connexion with drinking-water supplies to Berenplaat, which are taken from slightly south of the branch of the Hartel Canal and the Oude Maas.

4 Models applied to the development of locks having a low level of salt-water leakage

One of the main sources of salt contamination of our fresh waters in the western part of the Netherlands is — apart from seepage — the salt water that enters through a lock each time a vessel passes through.

Every time a vessel locks through, the lock chamber is levelled; and whenever the level of the sea is higher than that of the canal a layer of salt water (the 'lockage water') is taken into the chamber; the lockage water is then allowed to flow out into the canal, and consits of the water in the chamber with an admixture of salt. The lock problem is not, however, the most serious; it can be overcome by never emptying the chamber into the canal, but instead returning the lockage water to the sea using pumps. Far more difficult is the problem of 'exchange currents'; if the fresh water in the chamber is at the same level as the seawater, and the sea-gates of the lock are opened, then the salt seawater sinks down beneath the fresh water and a den-

Figure 10. Salt intrusion through a sea-lock.

sity current is set up. Eventually the water in the lock chamber becomes entirely salt; when, during a subsequent locking operation, the canal-gates (on the freshwater side) are opened the salt water in the lock sinks down and flows out over the bed of the canal, in time mixing with and contaminating the fresh water (see Fig. 10).

If no preventive measures are taken at a lock, the volume of salt that can be stored up in the lock chamber between sea level and the floor of the chamber passes out into the freshwater reach. Various systems have been developed for combatting this, and model tests have played an important part in perfecting them.

4.1 Air-bubble (pneumatic) screens

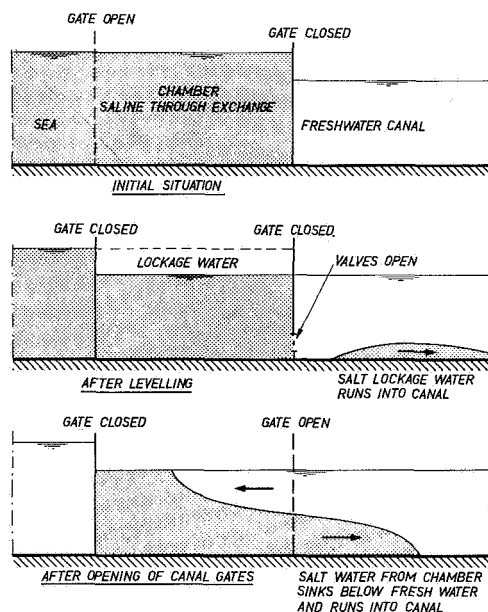Working from the fact as the salt water 'sinks' a two-layer flow is set up with velocities
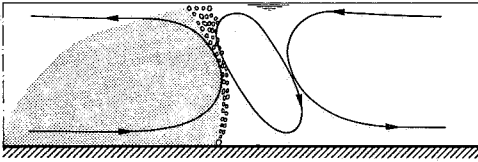
130

Figure 11. Principle of pneumatic barrier.

in different directions, the exchanging of particles moving in one direction with particles moving in the other direction will act as a brake [3]. This exchange is brought about by setting up a screen of air bubbles rising from the bottom. An important condition for this 'delaying' system is that the lock-gates should not remain open for too long a time, otherwise all the salt will eventually get through.

4.2 Direct drawing-off of the 'tongue' of salt water that flows out into the freshwater reach

This is done by arranging an extractor slot in the canal bottom on the freshwater side of the lock gates. The extraction rate at which no salt water gets into the reach, the
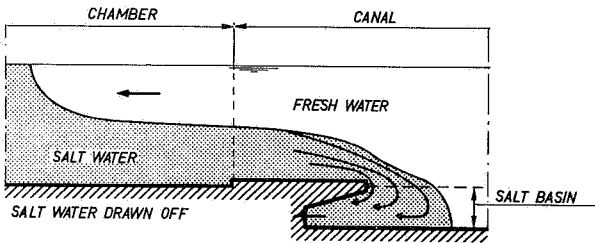

Figure 12. Direct drawing-off of the salt 'tongue'.

optimum shape for the slot and the effects of shipping can be accurately found from models.

Model research makes it possible simultaneously to study mixing, the speed at which the salt-water tongue moves, the extraction efficiency, etc.; and at the same time a study can be made of the problems likely to result for shipping from the locking procedure, the stratified flow pattern and the drawing-off of the salt water.

4.3 Pumping-out the salt water from the lock via the chamber bottom, simultaneously topping-up with fresh water at the top

This prevents any salinity at all from escaping into the freshwater reach when the lock gates on the canal side are opened. This system was very thoroughly studied under laboratory conditions while investigating ways of protecting the Delta waters when locks were being built at Kreekrakdam on the Antwerp/Rhine Link [4]. The

system stands or falls by a sound design for the bottom and walls of the chamber, in order that there shall be no oscillation at the boundary between the salt and fresh water (and thus a minimum of mixing). This system was first applied in France, for the lock at Dunkirk [5].
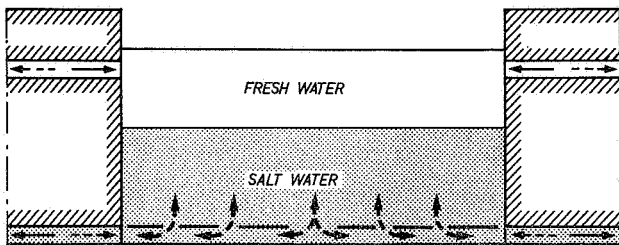

Figure 13. Exchanging chamber water with gates closed.

Before the system was used there was a separate investigation to discover to what scale such a model can be reduced. At the scale chosen, 1 : 30, it is found that all phenomena can still be satisfactorily reproduced; at most, the salt contamination of the fresh water at the top is slightly underestimated.

With both system 2 and system 3 it is possible, when locking a vessel through in the opposite direction to return the fresh water in the lock chamber back to the freshwater reach of the canal by letting in salt water through the bottom and allowing the fresh water to overflow at the top. It is found that with system 2, where a two-layer current is set up and maintained for longish periods, there is however so much mixing action that the fresh water in the lock chamber is appreciably contaminated with salt.

With both systems ships moored in the lock must, to reduce mixing to a minimum, not be allowed to keep their screws running.

We have seen, in the foregoing, how the difference in salinity in the adjoining reaches at a lock can prompt extra preventive measures. We have also said that if no precautions are taken an exchange current will be set up as the gates are opened, which will cause problems for vessels on the move.

This exchange current, occurring as the gates open, can also give rise to very substantial loads on mooring lines: yet even with the gates closed most systems for filling the chamber with the lockage water are highly vulnerable to density differences. If, for example, a chamber of fresh water is being topped up with salt water, the latter will flow across the chamber bottom and the fresh water will be forced up behind the vessel which will be, so to speak, 'sucked' up towards the gates. The reverse will happen when fresh water is let into a chamber of salt water.

132

5 The effect of density differences on the current pattern occurring during sluicing

The current pattern during sluicing is of importance from the viewpoint of ground-scouring and, because this happens in waters used by shipping, of the problems caused to vessels. A physical model has, again, often been used — very profitably — for studying these phenomena. In all the cases investigated the circumstances were those of sluicing (relatively) fresh water in a salt-water dock basin — the IJmuiden sluice, the Den Helder pumping station, the drainage ducts at the sea-lock at Terneuzen, the yacht harbour at Scheveningen, and many others. When the sluicing takes place at high flow-rates there is no great change from the homogeneous state; but at slow speeds the fresh water is forced back up to the upper layer while the salt water either remains stationary or is éven drawn towards the sluice. In the first instance we get an 'oil-patch' current pattern. Only when the current persists for a long time is it also possible for eddies to appear.
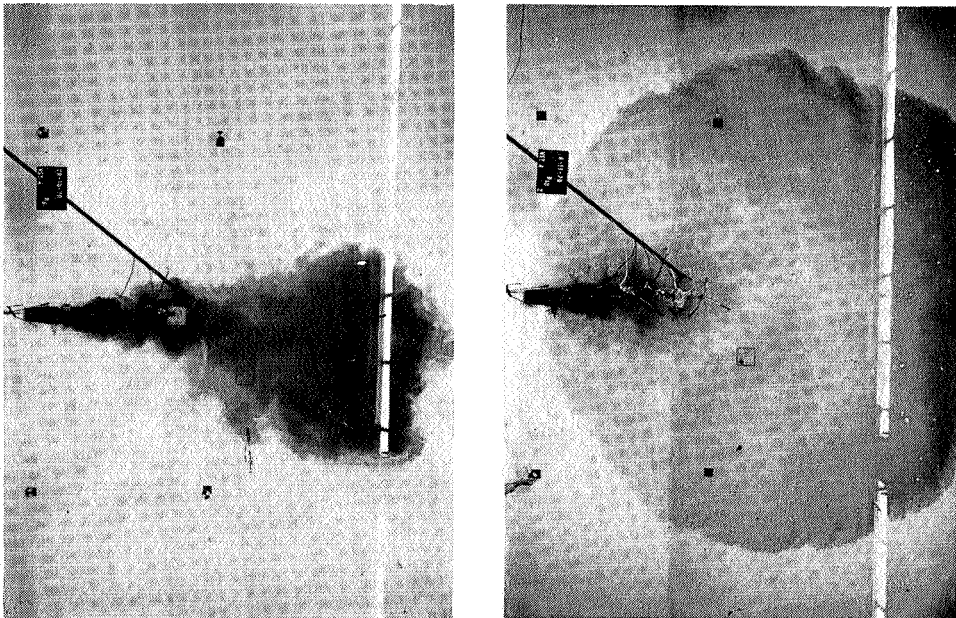

Figure 14.   An oil-patch current pattern compared to a normal pattern at an outlet (similar test with and without density differences).

6 Selective extraction from a stratified system

When combatting intrusive salt water, the two principles to be considered are flushing-through and selective extraction.

The former has to be used where the system is 'mixed,' i.e. in, say, a canal the salt content in one particular cross-section is virtually homogeneous, and varies only along the length of the canal. Flushing-through is effectual where the speed of the water is greater than the rate of saline intrusion through diffusion (consisting of molecular and turbulence diffusion).

In general, flushing-through in nature involves only low flow-rates, so that reproducing the associated turbulence in models is hardly feasible.

Selective extraction from a stratified system is possible provided that the suction nozzle is positioned deep enough below the interface, and the drawing-off rate is not too high. Even quite smal-scale models offer very good opportunities for developing an optimum design, and for finding out how much water is taken from the upper layer as well if the critical extraction rates are exceeded.

Fig. 15 shows, in a two-dimensional example of selective extraction, the relationship between the circumstances and the percentage of fresh water that is drawn off together with the salt.

The dimensionless presentation makes it possible to see how tests carried out with various density differences match each other; this is also an indication that the model technique hardly gives rise to scale deviations in the results.

Fig. 16 illustrates the results of an investigation of current inflow to deep-sited orifices, in relation to the selective draining-off of intrusive salt water. The case in question involved the recently built pumping station at Den Helder, where water from the Noord-Hollands Canal is pumped or discharged into the sea. It was intended to make use of this pumping station to remove all the salt penetration taking place through the locks
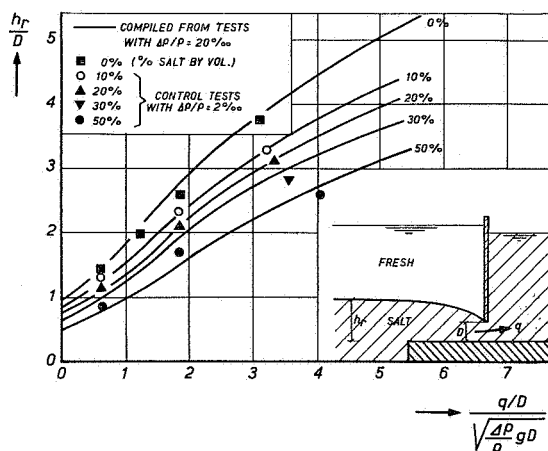

Figure 15. Percentage of fresh water carried out from upper layer during selective extraction.
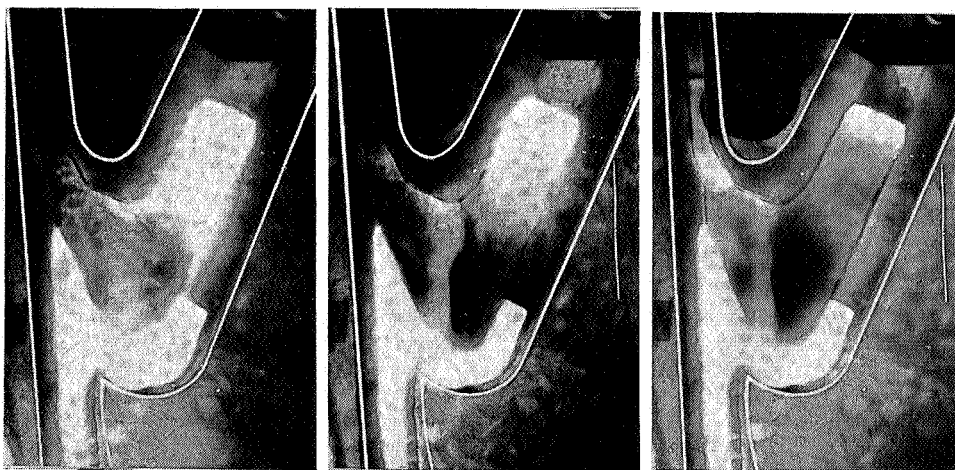
134
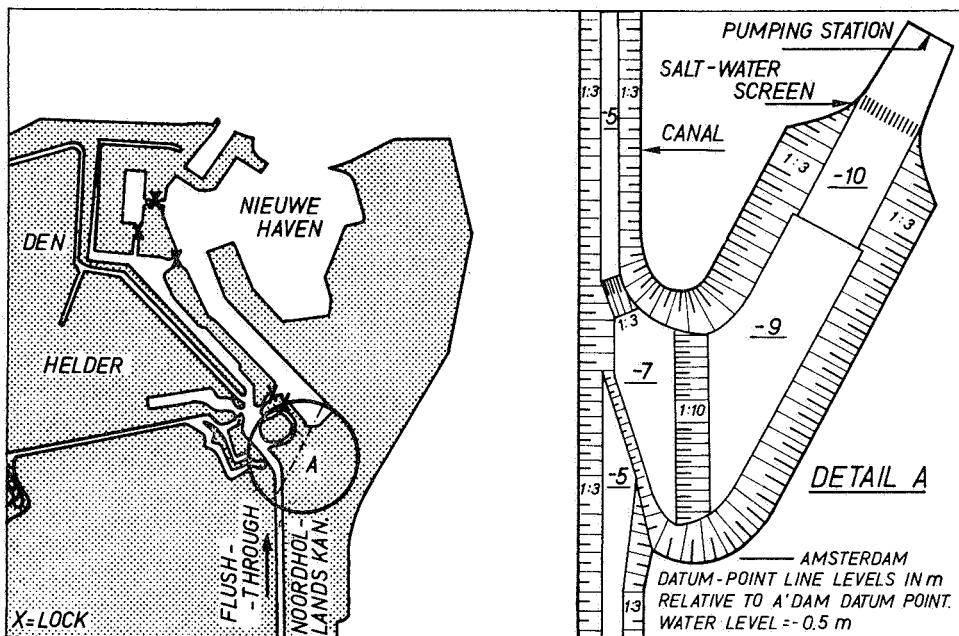
Figure 16. Pumping station at Den Helder, with salt water pit and barrier; test using salt water with stain.

135
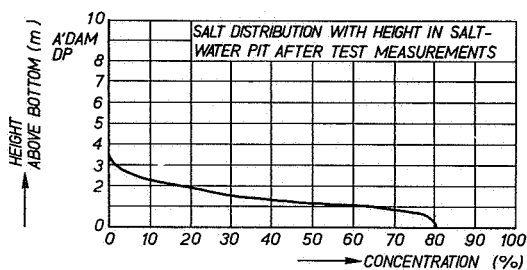
lying to the north of the plant. In broad terms, therefore, the canal north of the pumping station is more heavily saline than that to the south, the salt water tending to run into the freshwater canal as an undercurrent, with a northwards freshwater current set up in the upper layer. The salt undercurrent is now led off sideways into the branch, after which this current is forced to go round a curve. The curve results in the interface becoming inclined. In order to prevent the salt water from being able to run into the canal by the inclination of the interface, the curve is at some distance from the canal bank. Tests were carried out at a scale of 1 : 20, shutting off the northern canal pound with a partition, filling it with salt water and then removing the partition. The test was repeated at various salt concentrations, and it was found that there was no saline contamination of the southern canal reach, and also that the salt water in the deep part is to some extent mixed with fresh water. The mixing proves to be the same at the various salinity levels, and this is in line with the scaling laws applied. It has also been found, now the pumping station has been in operation for a few years, that salt penetration to the south of the station is hardly noticeable any more.

7 Conclusion

In the foregoing we have looked at the varying kinds of problem that arise in the prevention of saline intrusion, and the opportunities offered by model testing for finding optimum solutions and making sound forecasts. One may expect that the possibilities provided by this technique will develop further. Since similar problems arise with other flow phenomena where density differences have a part to play — such as coolant water currents, warm/cold currents in air (smoke distribution, draught patterns etc.), flow patterns in heat-exchangers, and so on — it is reasonable to assume that the range of application of such models will widen still further.

Literature

[1] B. P. Rigter. 'Minimum Length of Salt Intrusion in Estuaries', Journal of the Hydr. Div. A.S.C.E. HY, 9 Sep. 1973.

[2] A. J. van Rees, P. v. d. Kuur, H. J. Stroband. 'Experiences with tidal tidal salinity model Europoort', Proc. 13th Coastal Eng. Conf., Vancouver 1972, Vol. III, Chapter 135.

[3] G. Abraham and P. v. d. Burgh. 'Reduction of Salt Water Intrusion through Locks by Pneumatic Barriers', Delft Hydraulics Laboratory, Publication No. 28 and Rijkswaterstaat Communications No. 17.

[4] P. A. A. Volker, F. J. de Vos, P. Blokland. 'Netherlands Contribution at the 22nd Int. Navigation Congress of PIANC', Paris 1969, Sect. I, Sub. 3.

[5] G. Ribes and C. Blanchet. 'Les courants de densité et le projet de l'écluse de Mardyck à Dunkerque', La Houille Blanche 1965, No. 1, pp. 48–52.

Synthesis and its application to practical problems

by Prof. dr. ir. J. C. Schönfeld

1 Introduction

Let us start by recapitulating the lectures and the areas they covered within the framework of this conference, which was set up to deal with the following subjects interrelated as shown:

```
                    ┌─────────────────┐
                    │    Technical    │
                    │  problems and   │
                    │    solutions    │
                    └─────────────────┘
                             ↓
                             ↑
┌──────────────┐    ┌─────────────────┐    ┌──────────────┐
│  Laboratory  │────│    Analysis     │────│ Computation  │
│   research   │    │    synthesis    │    │   methods    │
└──────────────┘    └─────────────────┘    └──────────────┘
                             │
                    ┌─────────────────┐
                    │     On-site     │
                    │  measurements   │
                    └─────────────────┘
```
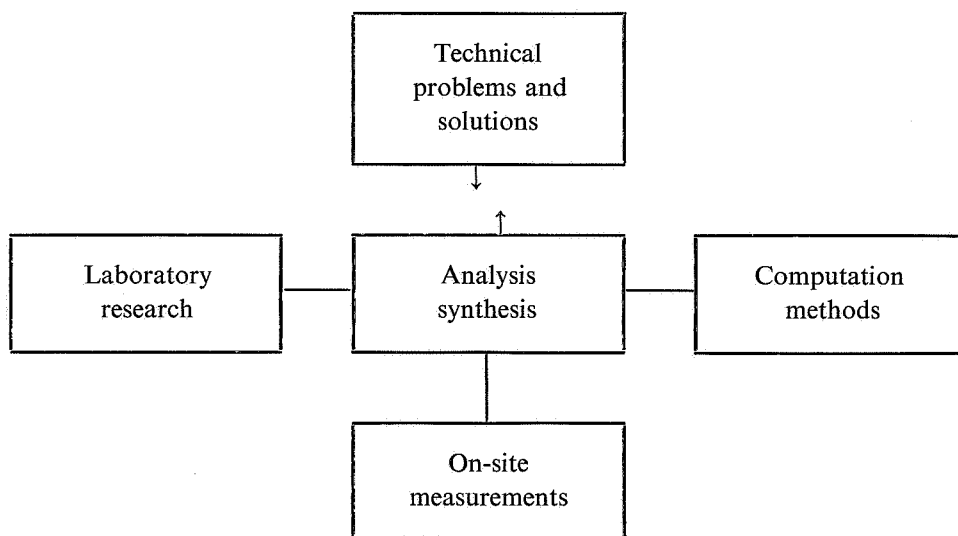
In the first lecture Ir. Blumenthal gave us an outline of the technical problems which we are considering here; they spring from the physical phenomena observed when salt occurs in surface water.

We then came to the analysis of the phenomena associated with the movements of salt and fresh water and their mixing. These phenomena were described to us by Dr. Abraham in the second lecture. He showed us that analysis led to three fields of research and that researchers in each field could help to supply us with the information we needed to solve the technical problems involved.

Then Ir. Langeweg took us out of doors and told us something about on-site measurements and the conclusions that might be drawn from them.

After that Dr. Vreugdenhil came to the computer and told us about developments in modern computation methods.

Lastly, Ir. Kolkman took us to the laboratory and showed us what could be achieved by using hydraulic models.

Having reconnoitred the fields of research, it is now time for us to return to the depar-

ture points of the analysis and try and consolidate our observations. Before attempting to do so, let us recall the two most important aspects of the salt and fresh water problem which emerged from the analysis.

The first was flow. It included the movements of fresh water originating from precipitation and brought down by the rivers, the movements of salt water from the sea, and also the relative movements, for instance of a layer of fresh water and a layer of salt water underneath it. In this context salt water and fresh water were regarded as two completely different fluids.

The second aspect of the salt and fresh water problem was that of mixing. The mixing of salt and fresh water resulted in brackish water, in a range of salinities extending from those of rain or river water to those of sea water.

Salt and fresh water phenomena have a far-reaching, and as a rule, upsetting effect on water management. Generally speaking, there are three items on the debit side: 1. the loss of fresh water; 2. the intrusion of salt water; 3. the mixing of salt and fresh water.

1.   There is a growing demand for fresh water. Supplies, such as precipitation and the international rivers, are decreasing rather than increasing, and they are steadily deteriorating, sometimes to a serious degree. That important commodity, water, is gradually becoming one of the raw materials in short supply, so every drop of fresh water that flows out to sea unused must be regarded in principle as a potential loss.

2.   Every influx of salt water from the sea which supersedes fresh water at a point where the latter is needed constitutes a loss because of the extra cost of obtaining the necessary fresh water from some other place.

3.   The mixing of fresh and salt water also involves a loss, but one which should be distinguished from the other two. If, for instance, 10 % of a quantity of fresh water is replaced by salt water, i.e. without mixing, the loss can be put at 10 %. If on the other hand the intruding 10% of salt water mixes with the remaining 90% of fresh water, the result will be brackish water, water whose quality is impaired by salinity to such an extent that its value may be reduced by very much more than 10 %.

Consequently, those responsible for water management will, generally speaking, have to concentrate on:

1.   Storing fresh water that is not for immediate use;
2.   Combating the intrusion of sea water;
3.   Preventing salt and fresh water mixing.

Measures for achieving 1) and 2), such as building storage basins or closing inlets, present few salt and fresh water problems. It is a different matter where masses of fresh and salt water are so close to each other that the risk of their mixing must be considered. Thorough research into fresh and salt water phenomena is then usually necessary if a technical solution is to be found that will satisfy all three points in an economically acceptable manner. Sea locks are an example.

A better understanding of flow phenomena and of the mixing of salt and fresh water will enable us to lay the foundations for an economically sound water management system.

Let us now summarise the research that has been done into fresh and salt water phenomena, first by considering what has been achieved and then by tentatively sketching developments in the immediate future.

2 Present position

2.1 On-site measurement: interpretation

Any analysis should start from the actual situation. Therefore on-site measurements provide the indispensable basis for research.

Research into fresh and salt water phenomena got well under way in this country around the beginning of the century. Extensive measurements were carried out in those days in the Rotterdam Waterway under Canter Cremers.

So long as the mixing of the two masses of water is a matter of minor importance, the movement of salt and fresh water can be treated as a conventional hydrodynamic problem. The underlying theoretical principles had been worked out at the beginning of the century.

Canter Cremers' great contribution was that he spotted the fundamental factors, especially salt and fresh water currents; others have been able to go forward from his astute beginnings.

Insofar as we may ignore mixing and turbulent friction, there is a good theoretical basis nowadays to explain and forecast salt and fresh water currents.

The mixing of salt and fresh water is a different matter. Mixing is a result of turbulence. At the beginning of the century, people still only had a more or less rudimentary understanding of this phenomenon. Nowadays, thanks to the outcome of an impressive series of experiments and theoretical studies, we know much more about turbulence. Yet the possibilities of applying this knowledge, especially in complicated situations, are still limited, because turbulence is not yet susceptible of general deductive treatment.

As a result, our knowledge is still not sufficient to enable us to find adequate theoretical deductive explanations for natural phenomena and, on the strength of them, make forecasts for future situations.

Since there are no fully satisfactory theoretical deductive models, various attempts have been made to interpret phenomena inductively and empirically, the aim being to extrapolate the results to future situations.

The disadvantage of such an approach is that where there is no adequate theoretical understanding, there is really no basis either for assessing the reliability of extrapolations.

In order to make the inductive empirical interpretation more easily extrapolated, attempts were made to condense the phenomena of several rivers into a single interpretation, so that observations for one river could support an extrapolation for another. It is doubtful, however, whether this really makes extrapolation more reliable. Mixing

phenomena in rivers are very complex and depend on many factors. If there is no clear understanding of the effect of these factors, one must also doubt the admissibility of transferring empirical results from one river to another.

Extrapolations from inductive and empirical results must be viewed with caution in the case of such complicated phenomena as we are dealing with here.

The limited direct value of on-site measurements for forecasting is offset by their indirect value, which is evident when combined with other forms of research.

On-site measurements are an essential basis, both for laboratory research and for computation methods. The observation of conditions in nature has a stimulating and corrective effect on the formation and testing of theories.

2.2   Laboratory research: scale models

The use of hydraulic scale models in hydraulic engineering has become increasingly common, especially since World War I; it was one of the factors that prompted the foundation of the Hydraulics Laboratory.

Scale models afford opportunities for systematic research by varying the parameters. They facilitate the study of the effects of variations in natural conditions, such as tides, river discharges etc. Moreover, all manner of technical solutions can be subjected to comparative examination beforehand in scale models.

Generally speaking, there are far more opportunities for quantitative observation, that is, for measuring, in a laboratory than there are in nature.

A hydraulic scale model is a physical system that closely resembles the real thing, but it reveals its secrets more readily. We can learn a lot about what happens in the prototype by studying models. The model allows of a certain amount of extrapolation of parameters for which no prototype measurements are available.

Scale models have two shortcomings, one of them intrinsic, the other practical.

The intrinsic shortcoming is the need to comply with the laws of scale. Generally speaking, various scale laws must be complied with, and this may involve conflicting requirements. This limits the usefulness of scale models, and may make the admissibility of extrapolations disputable.

A great deal of experience was gained, partly before and especially after World War II, with scale models without density differences. The models with density differences were evolved later.

The simulation of flow is theoretically the same as that in models without density differences. Measuring the density differences does, however, present a practical complication.

Simulation of mixing presents a more fundamental complication. In using scale models in problems where mixing plays a major part, the mixing processes in the model require special attention.

Generally speaking, a model for a particular situation will have to be calibrated, i.e.

the conformity of the model to its prototype must be established. This is only possible where enough on-site measurements are available.

Hydraulic models are a valuable supplement to measurements in nature, both because they contribute to a better understanding of the subject and because they afford more and better possibilities of forecasting.

2.3   Computation methods: schematisation

Like research by models, computation methods got well under way after World War I. The Lorentz Commission in particular did pioneer work in this field in connection with the Zuider Zee. Between the wars various computation methods based on its work were developed in this country for tides and storm surges.

As these methods were extremely labour-intensive, analogue computation techniques began to be developed in World War II. This development resulted in a tidal analogue computer, the Deltar, being specially constructed for the Delta Project. This computer, however, is not designed to deal with density differences, although theoretically this should be possible.

Computation methods using digital computers were developed about ten years later. They are being more and more widely used, especially for problems involving density differences and for fresh and salt water problems.

From now on we will restrict ourselves in this study to digital methods.

The computation method is based on a mathematical model, i.e. on a mathematical description of physical phenomena. The flow aspect (except the effect of friction) can be given its due by constructing the model on conventional hydrodynamic lines. Friction and mixing are usually dependent on the occurrence of turbulence. For the reasons given in 2.1, a more opportunistic approach must be made to problems involving friction and mixing, use being made of empirical and semi-empirical formulas. A numerical model for carrying out the actual computations is then set up from the mathematical model by schematisation, i.e. by more or less disregarding detailed physical information.

The limitations of a computation method lie in the imperfections of the mathematical model on the one hand and in the schematisation of the numerical model on the other. The imperfections of the mathematical model lie chiefly in the manner in which turbulence is represented and are therefore especially important for the mixing aspect. The degree of schematisation depends very much on the financial aspect and is also restricted by the availability of computers and programmes. Computations are still largely being made with fairly highly schematised numerical models, especially one-dimensional models in one, two or more layers. Two and three-dimensional models are being developed but have not yet been used to any great extent for practical problems.

Like scale models, computation models such as those used hitherto need to be calibrated by comparison with on-site measurements.

146

Because of the numerical schematisation, computation models are one step further removed from nature than scale models. Consequently, the usefulness of a computation model depends on the quality of the empirical or semi-empirical formulas for friction and mixing. Computation models are therefore somewhat less satisfactory than scale models.

On the other hand, a computation model is not subject to restrictive scale laws, and this is one of the reasons why it is more flexible. This may be a considerable advantage when extrapolating to new circumstances.

2.4   Combined research: cross-checking

Investigations based on on-site measurements, scale models or computation methods all offer possibilities for extrapolating and forecasting. But each of these methods has its specific limitations and weaknesses, besides its specific advantages.

It might be advisable to choose the most suitable forecasting method for each individual case in the light of circumstances. This does not alter the fact that the reliability of each method is low.

This difficulty can be overcome by comparing two, or possibly more, forecasts made by different methods.

Critical comparison, taking into account specific limitations and sources of error, can make our conclusions more reliable. This operation can be termed cross-checking. This kind of combined dialectical research more or less typifies the extent to which the three fields of hydraulic research have achieved cooperation, especially in the sphere of fresh and salt water phenomena.

3 The future

3.1 On-site measurements: systemisation

Because of the complicated nature of salt and fresh water phenomena, the regular recording of phenomena needs to be extended. This can be done by establishing recording networks and making use of automatic data-processing.

A better impression of the synoptic coherence of the phenomena in nature can be obtained by computer processing of the recordings by statistical methods such as cross-covariances etc.

There would presumably be less need for simultaneous recording campaigns if a permanent recording network were established.

Tracer experiments and recording campaigns using sophisticated recording techniques for observing turbulence mechanisms probably have a promising future. Purposeful recordings of this kind would help us to understand the physical mechanisms involved.

3.2 Laboratory research: fundamentalisation

In view of the development of computation methods, it seems questionable whether we can expect scale model techniques to develop very much further.

On the other hand, considerable progress will perhaps be made in laboratory research of a more fundamental nature.

Thanks to the development of new recording methods such as the laser-doppler method, a more fundamental form of research into turbulence by means of laboratory experiments is becoming a practical proposition. Laboratory experiments can help in no small measure to deepen our knowledge of turbulence problems. They may help us not merely to consolidate the theory of turbulence, but to develop sounder semi-empirical formulas for friction and mixing.

3.3 Computation methods: simulation

The further development of computation methods involving two or three-dimensional space grids for hydrodynamic and water quality parameters may be expected. Computation methods of this kind generally call for large and rapid — and therefore expensive — computers. Whether they can be made available or not, depends inter alia largely on financial considerations.

Theoretically, these computation methods will provide reliable simulations of fresh and salt water phenomena suitable for forecasting, provided sound formulas are used for friction and mixing.

It would probably still be necessary to calibrate with the help of on-site measurements, in order to test the simulation of the local situation.

Theoretically, there seems no reason why more complete simulation including turbulence should not be achieved, but three-dimensional fine-mesh grids would be required for the purpose. It is doubtful whether the scheme would be economically viable.

3.4 Cooperation: division of work

What the foregoing boils down to is that technical progress is likely to lessen the more practical limitations in the various fields of research, thus enabling us to take more effective advantage of the opportunities offered.

As a result, relations between the forms of research will be determined to a greater degree by the more essential limitations. This may lead to a certain amount of specialisation; cooperation will come to be more a question of the division of work.

In the division of work the main object of making on-site measurements should be to obtain a systematic documentation of actual conditions and the changes occurring in them.

The main object of laboratory research should be to increase the basic physical knowledge required for making sound forecasts.

The main function of the computation methods should be to extrapolate to future situations, starting from the available knowledge of actual conditions and making use of the available basic physical information.

The mathematical description of the physical phenomena will have to be of prime importance where laboratory research and computation methods are combined.

Where on-site measurements and laboratory research are combined, the phenomenological description would be the main factor. Purposeful on-site measurements and laboratory experiments can supplement each other.

The systems approach could be the main factor where on-site measurements and computation models interact. Models for the system being investigated could be set up either inductively and empirically from measurements in nature or deductively and theoretically from computation models. More direct calibration of the computation model can be achieved by comparing the computation model with the prototype in terms of correlations between synoptic observations rather than in terms of the observations themselves.

4 In conclusion

Let us complete this study by taking a look at salt and fresh water problems in a somewhat wider context. Water is one of the most essential elements of the human environment. The water's salinity is a significant parameter of its quality; and in this country we have always realised the importance of the quality of water.

Population growth and increased social and economic activities have enhanced the importance of many other water-quality parameters, such as temperature, oxygen content, radioactive components, bacteria content, silt content.

The mechanisms of flows and turbulent mixing which determine the distribution of salinity have a completely analogous effect on the distribution of temperatures and the other substances mentioned above. It should also be remembered that the mechanisms of flows and mixing may be strongly affected by density differences resulting from salinity differences. Consequently, research into salt and fresh water phenomena is often indispensable if the effect of flows and mixing on other water-quality parameters is to be determined.

Studies of fresh and salt water phenomena can therefore be regarded as an important part of research into water quality in space and time.

Salinity, by the way, is not the only parameter whose effect on density has a profound effect on currents and mixing; temperature is another. Heat released by power-stations, for example, into open water can also engender phenomena similar to those observed in fresh and salt water.

Vertical density differences resulting, for instance ,from salinity and/or temperature differences, can greatly suppress turbulence and so create a stratified instead of a well-mixed system. This can have a great effect on other quality parameters besides salinity and temperature.

Turbulence set up by strong currents counteracts the development of a stratified system.

Salt and fresh water phenomena were studied first and foremost in relation to major density differences such as those observed in estuaries like the Rotterdam Waterway, where sea and river water with comparatively high density differences meet. There may also be comparatively strong currents set up by river discharges and tides; both stratified and mixed systems may then occur.

Stratified systems hardly ever occurred when salinity levels in the inland waterways were very low. But nowadays such large quantities of waste salt are discharged into inland waters that the density differences are greater than they were, although the differences are usually less than those between sea and fresh water.

Nevertheless, when density differences are low, stratification can develop in slow-

flowing inland waters; the temperature, of course, can also play a part here. Comparatively little is known about the special problems involved in such situations.

The author hopes that these final remarks have made it clear that continued research into salt and fresh water phenomena will help in no small measure to improve our approach to water-quality problems.

COMMISSIE VOOR HYDROLOGISCH ONDERZOEK T.N.O.

Verslagen en Mededelingen

No. 1. Verslagen van de Technische Bijeenkomsten 1 — 6 (with summaries in English, avec des résumés en français), 1952.
1. Het waterhuishoudkundig onderzoek in de Rottegatspolder
2. De watervoorziening der gewassen I
3. Waarneming van grondwaterstanden
4. Lysimeteronderzoek in Nederland
5. De watervoorziening der gewassen II
6. Het vraagstuk van de verzouting van grond- en oppervlaktewater in Nederland

No. 2. Verslagen van de Technische Bijeenkomsten 7 — 10 en Verslag inzake het verdampingsonderzoek in de Rottegatspolder over de jaren 1947-1952 (with summaries in English, avec des résumés en français), 1955.
7. Bewerking van regenwaarnemingscijfers
8. Modelonderzoek van grondwaterstromingen
9. Metingen en verbeteringen in het stroomgebied van beken
10. Geo-electrisch bodemonderzoek

No. 3. Verslagen van de Technische Bijeenkomsten 11 — 12 (with summaries in English, avec des résumés en français) en Rapport inzake de lysimeters in Nederland (in de Engelse taal), 1958.
11. Watervoorziening van zandgronden
12. Kwaliteitseisen van oppervlaktewater

No. 4. Verdampingssymposium Agrohydrologisch Colloquium C.O.L.N. en Rapport inzake de lysimeters in Nederland II (with summaries in English), 1959.

No. 5. Verslagen van de Technische Bijeenkomsten 13 — 14 (with summaries in English), 1960.
13. Grondwaterstanden en grondwaterbeweging in de Nederlandse zandgronden
14. Het water in onverzadigde grond

No. 6. Verslag van de Technische Bijeenkomst 15 (with summaries in English, avec des résumés en français), 1961.
Enige onderzoekingen ten behoeve van de grondslagen van het beheer van de Rijn, het IJsselmeer en het Zeeuwse Meer

No. 7. Verslag van de Technische Bijeenkomst 16 (with summaries in English), 1962.
Het droge jaar 1959

No. 8. Verslag van de Technische Bijeenkomst 17 (with summaries in English), 1963.
De stromingswetten van het grondwater en de toepassing daarvan in de praktijk

No. 9. Verslag van de Technische Bijeenkomst 18 (with summaries in English), 1963.
Wateroverlast

No. 10. Steady flow of ground water towards wells, compiled by the Hydrologisch Colloquium, 1964.

No. 11. Verslag van de Technische Bijeenkomst 19 (avec des résumés en français, mit Zusammenfassungen in Deutsch), 1964.
Geo-hydrologische karteringen

No. 12. Proceeding of Technical Meeting 20 (in English), 1966.
Water balance studies

No. 13. Proceeding of Technical Meeting 21 (in English), 1966.
Recent trends in hydrograph synthesis

No. 14. Verslag van de Technische Bijeenkomst 22, 1968.
Regenwaarnemingscijfers (II) en
Rapport inzake Lysimeters in Nederland (III) (both reports with summaries in English)

No. 15. Proceedings and Informations no. 15 (in English), 1968.
Soil — Water — Plant

Verslag van de Technische Bijeenkomst 23, 1968.
Kwelverschijnselen
(Wordt niet gepubliceerd).

154

Verslag van de Technische Bijeenkomst 24, 1970.
Stroming door de onverzadigde zone van de bodem
(Wordt niet gepubliceerd).

No. 16.   Verslag van de Technische Bijeenkomst 29 (with summaries in English),
1975.
Het hydrologische onderzoek ten behoeve van het Structuurschema
Drink- en Industriewatervoorziening Nederland

No. 17.   Proceeding of Technical Meeting 25 (in English), 1973.
Automatic Processing of Hydrological Data

No. 18.   Proceeding of Technical Meeting 26 (in English), 1974.
Hydraulic Research for water management

No. 19.   Proceeding of Technical Meeting 27 (in English), 1974.
The hydrological investigation Programme in Salland (The Netherlands)

Verslag van de Technische Bijeenkomst 28, 1973.
Kwaliteitsaspecten van het Nederlandse oppervlaktewater in relatie tot de
waterhuishouding
(Wordt niet gepubliceerd).

No. 20.   Proceeding of Technical Meeting 30 (in English), 1976.
Salt distribution in estuaries

No. 21.   Proceeding of Technical Meeting 31 (in English), 1976.
Groundwater pollution

No. 22.   Verslag van de Technische Bijeenkomst 32 (with summaries in English),
1976.
Systeembenadering voor het waterbeheer

155

COMMITTEE FOR HYDROLOGICAL RESEARCH T.N.O.

Proceedings and Informations

No. 1.   Proceedings of Technical Meetings 1 — 6 (with summaries in English), 1952.
    1.   Investigations into the water balance of the Rottegatspolder
    2.   The water supply for crops I
    3.   Observations of groundwater levels
    4.   Investigations by drain gauges in the Netherlands
    5.   The water supply for crops II
    6.   The problem of the increasing salinity of ground and surface water in the Netherlands

No. 2.   Proceedings of Technical Meetings 7 — 10 and Report on the evaporation research in the Rottegatspolder 1947-1952 (with summaries in English), 1955.
    7.   The study of precipitation data
    8.   Model research on groundwater flows
    9.   Measurements and improvement works in basin of brooks
    10.   Geo-electrical research

No. 3.   Proceedings of Technical Meetings 11 — 12 (with summaries in English) and Report on the lysimeters in the Netherlands (in English), 1958.
    11.   The water supply of sandy soils
    12.   Quality requirements for surface waters

No. 4.   Evaporation Symposium and Report on the Lysimeters in the Netherlands II (with summaries in English), 1959.

No. 5.   Proceedings of Technical Meetings 13 — 14 (with summaries in English), 1960.
    13.   Groundwater levels and groundwater movement in the sandy areas of the Netherlands
    14.   Water in unsaturated soil

No. 6.   Proceeding of Technical Meeting 15 (with summaries in English and French, 1961.
The regimen of the Rhine, the Ysselmeer and Zeeland lake

156

No. 7.   Proceeding of Technical Meeting 16 (with summaries in English), 1962.
           The dry year 1959

No. 8.   Proceeding of Technical Meeting 17 (with summaries in English), 1963.
           The laws of groundwater flow and their application in practice

No. 9.   Proceeding of Technical Meeting 18 (with summaries in English), 1963.
           Water nuisance

No. 10.   Steady flow of ground water towards wells, compiled by the Hydrologisch
           Colloquium (in English), 1964.

No. 11.   Proceeding of Technical Meeting 19 (with summaries in French and Ger-
           man), 1964.
           Geo-hydrological cartography

No. 12.   Proceeding of Technical Meeting 20 (in English), 1966.
           Water balance studies

No. 13.   Proceeding of Technical Meeting 21 (in English), 1966.
           Recent trends in hydrograph synthesis

No. 14.   Proceeding of Technical Meeting 22, 1968.
           Precipitation Data (II) and
           Report on the Lysimeters in the Netherlands (III) (both with summaries in
           English)

No. 15.   Proceedings and Informations no. 15 (in English), 1969.
           Soil — Water — Plant

           Proceeding of Technical Meeting 23, 1968.
           (Will not be published).

           Proceeding of Technical Meeting 24, 1970.
           Flow in the unsaturated zone
           (Will not be published).

No. 16.   Proceeding of Technical Meeting 29 (with summaries in English), 1975.
           Hydrological investigations for masterplan for the future watersupply in
           The Netherlands

157

No. 17.   Proceeding of Technical Meeting 25 (in English), 1973.
           Automatic Processing of Hydrological Data

No. 18.   Proceeding of Technical Meeting 26 (in English), 1974.
           Hydraulic Research for water management

No. 19.   Proceeding of Technical Meeting 27 (in English), 1974.
           The hydrological Investigation Programme in Salland (The Netherlands)

           Proceeding of Technical Meeting 28, 1973.
           Water quality of Dutch rivers with respect to water management
           (Will not be published).

No. 20.   Proceeding of Technical Meeting 30, (in English), 1976.
           Salt distribution in estuaries

No. 21.   Proceeding of Technical Meeting 31, 1976.
           Groundwater Pollution

No. 22.   Proceeding of Technical Meeting 32, (with summaries in English), 1976.
           Systems Approach to the Management of Water Resources